

12

# Carnegie-Mellon University

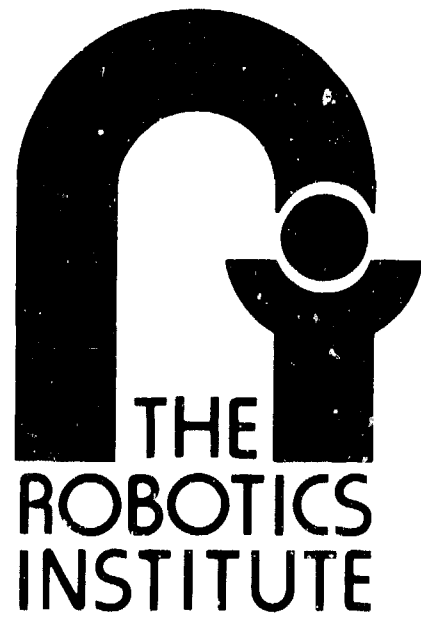
## DYNAMICALLY STABLE LEGGED LOCOMOTION

March H. Raibert, H. Benjamin Brown, Jr., Michael Chepponis  
Eugene Hastings, Seshashayee S. Murthy, Francis C. Wimberly

AD A 126369

DTIC  
APR 1983  
H

DESTROYED BY STATEMENT  
Approved for public release  
Distribution Unlimited



THIS IS A COPY

REPORT DOCUMENTATION PAGE		READ INSTRUCTIONS BEFORE COMPLETING FORM
1. REPORT NUMBER CMU-RI-TR-83-1	2. GOVT ACCESSION NO. ADA 126369	3. RECIPIENT'S CATALOG NUMBER
4. TITLE (And Subtitle)  DYNAMICALLY STABLE LEGGED LOCOMOTION	5. TYPE OF REPORT & PERIOD COVERED  Interim	
	6. PERFORMING ORG. REPORT NUMBER	
7. AUTHOR(s) Marc Raibert, H. Benjamin Brown, Jr., Michael Chepponis, Eugene Hastings, Seshashayec S. Murthy, Francis C. Wimberly	8. CONTRACT OR GRANT NUMBER(s)  ARPA 4148	
9. PERFORMING ORGANIZATION NAME AND ADDRESS Carnegie-Mellon University The Robotics Institute Pittsburgh, PA. 15213	10. PROGRAM ELEMENT, PROJECT, TASK AREA & WORK UNIT NUMBERS	
11. CONTROLLING OFFICE NAME AND ADDRESS  Office of Naval Research Arlington, VA 22217	12. REPORT DATE Oct. 1, 1982- Dec. 31, 1982	
	13. NUMBER OF PAGES 120	
14. MONITORING AGENCY NAME & ADDRESS (if different from Controlling Office)	15. SECURITY CLASS. (of this report)  UNCLASSIFIED	
	16. DECLASSIFICATION/DOWNGRADING SCHEDULE	
16. DISTRIBUTION STATEMENT (of this Report)		
17. DISTRIBUTION STATEMENT (of the abstract entered in Block 20, if different from Report)		
Approved for public release; distribution unlimited		
18. SUPPLEMENTARY NOTES		
19. KEY WORDS (Continue on reverse side if necessary and identify by block number)		
20. ABSTRACT (Continue on reverse side if necessary and identify by block number)		

# Dynamically Stable Legged Locomotion

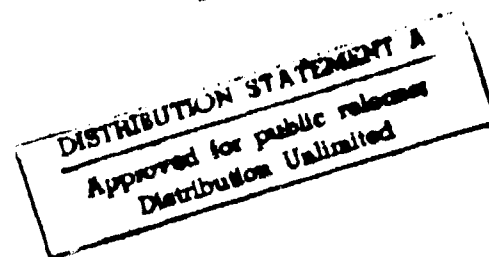
Second Report to DARPA

October 1, 1981 - December 31, 1982

✓ Marc H. Raibert, H. Benjamin Brown, Jr., Michael Chepponis  
Eugene Hastings, Seshashayee S. Murthy, Francis C. Wimberly

The Robotics Institute  
Carnegie-Mellon University  
Pittsburgh, PA. 15213

27 January 1983



Sponsored by the Defense Advanced Research Projects Agency (DoD), Systems Sciences Office, ARPA Order No. 4148. The views, opinions, and findings contained in this report are those of the authors and should not be construed as an official Department of Defense position, policy, or decision, unless so designated by other official documentation.

## Abstract

This report documents our recent progress in exploring balance and dynamic stability in legged systems. There have been five areas of progress, each described in a separate chapter in the pages that follow.

- Balance in 2D can be achieved with a surprisingly simple control system. The control system has three separate parts, one that controls hopping height, one that controls the velocity of forward travel, and one that controls body attitude. A physical 2D one-legged hopping machine that employs such a three-part control system hops in place, runs from place to place at speeds of up to 2.7 mph, maintains its balance when disturbed, and leaps over small obstacles.
- Control of locomotion in 3D can build upon the results obtained in 2D. Simulations suggest that a 3D one-legged machine could run and balance using the same three-part controller developed for 2D, provided that additional extra-planar mechanisms operate to suppress roll, yaw, and lateral motions.
- We have designed and built a physical one-legged system that will permit experimentation in the control of balance in 3D. The device has a simple pneumatic leg that is positioned by a hydraulic hip. It will hop on an open floor without a system of physical constraints.
- Last year we developed a method for obtaining balance that uses tabulated data. This year the method was extended by showing that the voluminous tabular data can be approximated by a polynomial surface of moderate degree, without much loss of control precision.
- We refined our understanding of the mechanisms responsible for balance by simulating and comparing three different algorithms for horizontal control: one just places the foot during flight, one places the foot during flight and sweeps the leg during stance, and the third places the foot during flight and controls body attitude during stance. Each of the three methods elucidates a different principle of dynamic stability.

The report closes with a bibliography on legged locomotion containing about 350 references.



Accession For	
NTIS GRA&I	<input checked="" type="checkbox"/>
DTIC TAB	<input type="checkbox"/>
Unannounced	<input type="checkbox"/>
Justification	
By _____	
Distribution/	
Availability Codes	
Dist	Avail and/or Special
A	

## Acknowledgements

We thank Wayne Book, Kirk Botula, Nancy Cornelius, Marc Donner, Ed Frank, Martin Liester, Matt Mason, Jeffrey Miller, Gregg Podnar, and Ken Salem for the numerous and varied contributions they have made to the project throughout the year. Sylvia Brahın worked on parts of this text, and helped out in many other ways throughout the year. Steve Talkington did most of the line drawings. We thank Andy Gruss for spending significant time helping us to design electronics for the 3D machine.

Ivor Durham's PLOT program generated the graphs used in this report. We thank him, not only for making the original program available to us, but for the many additions and changes he made specifically for our purposes.

Ivan Sutherland continues to be a source of motivation, encouragement, enthusiasm, guidance, and of course, good ideas.

# Table of Contents

<b>Abstract</b> .....	<b>iii</b>
<b>Acknowledgements</b> .....	<b>v</b>
<b>1 Introduction and Summary</b> .....	<b>1</b>
1.1 2D Experiments .....	1
1.2 Decomposing 3D Balance Into Planar and Extra-Planar Parts .....	3
1.3 Design and Construction of a 3D One-Legged Hopping Machine .....	3
1.4 Tabular Control in Legged Locomotion .....	4
1.5 Modeling and Simulation of 2D One-Legged Running.....	7
<b>2 Experiments with the 2D One-Legged Machine</b> .....	<b>9</b>
2.1 Abstract.....	9
2.2 Introduction .....	9
2.3 The One-Legged Device .....	10
2.4 Control.....	14
2.4.1 Height Control .....	14
2.4.2 Velocity Control .....	15
2.4.3 Attitude Control .....	17
2.4.4 Sequence Control.....	17
2.5 Experimental Results.....	19
2.5.1 Vertical Hopping .....	19
2.5.2 Horizontal Travel.....	20
2.5.3 Leaping .....	24
2.6 Discussion .....	25
2.7 Conclusions.....	26
2.8 Appendix I. Physical Parameters of One-Legged Hopping Machine.....	28
<b>3 3D Balance Using 2D Algorithms</b> .....	<b>29</b>
3.1 Abstract.....	29
3.2 Introduction .....	29
3.2.1 Background .....	30
3.3 Modeling and Simulation .....	31
3.3.1 Equations of motion.....	33
3.4 Control.....	34
3.4.1 Height control.....	35
3.4.2 Velocity control.....	35
3.4.3 Attitude control .....	37
3.4.4 Spin control.....	39
3.4.5 Path control.....	41

3.5	<b>Conclusion</b> .....	42
3.6	<b>Appendix II. Description of 3D Model</b> .....	43
<b>4</b>	<b>Design and Construction of 3D One-Legged Machine</b> .....	<b>45</b>
4.1	Introduction .....	45
4.2	Design Details .....	47
4.3	Sensors .....	50
4.4	Auxiliary Equipment .....	51
4.5	Appendix III. Specifications for 3D and 2D One-Legged Machines, Metric Units .....	52
4.6	Appendix IV. Specifications for 3D and 2D One-Legged Machines, English Units .....	53
<b>5</b>	<b>Using Tables for Dynamic Stability in a One-Legged System</b> .....	<b>55</b>
5.1	Abstract .....	55
5.2	Introduction .....	55
5.3	The Problem .....	56
5.4	Tabular Method .....	58
5.5	Polynomial Approximation to Tabular Data .....	60
5.6	Appendix V. Algorithm that Minimizes Performance Index for Tabular Data .....	65
5.7	Appendix VI. Algorithm that Minimizes Performance Index for Polynomial .....	66
<b>6</b>	<b>Control of Balance in 2D -- Modeling and Simulation for the One-Legged Case</b> ..	<b>67</b>
6.1	Abstract .....	67
6.2	Introduction .....	67
6.3	The Model .....	69
6.4	Vertical Control .....	72
6.5	IV. Horizontal Control .....	79
6.5.1	Method 1: Foot Placement .....	80
6.5.2	Method 2: Leg Sweeping .....	83
6.5.3	Method 3: Servo Attitude .....	87
6.6	V. Conclusion .....	89
6.7	Appendix VII. Equations of Motion for Model .....	92
6.8	Appendix VIII. Simulation Parameters .....	95
	<b>Bibliography</b> .....	<b>97</b>

# 1. Introduction and Summary

Humans and animals use their legs to locomote with great mobility, but we do not yet have a full understanding of how they do so. One sign of our ignorance is the lack of man-made vehicles that use legs to obtain high mobility. A legged vehicle might someday travel in difficult terrain, where softness or bumpiness makes wheeled and tracked vehicles ineffective. The research reported here was designed to address both the scientific problem of understanding how living legged systems operate, and the engineering problem of how to build useful legged vehicles.

Our research strategy is to focus on the problems of balance and dynamic stability, while postponing to later the study of gait and coupling among many legs. To do this we have modeled, simulated, and built a number of systems that hop and balance on just one leg. In the one-legged regime balance is of paramount importance, while coordination and coupling do not apply. A secondary strategy has been to examine systems with springy legs, so that the role of resonant oscillatory leg behavior might be better understood.

The main thrusts of the work during the past year has been to do experiments on a physical 2D one-legged hopping system that balances as it runs, to simulate a 3D one-legged system, to build a physical 3D machine for future experiments, and to refine our previous theoretical work on 2D balance. This report is a collection of five separate papers that describe these projects. The major findings are summarized here:

## 1.1 2D Experiments

A physical 2D one-legged hopping machine has been operating in the laboratory now for almost a year. A single set of control algorithms maintains balance as the machine hops in place, runs from one place to another, and leaps over small obstacles. Top recorded running speed is about 2.7 mph. When the machine is hopping in place, a person can disturb it by pushing sideways without causing it to lose balance.

The most important thing about the control system for the 2D one-legged machine is its simplicity. Three separate servos operate independently to control hopping height, forward travel, and body attitude:

- Hopping Height: The control system regulates hopping height by manipulating hopping energy. The leg is springy, so hopping is a bouncing motion that is generated by an actuator that excites the leg. Hopping height is determined by the energy recovered from the previous hop, the losses in the hopping cycle, and thrust developed in the leg actuator. Height is regulated by adjusting the amount of thrust on each cycle to just make up for losses.
- Velocity: The control system manipulates forward velocity by placing the foot with respect to the center of the *CG-print* on each step. The *CG-print* is the locus of points on the ground over which the center of gravity of the system will pass during stance. Displacing the foot from the center of the *CG-print* causes the system to run either faster or slower. The control system calculates the

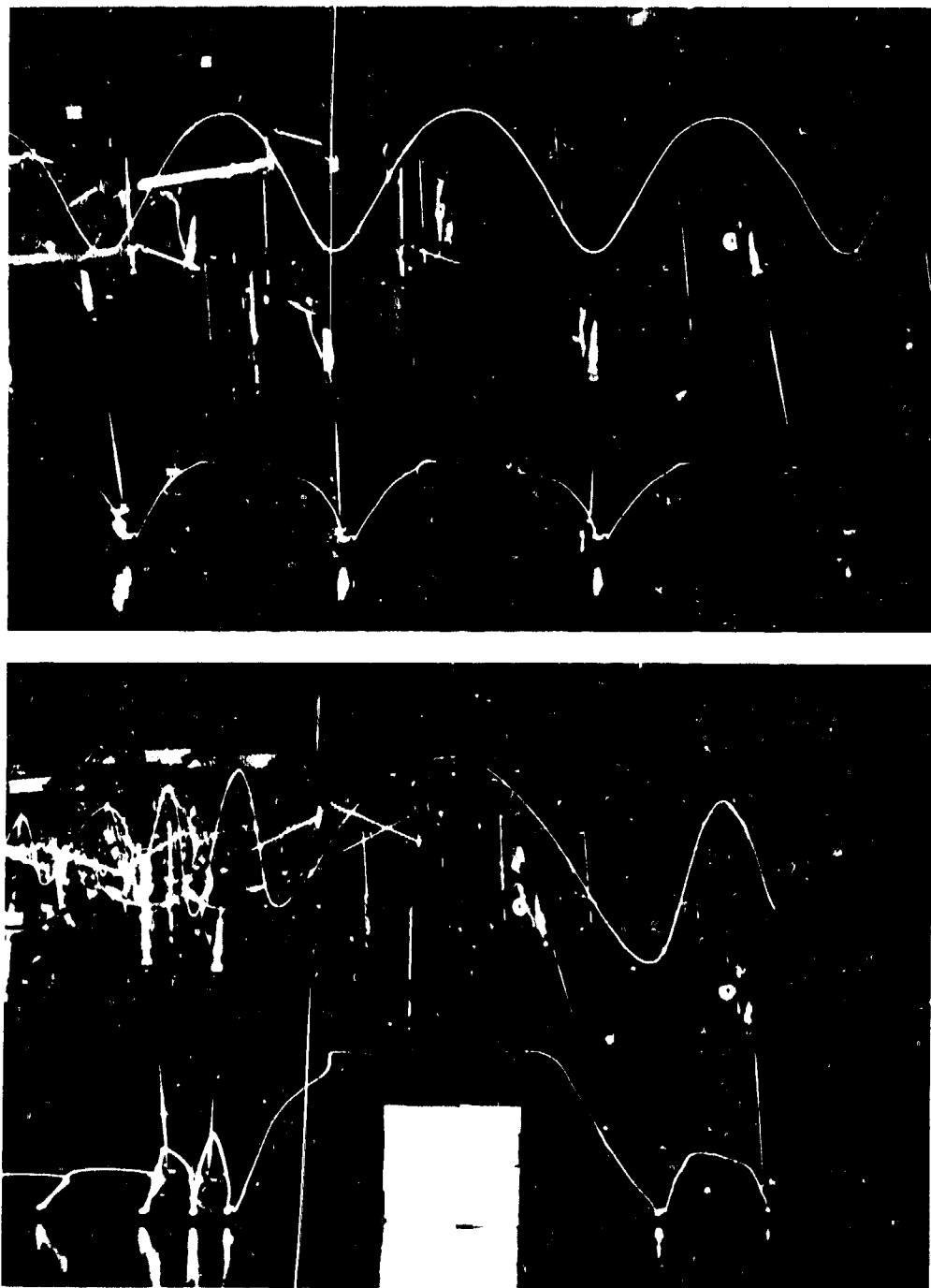


Figure 1-1: The 2D hopping machine running and leaping. Action is from right to left in both photographs. LEDs indicated paths of the foot and hip. TOP: Running at about 2 mph with 0.4 m stride. BOTTOM: The same controller that balances when hopping in place and when running forward, can be used during leaping. The vertical control program is modified to generate extra thrust and to retract the leg. Obstacle is 6 x 6 inches.

length of the CG-print from the measured forward velocity and an estimate of the duration of stance. The error in forward velocity determines a foot position that will maintain the correct speed of forward travel.

- **Attitude:** The control system maintains an erect body posture during running, by generating hip torques during stance that servo the body angle. During stance friction between the foot and ground permits large torques to be applied to the body without causing large accelerations of the leg. These torques are used to implement a simple proportional servo that moves the body toward an erect posture once each step.

## 1.2 Decomposing 3D Balance Into Planar and Extra-Planar Parts

The same three-part control system that operates to balance the 2D machine can be applied to balance in 3D. We have begun to explore the notion that motion of dynamically stable 3D legged systems can be decomposed into a planar part and an extra-planar part. The planar part is like that already described for 2D, controlling large leg and body motions that provide hopping and forward travel. The extra-planar part produces only subtle corrective motions that maintain planarity. These motions must eliminate errors in roll, yaw, and lateral translation.

Motivation for this approach came from observing animals. Running animals seem to operate in 2D, with their legs swinging fore and aft through large angles while the body bobs up and down. The body may also pitch back and forth quite markedly. These large planar motions do not tell the whole story, since locomotion takes place in 3-space where things can move with six degrees of freedom. Motions that enforce planarity are usually not obvious.

We have designed a controller that uses these ideas to balance a simulated 3D one-legged machine. In addition to the three parts developed for the 2D machine, there are controllers for roll and yaw. Control of heading is treated in a special way that needs further work, and we have not yet begun to study active turning while running. Simulation data show good control of velocity, body attitude and spin while traversing paths made up of straight segments. These findings indicate that decomposition results in a very simple solution that seems to be in concert with what we observe in natural systems.

## 1.3 Design and Construction of a 3D One-Legged Hopping Machine

While 2D experiments have taught us a great deal about control of hopping, forward velocity and attitude, real locomotion takes place in 3D where yaw, roll and lateral drift must also be controlled. We are anxious to extend our experimental results to the 3D case. The notion that control of locomotion can be very simple receives the acid test in 3D, because the dynamic equations that describe motion in 3D are much more complicated than in 2D.

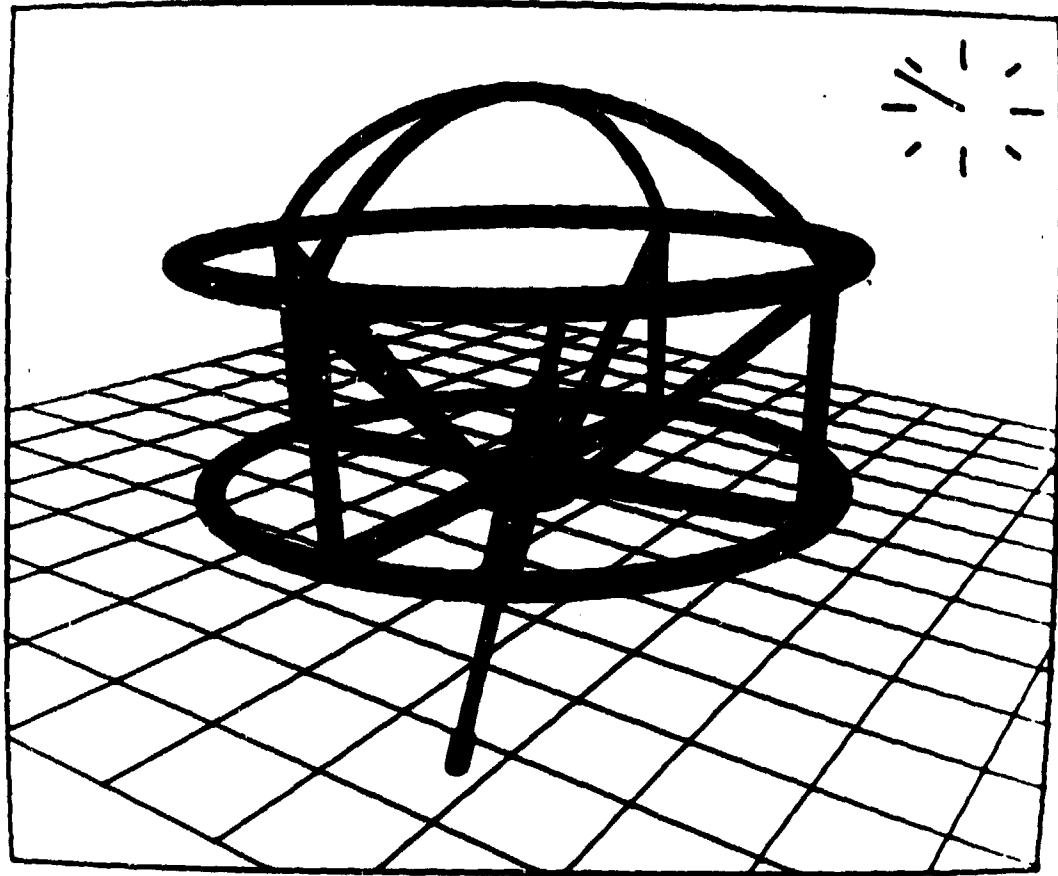


Figure 1-2: Simulated one-legged machine used to study algorithms for balance in 3D.

We have built a machine for these experiments. Like the 2D machine, it hops on one springy leg with hopping motions powered by compressed air. Hydraulic actuators control orientation of the leg with respect to the body. A 3-axis force sensing foot provides measurements of vertical loading and traction forces. A two-axis vertical gyro and an electronic compass provide measurements of the body's orientation in space. We are currently applying the principles of planar decomposition to the control and balance of this 3D one-legged machine.

#### 1.4 Tabular Control in Legged Locomotion

We have developed a tabular control method that is particularly well suited to controlling the non-linear dynamics of legged systems. Control of systems with non-linear dynamics is difficult when simple expressions that relate the behavior of the system to the available control signals are not available. Manipulators have been controlled using carefully organized tables that contain pre-computed data, but such tables are typically very large. We have found that it is possible to reduce the size of the tables needed for control, by capitalizing on the cyclic character of legged locomotion, in which movements are repeated one stride after another.

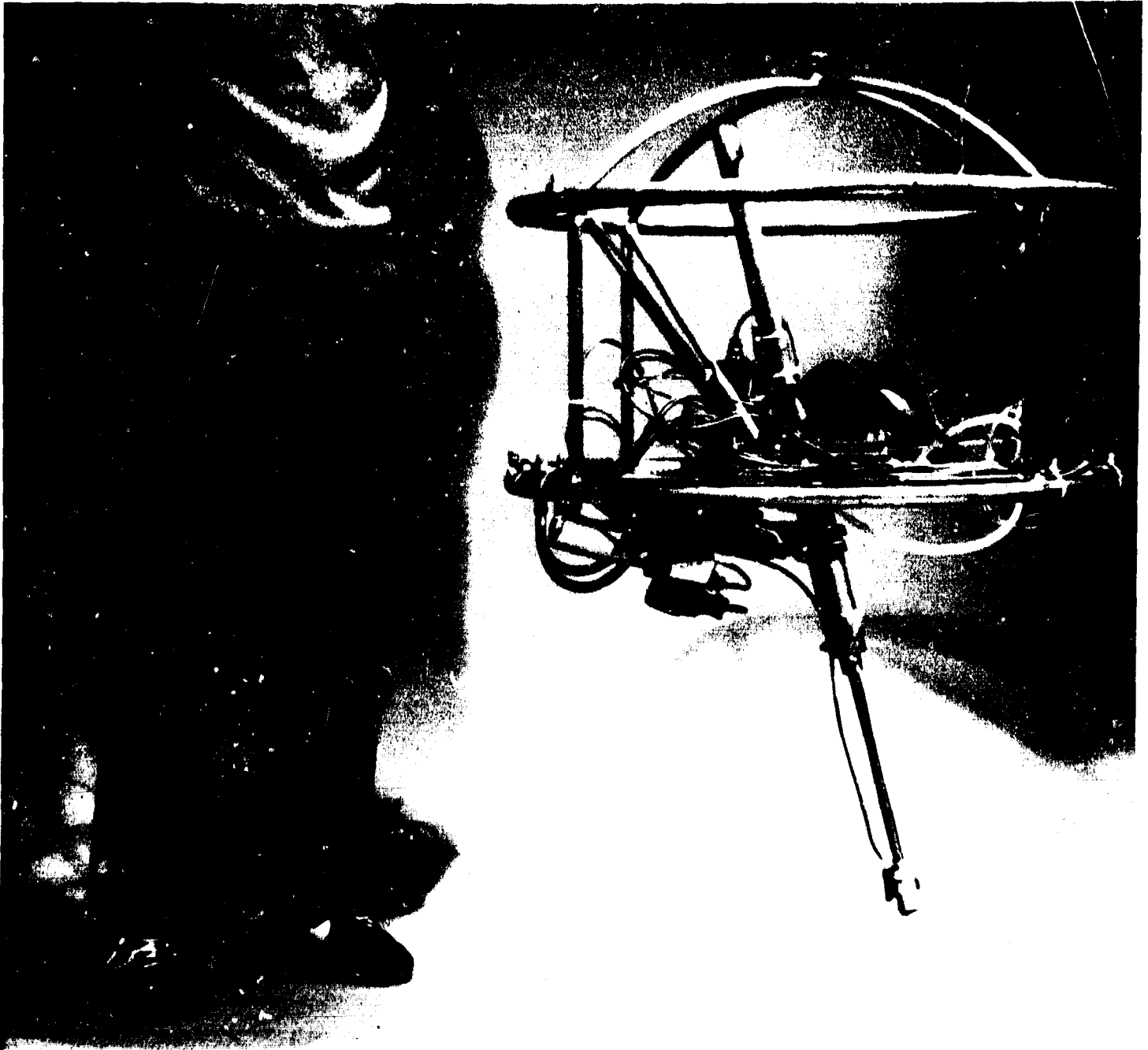


Figure 1-3: Machine to be used for experiments on balance in 3D. Hopping motion is powered by compressed air, but hydraulics are used to orient leg precisely with respect to the body. The foot can sense load and traction forces, and a gyroscope measures orientation of the body in space. An umbilical connects the machine to power supplies and the control computer, which are located nearby in the laboratory.

While the tables designed for manipulator control typically require one dimension for each state or configuration variable, the new tabular method employs a table that represents only a subset of the state variables. Behavior of the remaining state variables is nearly the same on each cycle, so they need not be represented explicitly in the table. For the case of the simulated 2D one-legged system, the control table has dimension 4, and stores about 20,000 numbers. Control using the tabular method results in very good performance, eliminating velocity limit cycles that occur when linear feedback is used.

We have also controlled the simulated 2D system with multi-variate polynomials that approximate the tabular data. This approach will permit treatment of problems larger than a pure tabular method can handle, provided additional computing power is available to evaluate the polynomials. Control data are presented for polynomials with 24, 40, 68, and 625 terms. We have found that the 40 term polynomial provides surprisingly good control, at only moderate storage and computational cost.

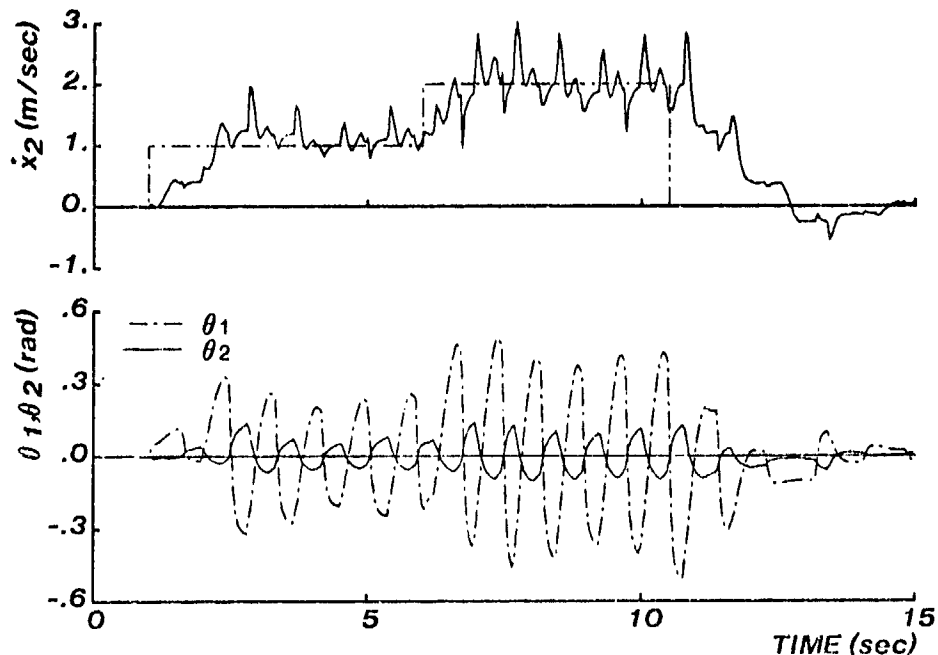


Figure 1-4: The three-part control algorithm responds to step changes in desired velocity, (shown stippled). Separate controllers modulate thrust to regulate hopping height, place foot during flight to control forward velocity, and generate hip torque during stance to control attitude of the body. These simulation data are designed to allow comparisons among the various mechanisms that contribute to control of balance and forward travel.

## 1.5 Modeling and Simulation of 2D One-Legged Running

Our understanding of balance has progressed through a number of stages. First we explored hopping itself, since balance could only be addressed once a locomotion cycle that alternated periods of support with periods of flight had been established. Then we examined the importance of foot placement as a means of controlling tipping and forward travel. Introducing the notion of the CG-print, the locus of points over which the center of gravity travels during stance, permitted us to generalize our results on foot placement to the case where forward velocity was important. This generalization led to sweep control. Finally, in doing physical experiments on the 2D hopping machine, we found that body attitude could be controlled separately from hopping and foot placement. The result was the three-part control algorithm mentioned earlier.

We reexamined these four aspects of control: hopping, foot placement, the CG-print, and three-part decomposition. We have gone back and produced a systematic set of equations, simulations, and tests that help to reveal the power and role played in legged locomotion by each mechanism.

## 2. Experiments with the 2D One-Legged Machine

### 2.1 Abstract

The ability to balance is important to the mobility of legged creatures found in nature. The study of this ability may someday lead to versatile legged vehicles. In order to study the role of balance in legged locomotion and to develop effective control strategies, a 2D hopping machine was constructed for experimentation. The machine has one leg on which it hops and runs, making balance a prime consideration. Control of the machine's locomotion was decomposed into three separate parts: a vertical height control part, a horizontal velocity part, and an angular attitude control part. Experiments showed that the three part control scheme, while very simple to implement, was powerful enough to permit the machine to hop in place, to run at a desired rate, to translate from place to place, and to leap over obstacles.

### 2.2 Introduction

A key to the mobility obtained by legged systems that are dynamically stabilized is their ability to remain upright without a broad continuous base of support. The ability to locomote on a narrow base permits travel where obstructions are closely spaced, or where the only support path is a narrow one. The ability to locomote using intermittent support, or support points that are separated from one another gives flexibility to the choice of where and when to place the feet. For instance in rough terrain feet are placed only on those locations that provide good support, even when they are separated by large distances. Biological legged systems routinely take advantage of these features of dynamic stability, narrow base and intermittent support, to traverse terrain that can not be traversed by wheel or tread.

Previous experimental work on balance began with Cannon's control of inverted pendulums that rode on a small powered truck [141]. His experiments included balance of a single pendulum, two pendulums one atop the other, two pendulums side by side, and a long limber pendulum. Matsuoka [197] implemented a very simple one-legged hopping machine that lay on a table inclined  $10^\circ$  from the horizontal. Kato et. al. [169] have studied quasi-dynamic walking in the biped. In their studies a 40 kg biped with 10 hydraulically driven degrees of freedom used a preplanned motion to dynamically transfer support from one foot to the other. Miura and his students [230] built an electrically powered biped that balanced itself in 3D using a tabular control scheme. With only three actuated degrees it used a shuffling gait to balance that reminds one of Charlie Chaplin.

The present study explores the control of a physical one-legged hopping machine. The objective of using a machine with only one leg was to avoid the problem of coordinating many legs, thereby simplifying the experiments, while at the same time drawing attention to the issues of dynamic stability that are central to versatile legged systems. Study of a one-legged system also addressed the question of intermittent support in locomotion, because the only gait available was hopping. A related objective was to explore the use of springy

legs in obtaining efficient hopping, as animals do [7]. Springy legs permit energy to be recovered from one step so that it may be used to power the next step. Experimental results obtained from a physical device with one springy leg confirm the feasibility of the control strategies, previously tested only in simulation.

This chapter reports experimental results obtained by controlling a physical one-legged device, which is described in the next section. Section 3 describes how control of the device can be decomposed into three simple parts, and presents the three corresponding control algorithms. Data are presented in section 4 that were obtained by using the three algorithms to control the hopping machine. They illustrate the ability of the algorithms to control hopping height, to maintain balance, to regulate travel from place to place, to respond to sudden disturbances, and to leap. Section 5 closes with conclusions and a summary.

### 2.3 The One-Legged Device

The 2D hopping machine shown in Fig. 2-1 was designed and constructed to do experiments in balance. Its main parts are a body and a leg connected by a simple hip. There is also a mechanism that constrains motion of the hopping machine to two dimensions. The body consists of a platform that mounts sensors, valves, actuators and computer interface electronics, and a weighted beam that increases the moment of inertia of the body.

The leg consists of a double acting air cylinder with a rubber cushion attached to the lower end of the rod to form a foot. The narrow foot, about 1. cm when fully loaded, provides a good approximation to a point of support. The coefficient of friction between the foot and the floor in our laboratory is about 0.6. Delivery of air pressure to the top end of the cylinder drives the piston and rod assembly downward, providing the vertical thrust for hopping. The leg air cylinder acts as a spring when the valves controlling air flow seal it off. This air cushion provides an opportunity to transfer the kinetic energy from one hop to the next hop, thereby reducing the energy cost of continuous hopping.

Under the best test condition the air spring recovered about 65% of the energy from one hop and returned it to the next hop. The ratio of body mass to the mass of the reciprocating portion of the leg is about 20:1. This results in a 5% energy loss when the device lands on the ground, and when it leaves the ground, as explained in Chapter 5. Friction in the leg actuator accounts for the other hopping losses.

The leg and body are connected by a hinge-type pivot joint that forms a hip. The angle between body and leg at the hip is controlled by a single stage proportional air servo valve that drives a pair of single acting air cylinders. A potentiometer provides a measurement of this angle to the control computer that serves the joint with a simple linear servo:

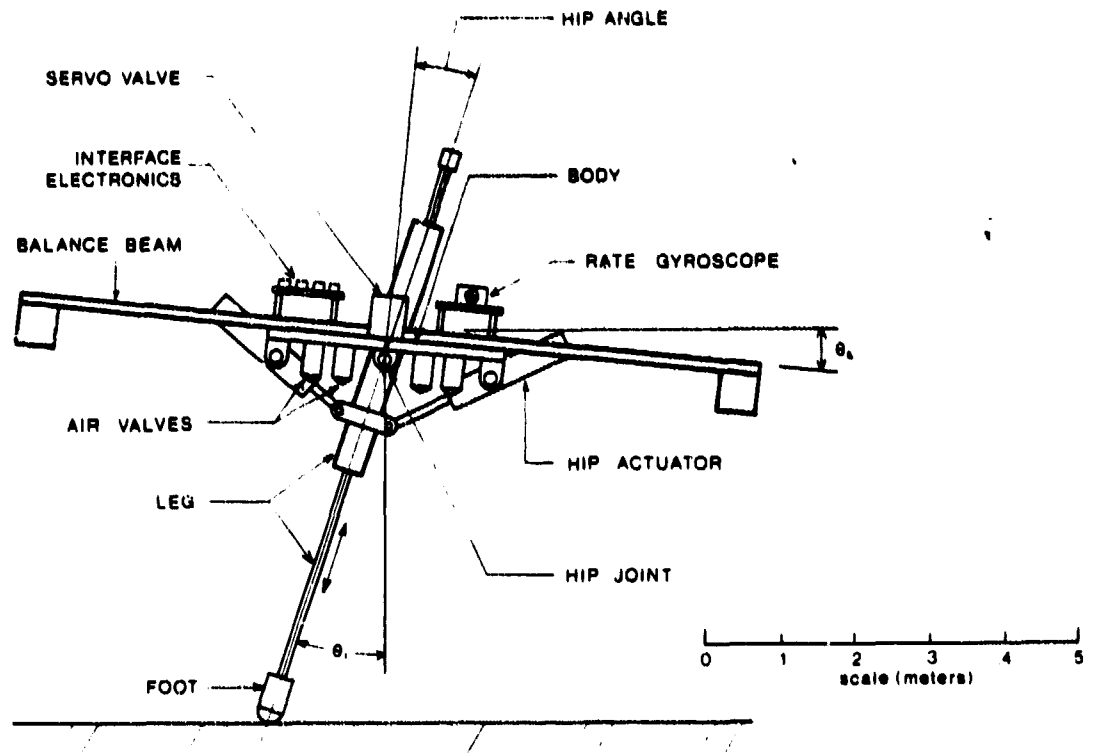


Figure 2-1: The one-legged device used for experiments has two primary parts: a body and a leg. The body provides mounting for valves, electronics and sensors, and has a balance beam that increases its moment of inertia. The leg is a double ended air cylinder that pivots with respect to the body, and that carries a padded foot on one end of the rod. Four two-way pneumatic valves control flow of compressed air to and from each end of the leg cylinder. Air can be trapped in the cylinder to make it act like a spring. Another set of pneumatic actuators powered by a proportional servo valve acts between the leg and body to control angle of the hip. On board sensors measure length of the leg, angle between leg and body, angle between leg and ground (only during stance), contact between foot and ground, pressure in the leg air cylinder, and inclination of the body with respect to the vertical.

$$\tau(t) = K_{P,FL}(\theta_1 - \theta_{1,d}) + K_{V,FL}(\dot{\theta}_1) \quad (2.1)$$

where

$\tau(t)$  is the actuator torque generated at the hip,  
 $K_{P,FL}, K_{V,FL}$  are position and velocity gains during flight, and  
 $\theta_{1,d}$  is the desired leg angle. (Values given in Appendix I.)

A full  $40^\circ$  sweep of the leg takes approximately 120 msec. The ratio of moment of inertia of the body to that of the leg is 15:1. This relatively high ratio ensures that the orientation of the leg may be changed during

flight without severely disturbing body attitude. The center of gravity of the body is located at the hip, so the only moments acting on the body are those generated by the hip actuator.

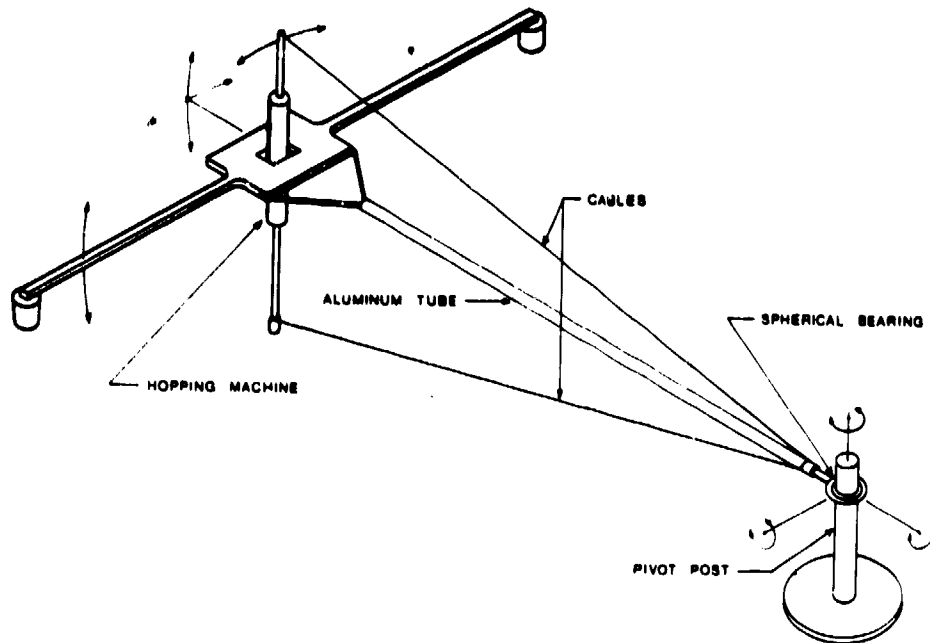


Figure 2-2: Tether boom mechanism constrains motion of one-legged device to surface of a sphere. The tether consists of a section of aluminum tubing with a spherical bearing at the stationary pivot end, and a fork pivot at the hopper end. The main boom holds the hopper 2.5 m from the pivot center, giving it radial and yaw stability, while a pair of nylon cables prevent roll. These cables also keep the foot a nearly constant radius from the pivot point as the leg changes length, minimizing radial scrubbing. Instrumentation mounted at the pivot provides measurement of the three primary motions: vertical translation, horizontal translation, and rotation about the axis of the boom.

Motion of the hopping machine is constrained to the 2D surface of a large sphere by the tether boom shown in Fig. 2-2. This mechanism permits the hopping machine to translate vertically and horizontally, and to rotate about the axis of the tether boom. Since the tether boom is made of cables and light-weight tubing, weight and friction are sufficiently small to be ignored. The tether boom arrangement permits the machine to travel around the laboratory on a circle of radius 2.5 m. Sensors mounted on the tether boom pivot provide measurements of the three free motions. An umbilical is attached to the tether boom that carries compressed air to drive the actuators, as well as electrical power and communication with the control computer.

Sensors mounted on the hopping machine provide state information to a nearby control computer and permit

performance to be measured. Potentiometers measure the angle between body and leg, the angle between leg and ground, and the length of the leg. A switch mounted on the foot senses contact with the ground. A pressure transducer measures compression of air in the leg air cylinder. A rate gyroscope mounted on the body of the hopper senses its angular rate. This signal is also integrated to estimate attitude of the body with respect to the ground; this estimate is periodically corrected for drift using the combined leg and hip angle measurements. The pitch motion to which the gyroscope is sensitive is also measured by instrumentation of the tether boom.

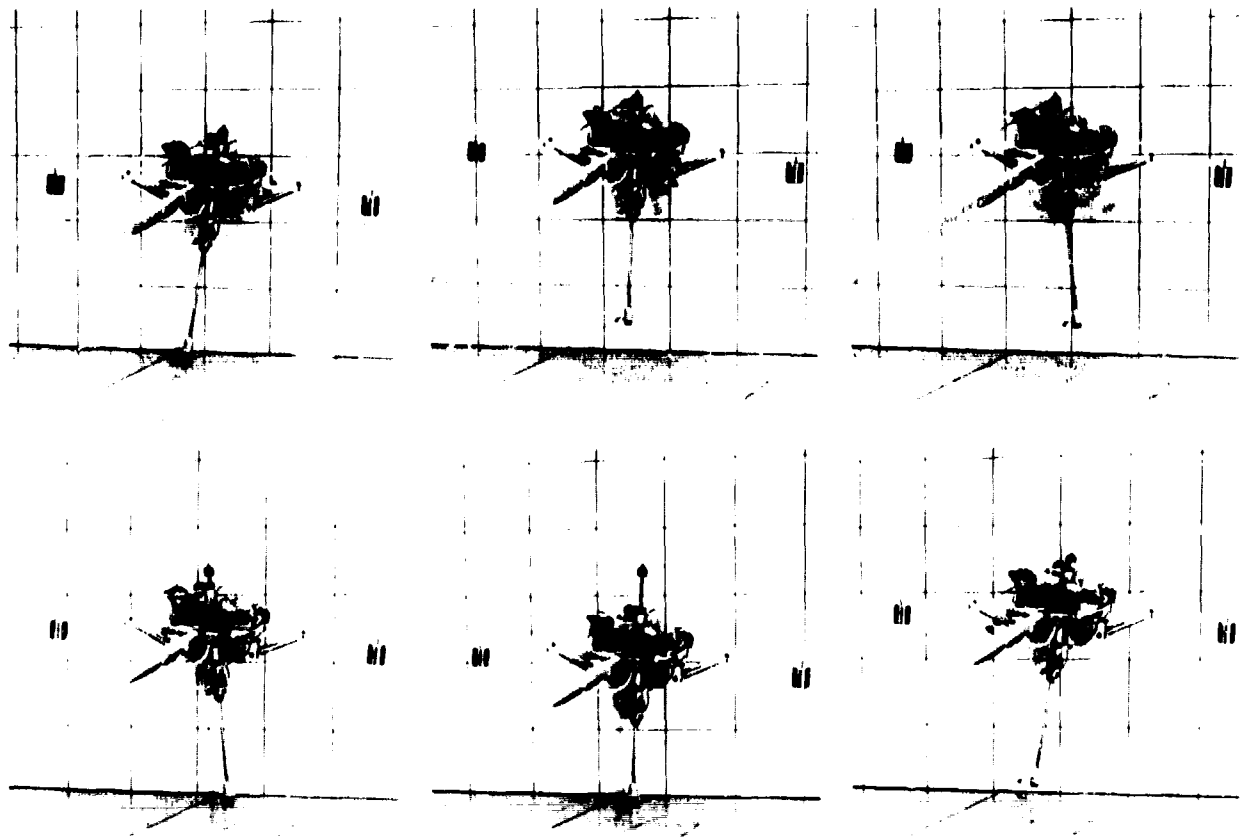


Figure 2-3: Sequence of photos showing one complete stride of the hopping machine running from left to right. Background grid spacing is 2 m. Running speed here is .75 m/sec. Stride .45 m, stride period 680 msec. Adjacent frames separated by 100 msec.

To make the machine hop the leg actuator is pressurized during the stance phase of each cycle and partially exhausted during the flight phase. The timing of pressure and exhaust are chosen to excite the spring-mass oscillator formed by the leg and body. Peak to peak amplitude of body oscillation can be varied between .04 and .3 m, with corresponding bouncing frequencies of about 3 to 1.5 per second. Over this range of bouncing frequencies the stance period is nearly constant varying by only a few percent, as expected for a spring-mass system.

To make the machine balance while traveling from place to place, the foot is positioned during flight and the hip is torqued during stance. During flight, a forward position for the foot is chosen appropriate to the machine's rate of travel. During stance, torques are developed at the hip to maintain the body's upright posture. The resulting control system produces running at rates of up to 1.2 m/sec (2.7 mph) with strides of up to .6 m. General operation of the machine is shown in Figure 2-3. These photographs, taken in rapid sequence throughout one stride, show the machine running at .75 m/sec (1.7 mph).

## 2.4 Control

Control of running in the one-legged device was decomposed into three separate parts. One part controls the height to which the device hops by modulating the vertical thrust generated in the leg. A second part controls forward velocity by positioning the foot on each step prior to landing. The third part controls attitude of the body by generating torques at the hip during the stance phase. The timing of these three controllers is synchronized to the ongoing activity of the hopping machine by a sequencer that receives input from the various sensors. Beyond coordinated timing, there are no explicit interdependencies among the three control parts. This independence results in a particularly simple control design that is effective when the system is hopping in place, when it translates from one point to another, when it accelerates to change running speed, and when it leaps.

### 2.4.1 Height Control

Hopping height is regulated by manipulating the duration of thrust of the leg. If the system were left to bounce passively on the springy leg, losses in the sliding friction of the air cylinder and in accelerating and decelerating the unsprung mass of the leg would soon cause the device to come to rest. Measurements of the decay in hopping height during passive hopping showed that such energy losses amounted to about 35% on each cycle. A vertical thrust is provided every cycle that just compensates for these losses.

Thrust is produced by permitting compressed air at supply pressure to flow into the upper part of the leg cylinder. The inflowing compressed air is added to that compressed by shortening of the leg as it absorbs kinetic energy on the previous hop. Pressure in the cylinder acts on the leg to accelerate the body upward. The magnitude of this acceleration, and therefore, the velocity of the device when the leg is fully extended, are determined by the amount of kinetic energy recovered from the previous hop and the length of time the intake valve is left open.

Equilibrium occurs when the energy lost in one hopping cycle equals the energy introduced through the intake valve. Since losses are monotonic with hopping height, a unique stable hopping height exists for each value of thrust. Details of the relationship between hopping height and duration of thrust were determined empirically. The height controller regulates the height of hopping by manipulating the duration that the intake valve is left open.

This scheme works quite well provided the thrusting direction of the leg is vertical. During running significant deviations from vertical occur, so variations in hopping height occur. Uniform hopping height could be obtained during running with an algorithm that took the changing kinematics of the device into account, but this was not done here.

#### 2.4.2 Velocity Control

Each time a hopping or running system leaves the ground, a foot must be moved to a position that will balance the system during the next stance interval. The goal is to ensure that there is support and to control horizontal motion of the machine. The forward velocity of the system during flight is used to calculate an appropriate foot position for landing.

During stance the system behaves like an inverted pendulum. Gravity generates a moment about the foot proportional to the horizontal displacement of the foot from the projection of the center of gravity of the system. When the foot is located directly under the center of gravity, the device tips neither forward nor backward. If the foot is offset from the projection of the center of mass, say to the rear, the device will tip in the opposite direction, to the front. When the device tips the body accelerates horizontally. In such a dynamically stable system it is not possible to prohibit tipping at all times. Rather, the velocity control algorithm must manipulate these tipping motions and the ensuing accelerations to control forward movement.

The strategy used here was to choose a foot position based on the predictable nature of the alternation between stance and flight, and constraints imposed by a system moving at constant velocity. When the device travels with constant horizontal velocity, balance is maintained by causing the average tipping moment to be approximately zero over each stride. This results in no average horizontal acceleration over each stride, and no average angular acceleration.

The distance traveled during stance is:

$$\Delta x = \dot{x}_2 T_{ST} \quad (2.2)$$

where

$\dot{x}_2$  is the horizontal velocity of the body, assumed to be constant, and  
 $T_{ST}$  is the duration of the stance phase.

The locus of points over which the center of gravity travels during the stance period, called the *CG-print*, extends from  $x_{2,TD}$  to  $x_{2,TD} + \Delta x$ , where  $x_{2,TD}$  is the position of the CG at touch-down. To minimize the tipping moment during stance, the foot should be placed in the center of the CG-print:

$$x_0 = x_{2,TD} + \frac{\Delta x}{2} \quad (2.3)$$

where

$x_0, x_2$  are the horizontal positions of the foot and body.

This positioning of the foot causes the horizontal and vertical motions of the leg to be symmetrical about the midpoint of the stance interval, at which point the leg is vertical and maximally compressed. During stance:

$$\theta_1(t_{TD} + t) = \theta_1(t_{LO} - t) \quad (2.4)$$

$$w(t_{TD} + t) = w(t_{LO} - t) \quad (2.5)$$

where

$t_{TD}$  is the time of touch-down and

$t_{LO}$  is the time of lift-off.

Tipping moments and forward accelerations are also nearly symmetrical, and therefore average to zero.

When the foot lands precisely in the center of the CG-print, forward velocity is not affected. To accelerate the system, either to compensate for velocity errors or to change speed, a tipping moment is purposely generated. When the foot is placed forward of the center of the CG-print, then the device will tend to tip backward, which slows it down. If the foot is placed rearward, then it will tip forward, increasing forward velocity. A linear function of velocity error is used to generate deviations in foot placement from the center of the CG-print:

$$x_{ERR} = K(\dot{x}_2 - \dot{x}_{2,d}) \quad (2.6)$$

where

$\dot{x}_{2,d}$  is the desired values for  $\dot{x}_2$  and

$K$  is a feedback gain.

Augmenting (2.3) with (2.6) yields:

$$x_0 = x_2 + \frac{\Delta x}{2} + K(\dot{x}_2 - \dot{x}_{2,d}) \quad (2.7)$$

The corresponding angle of the leg that will yield this foot position is given by:

$$\theta_{1,TD} = \text{Arcsin} \left( \frac{\Delta x + 2x_{ERR}}{2w} \right) \quad (2.8)$$

$$= \text{Arcsin} \left( \frac{\dot{x} T_{ST} + 2 K(\dot{x}_2 - \dot{x}_{2,d})}{2w} \right)$$

The algorithm of (2.8) has limitations at high velocity. As long as  $(\Delta x/2) \ll w_{MAX}$  and  $\theta_{1,MAX}$  is small, horizontal forces generated by compression of the leg are small and (2.8) is reasonably accurate. However, this condition is not satisfied in fast running. In that case  $x_{TD} \sim w_{MAX}$  and  $\theta_{1,MAX}$  is large; horizontal forces decelerate the system during the first half of stance, then accelerate it during the second half, making the average forward velocity during stance less than the overall average. Under these circumstances the CG-print is substantially shorter than estimated by (2.8). As a practical matter this problem was avoided by substituting the average value of  $x_2$  during stance in (2.8) for the overall average.

### 2.4.3 Attitude Control

Since angular momentum of the system is conserved during flight, the control system can manipulate attitude of the body only during stance when ground forces act on the foot. Torques generated during stance between the leg and body can be used to servo the attitude of the body to any desired orientation:

$$\tau(t) = K_{P,ST}(\theta_2 - \theta_{2,d}) + K_{V,ST}(\dot{\theta}_2) \quad (2.9)$$

where

$K_{P,ST}$ ,  $K_{V,ST}$  are position and velocity gains used for the hip servo during stance, and  $\theta_{2,d}$  is the desired attitude of the body, zero in this report.

### 2.4.4 Sequence Control

For a legged system to locomote each leg must alternate between a support phase in which the foot touches the ground and bears weight, and a transfer phase when the foot is elevated to move from one foothold to another. At the heart of the control system lies a sequencer that ensures such an alternation by coordinating height, velocity, and attitude controllers to the timing of the machine's support and transfer phases. This coordination relies on sensors that signal the transition from one phase to another. For example, support begins when pressure begins to build in the leg cylinder, and the leg begins to shorten. The remaining transitions and transition states for the hopping cycle are shown in Fig. 2-4.

As the hopping system nears the ground two events happen in rapid succession. First there is contact with the ground, then the leg bears a load. Contact is important because horizontal motions of the leg required for foot placement during flight should not continue when the foot is very close to the ground. If they do, then unwanted torques may be inadvertently generated on the body, upsetting its attitude. Since friction between foot and ground develops in proportion to the normal force, generation of hip torques to control the attitude of the body must await adequate vertical loading. For these reasons the time between first contact and load-bearing support is treated as a *twilight-zone* during which thrust, foot placement, and attitude control processes are inoperative. Another twilight-zone occurs when the system leaves the ground. Lift-off begins

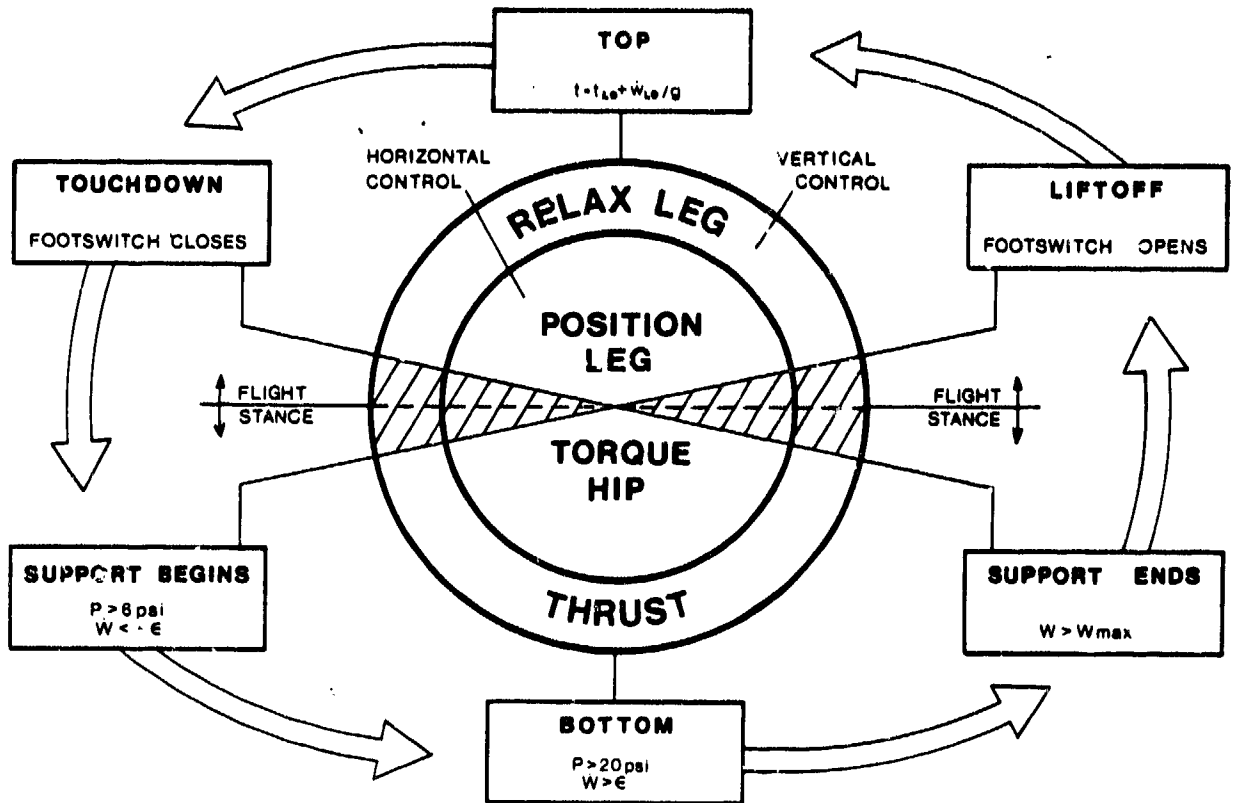


Figure 2-4: Finite state controller uses sensor measurements to synchronize the various phases of control with the cyclic activity of the locomotion system. Actions of the height, velocity, and attitude controls are coordinated by this state controller as it sequences through the hopping cycle.

and attitude control ends when extension of the leg is nearly complete. However, to ensure that the foot is fully unloaded before it is moved, no torques are generated at the hip until the foot switch opens.

The precautions taken during touch-down and lift-off to avoid motion of the foot when it is not fully loaded are not optimal for high speed running. When running at high speed the foot should not merely be left motionless during touch-down, but should accelerate to match the relative speed of the moving ground before actually touching it. At lift-off the foot should continue moving backward until it is fully unloaded. Running animals such as the kangaroo and cat match their feet to ground speed in this way [7], but the hopping machine has not yet been made to do so.

## 2.5 Experimental Results

The experimental hardware and control algorithms described above were used to verify the effectiveness and workability of the three-part control decomposition, to evaluate and refine the control algorithms, and to demonstrate balance in a man-made running system. The height, velocity, and attitude control algorithms and the sequence controller of the last section were implemented in a set of control programs that ran on a minicomputer. They controlled the hopping machine and recorded its behavior. The experiments tested vertical hopping, horizontal travel, and leaping.

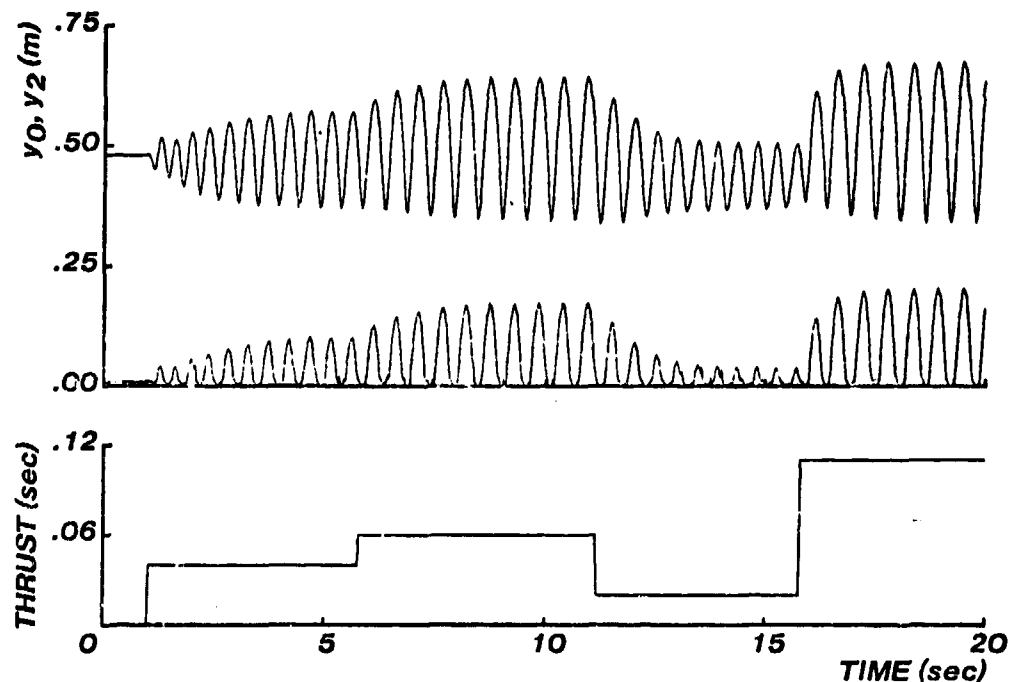


Figure 2-5: Data recorded while hopping machine hopped in place. Every 5 seconds duration of vertical thrust was adjusted to change hopping height. In each case it took about 2 seconds and 4 cycles to adjust. Upper curve is elevation of hip, middle curve is elevation of foot. Lower curve indicates duration of thrust. (a323.10)

### 2.5.1 Vertical Hopping

To demonstrate control of hopping height, data were recorded by the control computer while a new height setpoint was specified every 5 seconds. The results are plotted in Fig. 2-5. Each time the setpoint was changed it took four or five hops for the height to stabilize. In these records the machine hopped vertically in one place with no translation. Four cycles of these data are replotted in the  $y_2$  vs.  $\dot{y}_2$  phase plot of Fig. 2-6. The indentation at the upper right is due to the sudden acceleration experienced by the body when the leg

was accelerated to body speed. The upper part of this diagram is parabolic due to gravity's constant acceleration, while the lower part would be harmonic for a linear spring. Since the air spring is *hard*, the trajectory is not quite harmonic.

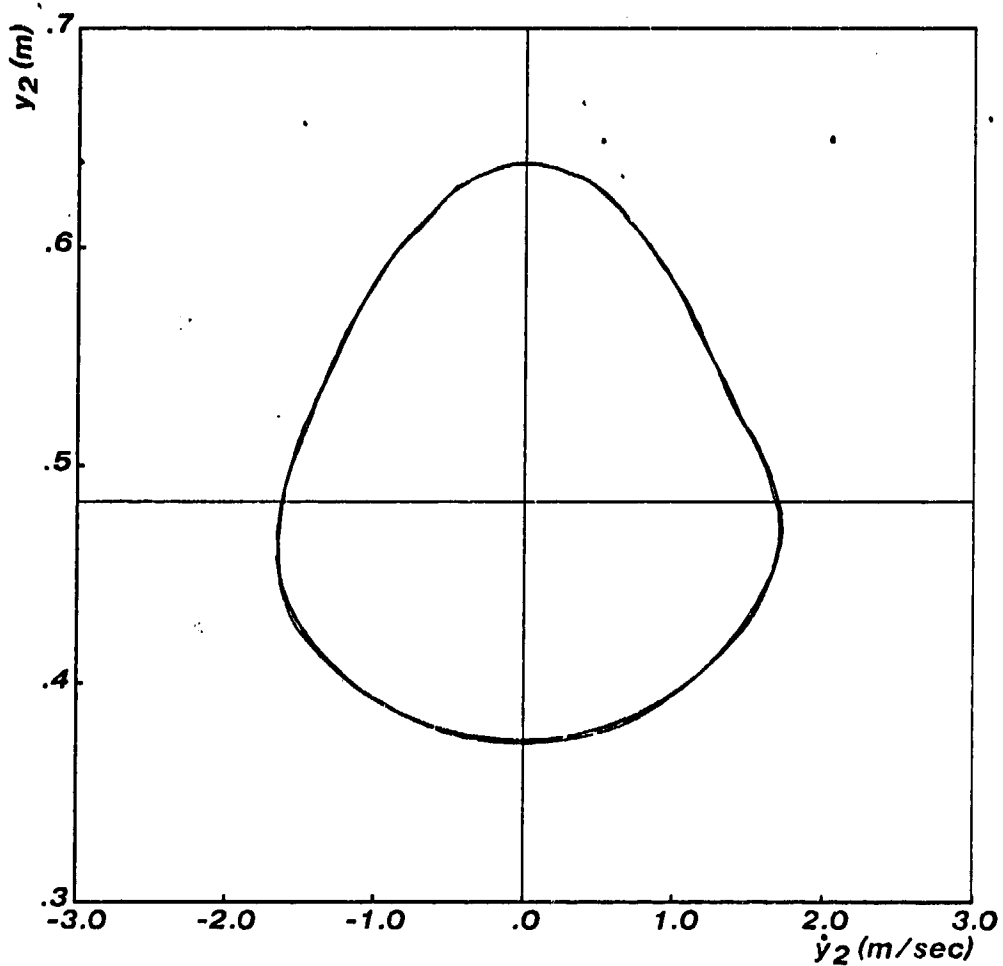


Figure 2-6: Four cycles like those shown in Fig. 2-5 replotted here in phase diagram form. The curves cross the axes at LIFT-OFF, TOP, TOUCH-DOWN, and BOTTOM. Note that position is plotted on ordinate, velocity on abscissa, and time progresses in counterclockwise direction. (a344.1)

### 2.5.2 Horizontal Travel

We examined the system's ability to regulate rate of translation during running by having the control computer specify a ramp in desired velocity while recording. The results are plotted in Fig. 2-7. These data show the machine, first hopping in place, then running at increasing rates up to about .9 m/sec. Throughout the run velocity was controlled to within about .25 m/sec of the desired value. This accuracy is typical. It was

possible to improve velocity regulation at lower rates by reducing the velocity error gain of (2.7), and at higher rates by increasing this gain. With a high velocity error gain, stable running at 1.2 m/sec (2.7 mph) was obtained for a few seconds at a time. Algorithms that use non-linear velocity error feedback provided promising results, but were not adequately developed to be included here.

During running, the leg and body counter-oscillate as shown in the plots of  $\theta_1$  and  $\theta_2$ . The back and forth motions of the leg were not explicitly programmed, but resulted from interactions between the velocity controller that operated during flight, and the attitude controller that operated during stance. Oscillations of the body are to be expected because angular momentum is conserved during flight, and attitude correction occurs only during stance.

The plot of  $\theta_2$  also shows that average body angle deviated from zero, the setpoint, in rough proportion to running speed. These deviations were very small, typically only a few degrees, even for rapid running. The average deviation of body inclination from the desired value could be further minimized by taking the expected body rotation into account when specifying the setpoint used by the attitude controller:

$$\theta'_{2,d} = \theta_{2,d} + \frac{I_1}{I_2} \text{Arcsin} \left( \frac{\dot{x} T_{ST}}{2w} \right) \quad (2.10)$$

where

$I_1, I_2$  are the moments of inertia of the leg and body respectively.

Hopping height and stride frequency were also affected by running speed, as indicated by the plot of body altitude,  $y_2$ . Actually, the relevant factor is not running speed directly, but the angle of the leg at touch-down. Faster running resulted in large deviations of the leg from vertical, and therefore, shallower hops. These shallower hops took less flight time resulting in more rapid stepping. At 0.9 m/sec peak foot clearance was reduced by 20%, and stride period was reduced by 8.6%. This result is reminiscent of data showing that kangaroos hopped at slightly higher frequency as their forward velocities increased [64].

A position controller was used to make the hopping machine translate from place to place. Position control was implemented with a controller that transformed position errors into desired velocities:

$$\dot{x}_{2,d} = K \min\{ (x_2 - x_{2,d}), \dot{x}_{2,max} \} \quad (2.11)$$

This algorithm prevented the machine from attempting very rapid translations when it was far from the target. Desired positions were sometimes specified with a joystick that was manipulated by the operator, and sometimes specified by the control computer according to a preplanned sequence. Data obtained while the device was position controlled is plotted in Fig. 2-8. A limit cycle of about  $\pm .1$  m is present whenever the machine is hopping in place.

Also shown in this Fig. 2-8 is the response to an external disturbance. After about 25 seconds the experimenter delivered a sharp horizontal jab to the body as the machine hopped in place. (See dotted vertical line in figure.) Balance was recovered and the machine returned to its commanded position after a few seconds. The control system tolerated fairly strong disturbances of this sort, provided the forces exerted on the body were primarily horizontal. Disturbances that introduced large rotations of the body often led to a crash.

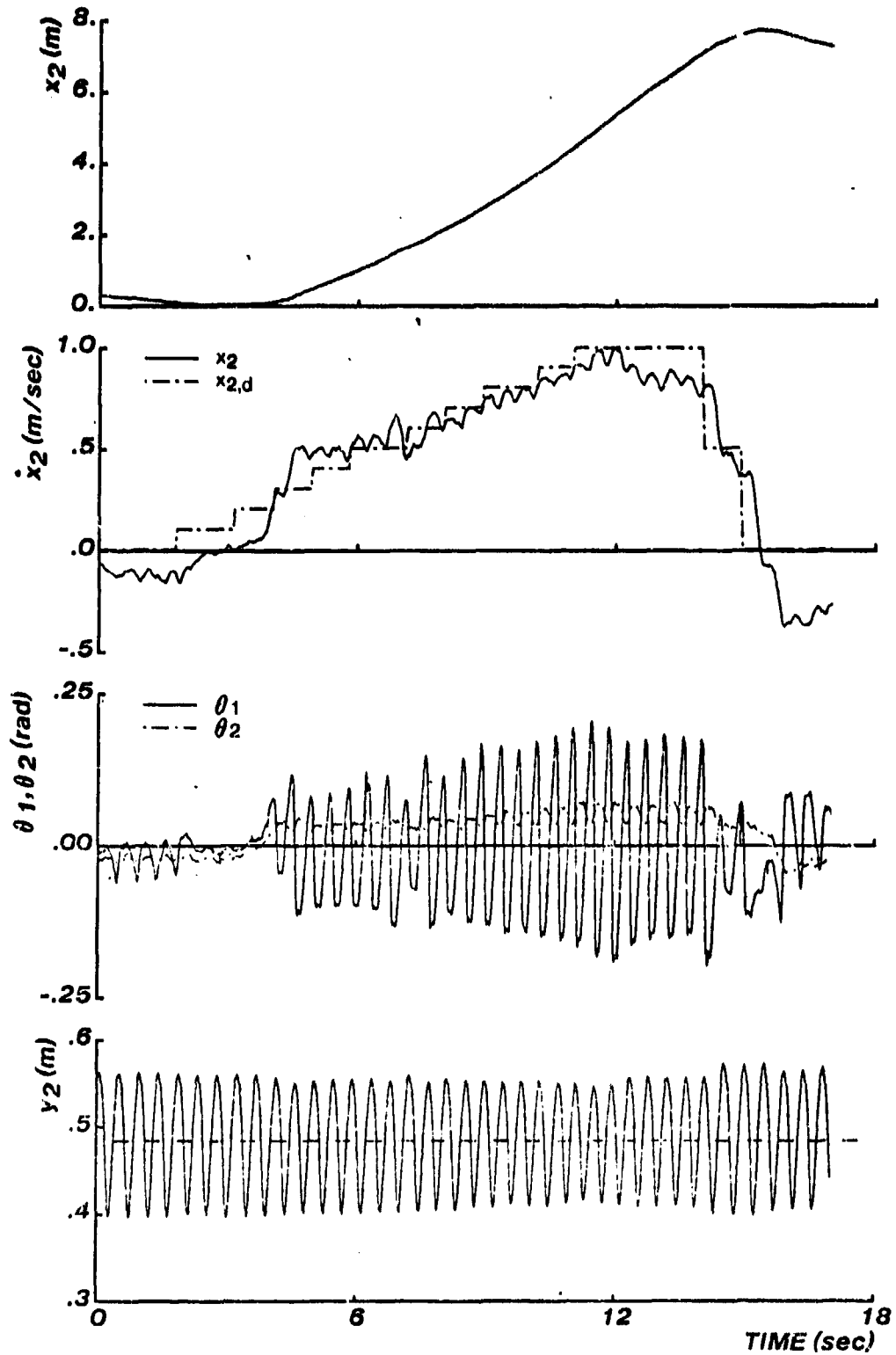


Figure 2-7: Rate control of the hopping machine was tested by varying  $\dot{x}_{2,d}$ , the rate set point (shown stippled), along a ramp from 0. to 1.0 m/sec in 10 sec. The maximum speed obtained in this trial over an entire stride was about .95 m/sec (2.1 mph). Dashed line on  $y_2$  curve separates stance, data below line, from flight. (a337.12)

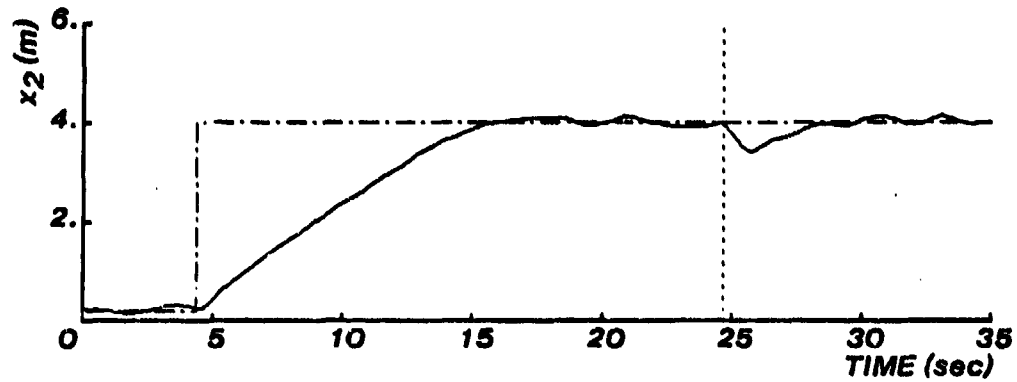


Figure 2-8: Position control was achieved by manipulating desired rate of translation, as described in text. After 4.3 seconds of stationary hopping the computer specified a 4 meter step change in desired position. (Vertical dotted line): Experimenter disturbed the machine by delivering a sharp horizontal jab with his hand. It returned to the setpoint within a few seconds. (a324.19)

### 2.5.3 Leaping

A specialized vertical control program was used to make the hopping machine leap while the standard velocity and attitude controls operated normally. During such experiments the machine approaches the obstacle with a moderate running rate. One step before the obstacle the operator presses the *leap* button, initiating a preplanned sequence synchronized to vertical hopping:

1. During the next stance phase, thrust is delayed so that the leg shortens more than normal under load of the body. This is done to prepare for a hop of maximum height. Thrust begins at bottom, not stopping until the leg has fully lengthened.
2. Once airborne, the leg shortens and its swinging motion is delayed; both provide extra clearance.
3. When top is reached hip angle is servoed to the correct landing angle as usual. There is less time to position the foot than normal, but the shorter leg is moved more quickly due to its reduced moment of inertia.
4. The leg is lengthened in preparation for landing.
5. Upon landing, the standard hopping sequence is re-established.

During the leaping sequence, velocity and attitude controls continued to operate in the usual manner.

This procedure was used to leap over a stack of styrofoam blocks, as shown in Fig. 2-9. While many successful leaps were obtained in this manner, equally many resulted in crashes. Clearing an obstacle requires that the foot be placed quite precisely before the leap, that the leap have sufficient altitude, and that the leap have sufficient span. The existing algorithm does a good job with height and span, but has no means for adjusting the take-off point.

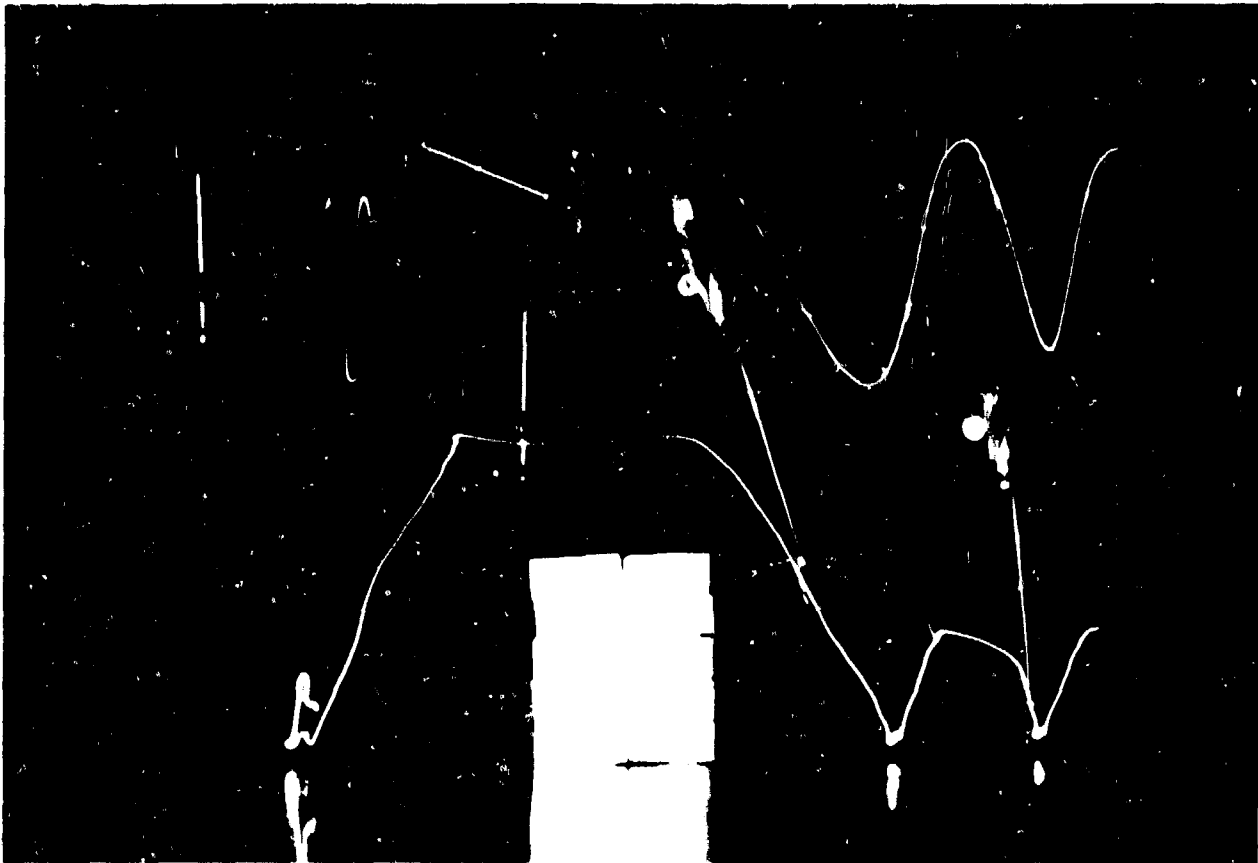


Figure 2-9: Hopping machine leaping over an obstacle. Machine approaches from right. The leaping sequence is described in text. Travel continues to the left after leap. Obstacle is .19 m tall and .15 m wide. The photograph was made with a low frequency strobe, while small light sources indicated paths of the foot and hip.

## 2.6 Discussion

While the primary purpose of using a one-legged apparatus for these experiments was to focus on balance, an additional goal was to develop a model that could explain the behavior of each leg in more complicated systems that run. If we ignore the third dimension, generalizing from the one-legged machine to the two-legged hopping kangaroo is very easy. A direct comparison can be made between the motions of the hopping machine's one leg and the motions of the kangaroo's pair of legs. The primary difference is that the kangaroo uses its tail to help compensate for the large sweeping motions of the legs, so that the body need not react by pitching so much on each hop. The control system can still regulate hopping height, body attitude, and velocity as before.

Many characteristics of the running biped are also similar to the running one-legged machine, including the alternation between stance and flight, the regular vertical oscillations, and the periods of support by only one leg. In the case of the biped, the two legs always swing in opposite directions, making rotations of the body or a tail unnecessary. Think of a biped as a hopping machine that substitutes a different leg on each stride. The three part decomposition can be employed as before. The three part control system can also be used to understand how a quadruped runs. This is described elsewhere by Raibert and Sutherland [290].

The specific algorithms described here might be useful in discovering the locomotion mechanisms used by biological systems. While the parallels between behavior of the one-legged hopping machine and various biological systems are provocative, the mechanisms responsible for control in biological systems are still not known. The algorithms described in this report allow specific predictions that could be explored experimentally. The most clear cut predictions are that hip torque during stance is uniquely used to adjust body attitude, and that speed is controlled through placement of the feet. The following experiments might elucidate these questions:

- Examine kinematic data to determine if human runners position their feet according to (2.7).
- Suppose a human running at constant speed were externally accelerated forward during flight, or made to think he was accelerated forward. Would the angle of the leg with respect to the vertical at touch-down change according to the algorithm given above?
- Suppose a human running at constant speed were externally rotated forward during flight, with no linear acceleration of the CG. Would leg angle change in that case?
- If the body of a running human were linearly accelerated during stance without disturbing body attitude, would there be a correction before the next step?

We do not know if it is technically feasible to do such experiments, but the results could provide important clues to the mechanisms responsible for balance in existing legged systems.

## 2.7 Conclusions

This chapter describes an experimental hopping machine and a set of experiments designed to elucidate the basic problems of dynamic stability and balance in legged systems that hop and run. The present work was done in order to verify the correctness of principles originally developed in simulation, and to get practical experience that might some day be valuable in designing a practical vehicle.

It was found that control of the one-legged hopping machine can be decomposed into three separate parts that are synchronized by the behavior of the machine. One part controls hopping height by choosing a fixed amount of energy to inject on each hopping cycle. A second control part regulates the forward travel of the system by placing the foot a specific distance in front of the hip as the device approaches the ground on each step. The third controller corrects the attitude of the body by applying appropriate torques to the hip during

stance when vertical loading permits horizontal forces to be generated at the foot. A finite state sequencer provides the glue that synchronizes the actions of the three controllers to the ongoing behavior of the device.

Experiments showed that the relatively simple control algorithms obtained good control of the machine. They maintained consistent hopping heights, reaching equilibrium after a change within a few hopping cycles. The device ran at speeds of up to 1.2 m/sec. At low velocity, speed regulation was rather poor, but improved when traveling at higher rates. The machine traveled from place to place using position control. A modification to the vertical control algorithm enabled the machine to leap over small obstacles.

## 2.8 Appendix I. Physical Parameters of One-Legged Hopping Machine

Leg mass - 1.31 kg

Leg moment of inertia - .036 kg-m<sup>2</sup>

Body mass - 7.18 kg

Body moment of inertia - .52 kg-m<sup>2</sup>

$K = .035 \text{ m}/(\text{m}/\text{sec})$

$K_{P,ST} = 153. \text{ Nt}\cdot\text{m}/\text{rad}$

$K_{V,ST} = 14. \text{ Nt}\cdot\text{m}/(\text{rad}/\text{sec})$

$K_{P,FL} = 47. \text{ Nt}\cdot\text{m}/\text{rad}$

$K_{V,FL} = 1.26 \text{ Nt}\cdot\text{m}/(\text{rad}/\text{sec})$

## 3. 3D Balance Using 2D Algorithms

### 3.1 Abstract

This chapter explores the notion that the motion of dynamically stable 3D legged systems can be decomposed into a planar part that accounts for large leg and body motions that provide locomotion, and an extra-planar part that accounts for subtle corrective motions that maintain planarity. The large planar motions raise and lower the legs to achieve stepping, and they propel the system forward. The extra-planar motions ensure that the legged system remains in the plane. A solution of this form is simple because 3D dynamics do not play an important role.

We develop a model of a 3D one legged hopping machine that incorporates a springy leg of non-zero mass and a two axis hip. The hopping machine is modeled as an open loop linkage that has different configurations in flight and in stance. Behavior at transitions between phases is calculated by invoking conservation of momentum. We have decomposed control of the model into four parts that control hopping height, forward velocity, body attitude, and spin. Hopping height is controlled by regulation of vertical energy. Velocity is controlled by placing the foot fore or aft during flight. Body attitude is controlled by torquing the hip during stance. Spin is controlled by placing the foot outside the plane of motion. Simulation data are presented which show that these control algorithms result in good control of velocity, body attitude and spin, while moving on a straight desired path.

### 3.2 Introduction

The locomotion of legged systems is a form of motion that has gained the attention of biologists seeking to understand the behavior they observe in natural organisms, and of engineers who attempt to build useful legged vehicles. Animators and film makers have also shown interest, but mostly in simulating the appearance of systems that use legs to locomote. Our interest is not so much in the appearance or description of locomotion, as it is in the underlying mechanisms that are responsible for production and control of such motion. In particular we have focused on the problem of controlling the motion of systems that balance as they run.

Dynamic stability is a key ingredient in the mobility exhibited by legged systems. Systems that balance can move on a narrow base of support, permitting travel where obstacles are closely spaced or where the support path is narrow. A dynamically stabilized system need not be supported at all times and may therefore use support points that are widely separated or erratically placed. These characteristics relax the constraints on the type of terrain a legged system can negotiate.

Casual observation of a running animal, say a cat, a horse, or a kangaroo, might lead one to conclude that running in a straight line is a 2D activity. The legs swing fore and aft through large angles while the body

bobs up and down. The body may also undergo pitching motions that are quite pronounced. These large motions of the legs and body propel the animal upward so that the feet may be picked up and placed on a new spot, they allow the animal to balance itself so that it does not tip either forward or backward, and they propel the animal forward so that transportation takes place. However, these large planar motions do not tell the whole story. Natural legged locomotion takes place in a 3-space where motion with six degrees of freedom is possible.

To study dynamically stable locomotion in 3D we have modeled a system with just one leg and a very small foot. This simple one-legged model allows us to address the dynamic stability problem squarely, while totally ignoring the coupling problem that complicates the analysis of systems with many legs. Our goal is to test the idea that control for legged systems running in 3-space need not explicitly deal with the complications of 3D dynamics. Rather it may be feasible to decompose the problem into a planar part that controls locomotion using the large motions described above, and an extra-planar part that uses only very subtle motions to restrict behavior to the plane. Decomposition results in a very simple solution that seems to be in concert with what we observe in natural systems.

### 3.2.1 Background

Previous studies of balance in 3D legged systems have been carried out by a number of workers, most notably in Europe and Japan. Vukobratovic and his co-workers [164, 338, 342] have developed the notion of *zero moment point, ZMP*, control. They have shown in simulation how a 3D multi-linked walking biped can be balanced by manipulating the relationship between the projection of the center of gravity and the support areas provided by the feet. Kato et. al. [169] have studied quasi-dynamic walking in the biped. In their studies a physical biped with 10 hydraulically driven degrees of freedom used a preplanned sequence of quasi-static motions to dynamically transfer support from one large foot to the other. Miura and his students [230] have built a number of small electrically powered walking bipeds that balance using tabular control schemes. Their most advanced model demonstrates dynamic balance without large feet. It has three actuated degrees of freedom that permit each leg to move fore and aft, to move sideways, and to lift slightly off the floor. This machine balances with a shuffling gait that reminds one of Charlie Chaplin's stiff-kneed walk.

Hopping has also been studied. Fifteen years ago Seifert [302] explored the idea of using a large pogo stick for transportation on the moon, where low gravity would permit very long hops. Matsuoka [196] analyzed 2D hopping in humans with a one-legged model, assuming that the leg could be massless, and that the stance period could be of very short duration. He derived a time-optimal state feedback controller that stabilized his system. Matsuoka [197] also implemented a very simple one-legged hopping machine that lay on a table inclined  $10^\circ$  from the horizontal.

Summarizing work that appears elsewhere in this report, we have found that for the a 2D one-legged machine, the control of locomotion could be subdivided into three largely independent parts: regulation of hopping height, control of forward velocity, and control of attitude.

- **Height:** The control system regulated hopping height by manipulating hopping energy. The machine had a springy leg, so hopping was a bouncing motion that was generated by an actuator that excited the leg spring. Hopping energy was conserved by the leg spring from hop to hop. The height to which the machine hopped was determined by the energy recovered from the previous hop, and by the losses in the hopping cycle. Since all energy in the system is converted to potential energy by the peak of a hop, hopping height could be regulated by injecting an appropriate amount of energy during each step.
- **Velocity:** The control system manipulated forward velocity by moving the leg during the flight part of each hop to properly position the foot with respect to the *CG-print*. The *CG-print* is the locus of points on the ground over which the center of gravity of the system will pass during the next stance period. If the foot is placed in the center of the *CG-print*, the device will tip neither forward nor backward, but will continue its forward motion at about the same rate as before. If the foot is placed rearward of the center of *CG-print*, then the device will tip forward, increasing its forward velocity. If the foot is placed forward of the center *CG-print*, then the device will tip backward, decreasing its velocity. The control system calculated the length of the *CG-print* from the measured forward velocity of the device and the estimated duration of stance. The control system then used the error in forward velocity to position the foot to control and correct the forward speed of locomotion.
- **Attitude:** The control system maintained an erect body posture during running, by generating hip torques during stance that servoed the body angle. During stance, friction between the foot and ground permitted large torques to be applied to the body without causing large accelerations of the leg. These torques were used to implement a simple proportional servo that returned the body to an erect posture once each step.

In this chapter we extend this approach to 3D locomotion for the case of straight line running. To do so we have modeled and simulated a 3D one-legged hopping machine that moves freely on an open floor. Hopping height is controlled as before in the 2D case. In order to extend the 2D control system to 3D, we must modify it to handle three new degrees of freedom: lateral translation, roll orientation, and yaw orientation.

### 3.3 Modeling and Simulation

The model, shown in Fig. 3-1, has two primary parts: a body and a leg. The body is represented by a rigid mass with substantial moment of inertia about its three primary axes. (See Appendix II for simulation parameters.) The leg is a long slender linkage that is springy in its axial dimension, with a small foot at one end. The leg is connected to the body by a universal hip joint that provides two degrees of freedom.

All three joints in the machine are actuated. The hip is driven by a pair of torque actuators that can be used to orient the leg with respect to the body, or to change the attitude of the body when the foot is in contact with the ground. The leg is driven by a third actuator that operates in series with a passive spring. Changes in the length of this actuator are used to excite the leg spring and to make the machine hop.

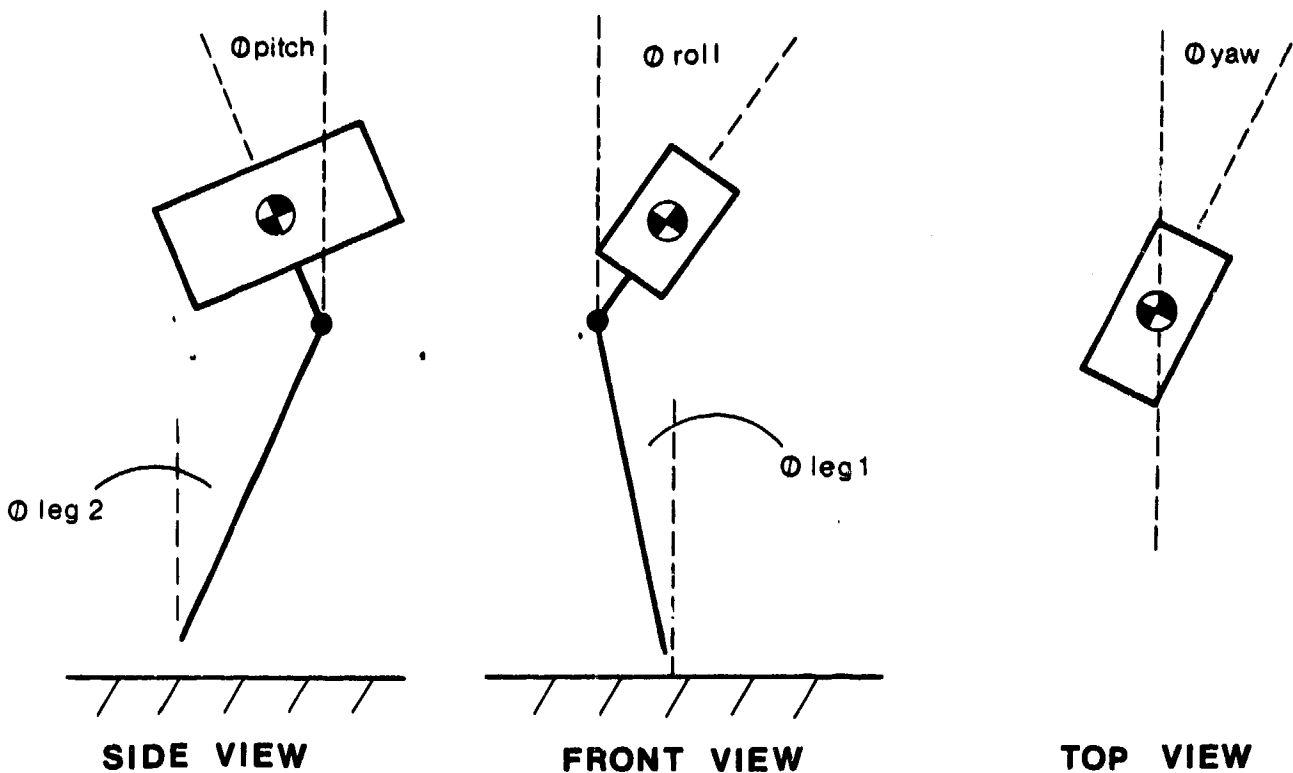


Figure 3-1: The 3D one-legged system modeled in this report. It has a body and a leg, connected by a hip. The body is a rigid structure with mass and moment of inertia. The leg has mass and moment of inertia, and an actuated spring along its long axis. The body and leg are connected by a hip with two orthogonal axes of rotation, both driven by a torque source. Model parameters are given in Appendix II

In addition to the model's three actuated joints, called *internal* degrees of freedom, the model has *external* degrees of freedom that permit it to move with respect to its surroundings. During stance, when the foot touches the ground, there are three external degrees of freedom that give the model's orientation in space. During flight when the foot leaves the ground, there are three additional external degrees of freedom, a total of six, that specify Cartesian position in space. Unlike the three internal joints that are driven directly by actuators, and therefore easily controlled, the external degrees of freedom are indirectly driven by dynamic interactions among the model, gravity, and the ground. At the heart of the legged locomotion problem lies the need to find ways to use direct control of internal degrees of freedom to achieve indirect control of external degrees of freedom.

Basic operation of the model is to bounce on the springy leg in a hopping motion that alternates between periods of support and periods of flight. Four events characterize this alternating cycle: *lift-off* - the moment in the hopping cycle when the foot loses contact with the ground, *top* - the moment the body achieves peak altitude, *touch-down* - the moment the foot first touches the ground, and *bottom* - the moment the body has minimum altitude and the leg is fully compressed. These four events help to synchronize control to the behavior of the model.

### 3.3.1 Equations of motion

The 3D hopper is modeled as an open loop dynamic linkage. This allows simulation using existing computer programs originally intended for robot arms [346]. In order to model the hopper as an open loop linkage the external degrees of freedom were modeled as joints with zero mass and zero moment of inertia. The kinematics of these joints are described in the Appendix II.

The state of the model is described by  $Q$  and  $Q'$ , where  $Q$  is the position vector describing the position of each of the links and  $Q'$  is the velocity vector describing the velocity of each of the links. To obtain the equations of motion we must find the acceleration vector  $Q''$  given the state of the model and the forces acting at each joint:

$$Q'' = f(Q, Q', \tau, g) \quad (3.1)$$

where

- $\tau$  is the vector of torques that acts on the internal joints of the mechanism, and
- $g$  is the gravitational vector.

The derivation and of the equations of motion were described by Luh, Walker, and Paul [192], and efficient methods for solving them numerically were given by Walker and Orin [346]. We used Walker and Orin's 3rd method to determine  $Q''$ .

The analysis is divided into a set of equations that describes the system when it is on the ground, and another set that describes the system when it is in flight. It is also necessary to determine what happens at transitions between these two phases. During stance the machine is an inverted pendulum that can tip in two directions, in addition to rotating about its own axis. Ground forces resulting from impact, internal forces and torques, and gravity affect the angular and linear momentum of the hopper during stance. In flight overall motion of the system is ballistic, affected only by gravitational forces. The horizontal component of the linear momentum and the angular momentum about the center of gravity remain unaltered during flight. Solution of (3.1) gives the trajectory of the system as a function of time, during either stance or flight.

At the transition between stance and flight, lift-off, and between flight and stance, touch-down, the simulation has discontinuities. At these transitions the laws of conservation of momentum are invoked in order to determine changes in state. If we assume the ground to be rigid with no compliance, then at touch-down an impulse force of duration  $\epsilon$  acts on the foot. As a result the velocities  $Q'$  are changed while the position  $Q$  remains unaltered. Simulation of the hopper in the ground phase requires calculation of the change in  $Q'$ . The following assumptions are made about the nature of the impact.

- An impulse of magnitude  $\delta = \int_{t-\epsilon/2}^{t+\epsilon/2} F dt$  acts on the foot at the time of impact. No torques act on the foot.
- The force  $F$  is very large compared to other forces acting on the system, such as gravity and internal forces and torques.

- The duration of transition between phases,  $\epsilon$ , is very small.

Using generalized coordinates,  $\tau$  is a vector of forces and torques that acts on the joints. Since angular momentum is conserved about the z-axis of a rotary joint during impact and linear momentum is conserved along the z-axis of a translational joint:

$$\int_{t-\epsilon/2}^{t+\epsilon/2} \tau dt = \tau \epsilon = J \Delta Q \quad (3.2)$$

By applying conservation of momentum about the z-axis of the three external rotational joints and the three internal joints we get six simultaneous equations:

$$\sum_{j=i}^9 a_{ij} Q_j' = L_i \text{ for } i = 4 \text{ through } 9 \quad (3.3)$$

where

$Q_j'$  is the velocity at joint j.

$a_{ij}$  is a linear constant that depends on  $Q_i$  to  $Q_9$ .

If joint i is rotational then  $L_i$  is the total angular momentum of links i through 9, about the axis of joint i, prior to touchdown. If joint i is translational then  $L_i$  is the total linear momentum of links i through 9 prior to touchdown.

Once the state is known at  $t-\epsilon/2$ , (3.3) can be solved for the velocity vector after touch-down. The state at  $t+\epsilon/2$  can then be computed without knowing the impulse forces acting on the foot.

At lift-off the leg and body assume the same velocity, which is the velocity of the center of gravity. An inelastic collision between body and leg is assumed. The effect of this impact is calculated in a similar fashion. Conserving momentum about the remaining eight joints provides the velocity vector at lift-off. This procedure permits modeling of the transitions from flight to stance and from stance to flight with very little computation.

### 3.4 Control

The strategy employed here to control locomotion of the 3D model is to decompose its motion into a planar part and an extra-planar part. There is a plane that contains the gravity vector, the center of gravity, and the forward velocity vector. We call this the *plane of motion*. We call the line where this plane intersects the ground the line of motion. If the control system were always to place the foot on the line of motion, then all forces acting on the model would lie in the plane of motion. In that case the machine would never leave the plane of motion and the planar control system mentioned earlier would be adequate to regulate hopping, attitude, and forward travel.

The extra-planar control part corrects three types of errors introduced by external disturbances and noisy control. These errors are roll rotation, yaw rotation, and lateral translation. Corrections for roll error are made by the attitude control algorithm, much as pitch corrections are made. Yaw errors are corrected by placing the foot outside the plane of motion, and applying suitable hip torque during stance. Lateral translations are not actually corrected in the present scheme, but they are taken into account when the plane of motion is redefined on each step. The planar control part operates properly in 3D only when the extra-planar part successfully limits each of these error motions to small magnitude.

By augmenting the planar 3-part controller with additional extra-planar controls, we arrive at a 3D control system with 4 separate control algorithms. They control hopping height, forward velocity, body attitude, and spin.

### 3.4.1 Height control

Control of hopping height for the 2D case has been explored elsewhere in simulation and physical experiments [284, 286, 287]. Simple control of hopping height is a 1D problem that is substantially the same for locomotion in 2 and 3D. Therefore we have simplified the present model.

The simulation of the hopper does not incorporate the various losses that occur due to friction in the actual machine. The only losses that occur are due to impact at touch-down and lift-off. Therefore, very little has to be done to maintain correct hopping height once it is attained.

### 3.4.2 Velocity control

The primary mechanism used for controlling the velocity of the hopper is proper placement of the foot at touch-down. During flight the control system orients the leg so as to position the foot with respect to the center of the CG-print. The algorithm is described below.

At touch-down:

$$L_0 = m r \times v + L_{cg} = m v r \sin(\theta_0 - \theta_1) + L_{cg} \quad (3.4)$$

where

- $L_0$  is the angular momentum of the model about the point of touch-down,
- $L_{cg}$  is the angular momentum of the model about its own center of gravity,
- $r$  is the vector from the point of touch-down to the center of gravity of the model,
- $v$  is the velocity of the center of gravity,
- $m$  is the combined mass of the body and leg,
- $\theta_0$  is the angle formed by the gravity vector and  $v$ , and
- $\theta_1$  is the angle formed by the gravity vector and  $r$ .

See Fig. 3-2.

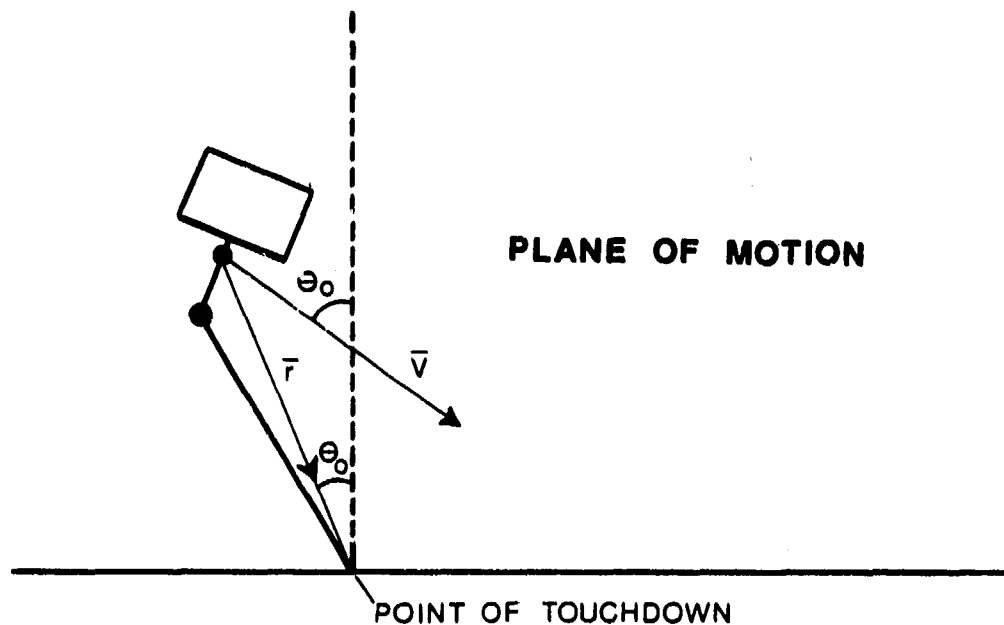


Figure 3-2: Configuration of model in plane of motion.

We make the assumption that  $r$ ,  $v$ , and the gravity vector lie in the same plane. The first term in (3.4) is dependent on the placement of the foot. It determines whether the system tips forward or backward after touch-down. During the normal hopping cycle, the horizontal velocity at touch-down is large and the angular momentum about the center of gravity is small. The major component of the angular momentum is the first term.

During stance the change in angular momentum is:

$$\Delta L = \int_{\text{touch-down}}^{\text{lift-off}} r \times mg \, dt = \int_{\text{touch-down}}^{\text{lift-off}} m g r \sin(\theta) dt = \int_{\text{touch-down}}^{\text{lift-off}} m g r \sin(\theta) d\theta / \theta' \quad (3.5)$$

where  $g$  is the gravitational acceleration vector.

The change  $\Delta L$  is a nonlinear function of  $\theta_0$ ,  $\theta_1$ ,  $v$ ,  $r(t)$  and  $\theta(t)$ . Its exact evaluation would require solution of the equations of motion for the stance phase. We have no closed form solution. Data generated by a systematic set of simulations for a large range of initial conditions are shown in Fig. 3-3. They show that the relationships between lift-off velocity, on the one hand, and touch-down velocity, vertical velocity, and leg angle, on the other hand, are all nearly linear over a wide range of values. We have used the linear approximation for control with good success.

Figure 3-4 shows the trajectory of the center of gravity as a function of time when this control is used. A constant desired velocity was specified until the model had translated 2 m, at which point the desired velocity

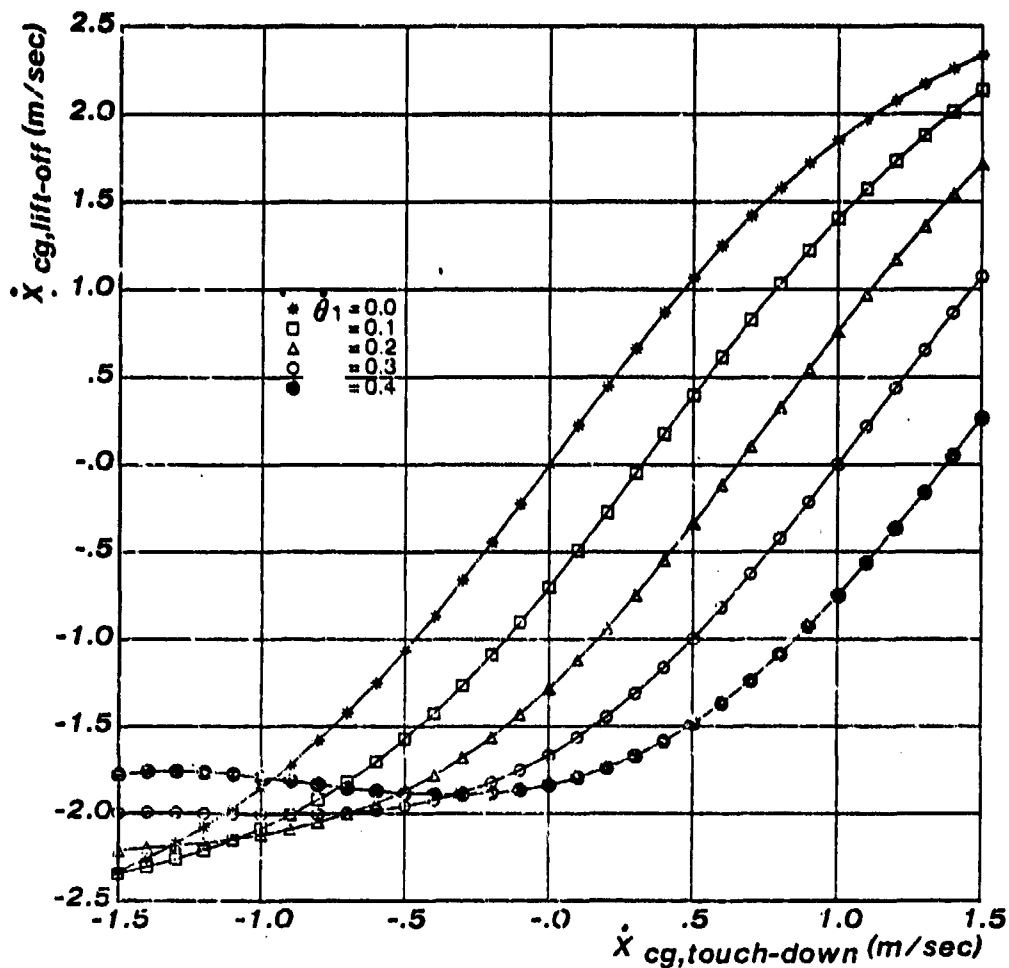


Figure 3-3: The effect of foot placement on forward velocity was determined empirically by simulating stance for a set of initial conditions and foot placements. Once forward velocity is known, it is possible to use these data to select a foot placement that will change the forward velocity to a desired value. The data in this figure are for  $\dot{z}_{cg,touch-down} = 1$  m/sec.

was brought to zero. Average velocity was controlled with good precision. The temporary deviations from the average velocity visible in the plot were caused by the attitude control servo, which begins to erect the body right after touch-down.

### 3.4.3 Attitude control

During stance it is possible to take advantage of friction between the foot and the ground to generate hip torques that will erect the body. The attitude controller must correct errors in both pitch and roll. Roll errors will generally be small while pitch errors are large. Pitch errors are caused by the reaction of the body to the swinging motion of the leg made when the foot is swung forward in preparation for the next step. Roll errors are caused by disturbances.

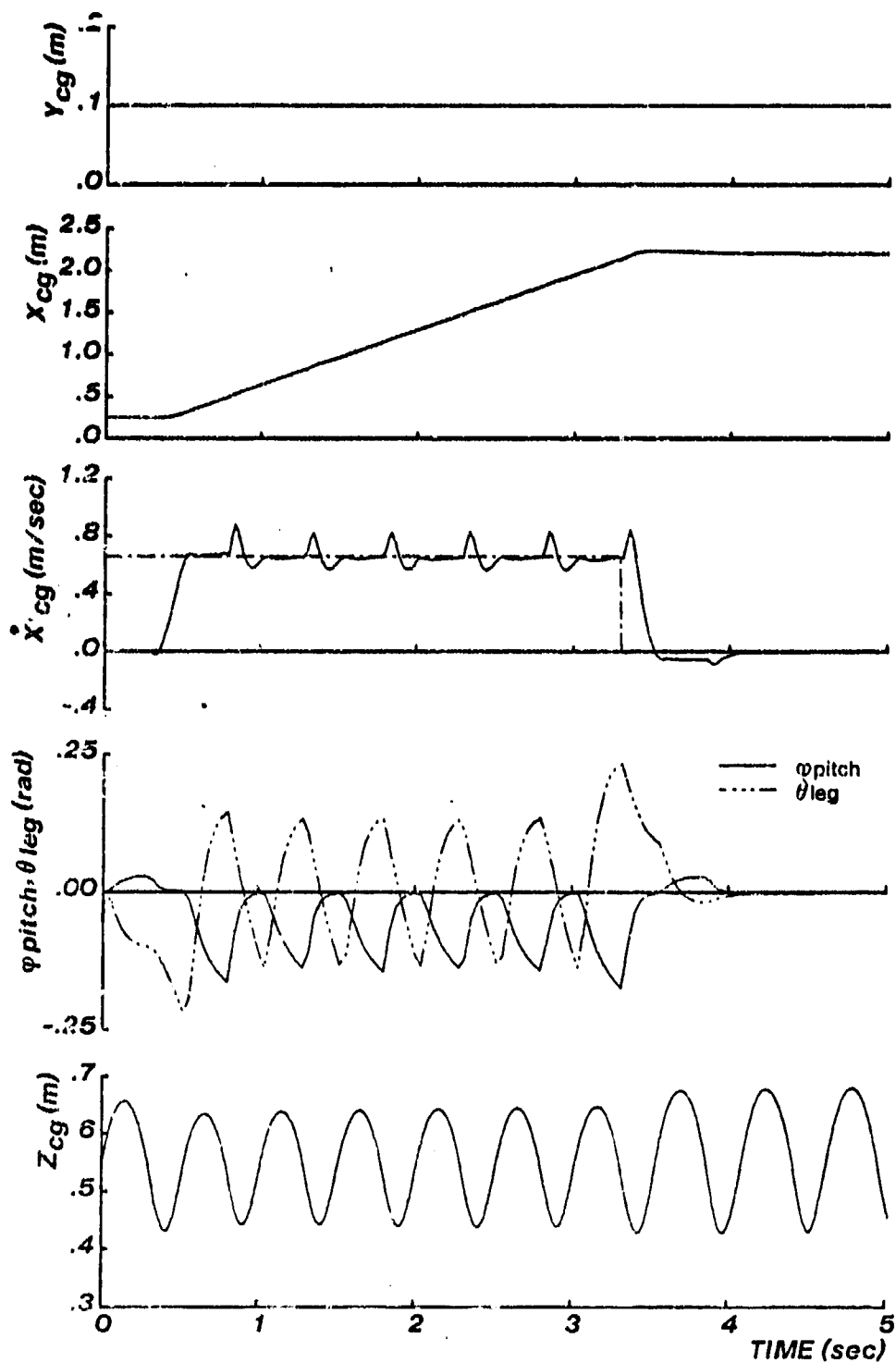


Figure 3-4: The 3D one-legged machine traveling in a straight line for 2 m. Plots show simulation data of trajectory of the center of gravity of the model, velocity of the center of gravity in the plane of motion, body and leg angle in the plane of motion, and the vertical position of the center of gravity.

The attitude controller is a linear PID servo that is neither too stiff nor too soft. It must be stiff enough to have settled by the end of stance. If this is not so the servo will disturb the body's attitude at lift-off, rather than correct it. The servo must not be so stiff that it causes the foot to slip when it generates hip torques. The weight of the system and the coefficient of friction of the foot are the limiting factors. Independent servo controllers are used about both the pitch and roll axes, each with  $\zeta = .707$ .

$$\tau_{pitch} = -k_p(\varphi_{pitch} - \varphi_{pitch,d}) - k_d\dot{\varphi}_{pitch} \quad (3.6)$$

$$\tau_{roll} = -k_p(\varphi_{roll} - \varphi_{roll,d}) - k_d\dot{\varphi}_{roll} \quad (3.7)$$

where

$\tau_{pitch}, \tau_{roll}$	are the torques applied at the pitch and roll axes,
$\varphi_{pitch}, \varphi_{roll}$	are the pitch and roll angles of the body,
$\varphi_{pitch,d}, \varphi_{roll,d}$	are the desired pitch and roll angles of the body at lift-off, and
$k_p, k_d$	are the proportional and derivative feedback gains.

The fourth curve in Fig. 3-4 is a plot of body pitch angle and the leg angle as a function of time during constant velocity running. The body tilts forward in the flight phase as the leg swings forward. At touch-down the body angle reaches a maximum. During stance the controller forces the body angle toward zero. Roll motions are similarly corrected.

#### 3.4.4 Spin control

The control system suppresses spin by placing the foot outside of the plane of motion. Fore and aft forces on the foot, generated both by the foot's impact during touch-down and by hip torque during stance, produce a torque about the yaw axis when the foot is placed outside of the plane of motion. Let the distance of the foot from the plane of motion be  $d_{\perp}$ . On touch-down an impact torque causes a change in spin momentum:

$$\Delta L_{yaw} = d_{\perp} m v_{horz} \quad (3.8)$$

where  $L_{yaw}$  is the angular momentum about the yaw axis.

In this equation  $m v_{horz}$  is the linear momentum of the hepper in the direction of the line of motion, and  $d_{\perp}$  is the horizontal distance between the center of gravity and the point of touch-down in a direction perpendicular to the plane of motion.

When a hip torque is applied to the body about the axis perpendicular to the plane of motion, it causes a ground reaction force at the base of the foot in the direction of the line of motion.

$$F_{horz} = \tau_{hip} \times r \cos\theta \quad (3.9)$$

where  $\theta$  is the angle between  $r$  and  $g$ .

This force causes a torque to act about a vertical axis through the center of gravity. The total change in the spin angular momentum during stance is:

$$\Delta L_{yaw} = \int_{\text{touch-down}}^{\text{lift-off}} F_{\text{horz}} d_{\perp} dt \quad (3.10)$$

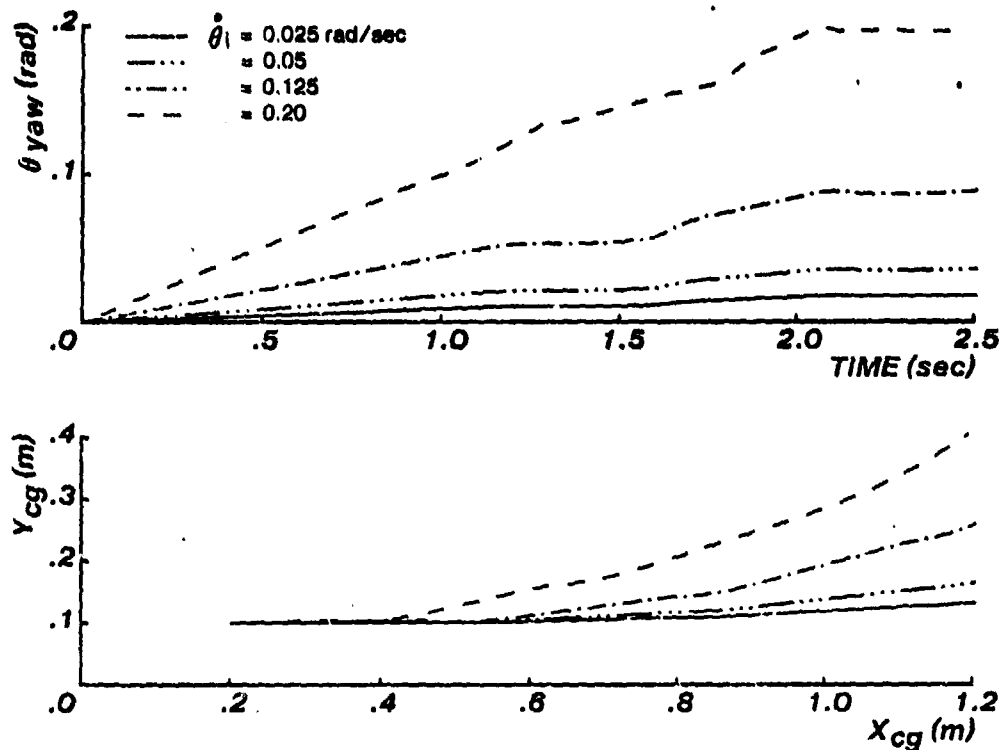
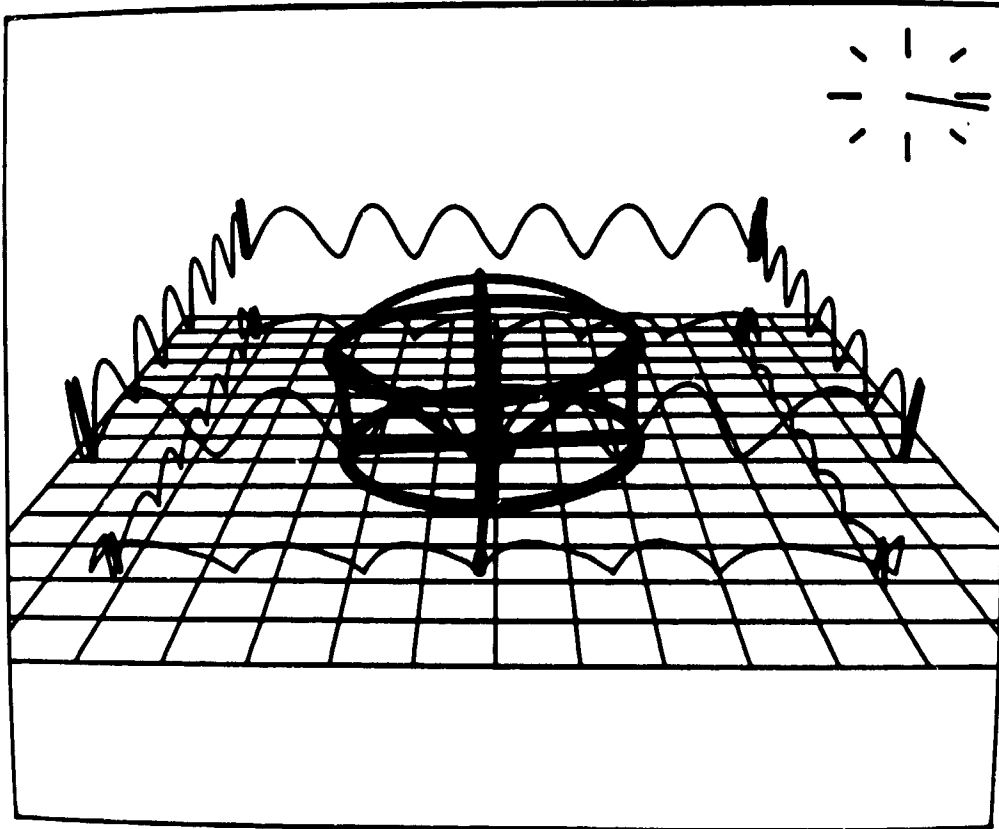


Figure 3-5: Spin control. Top: Angular position about the yaw axis is plotted as a function of time for various initial spin rates. The spin velocity is suppressed in a short time for initial spin rates of up to .2 rad/sec. Bottom: Path followed by center of gravity while spin is suppressed. Spin suppression places the foot outside the plane of motion, with the side-effect of altering the direction of travel.

Figure 3-5 (top) plots spin about the yaw axis as a function of time for four different initial spin rates. For initial rates of .2 rad/sec or less, spin is quickly controlled. The present technique does not work when the spin rate exceeds 0.2 rad/sec. For instance, at an initial spin rate of .25 rad/sec oscillations in the spin occur that cause the body to go unstable. Figure 3-5 (bottom) shows the path followed by the hopper during the spin suppression maneuver. Placement of the foot outside the plane of motion to correct spin, has the side-effect of changing the direction of travel.

The various controllers may require conflicting actions to achieve their goals. There are two cases where this is apparent. First, spin control may require the foot to be placed at a large distance from the plane of motion. However if  $d_{\perp}$  is large the trajectory in the plane of motion is affected. Care should be taken to see that

$\sin^{-1}(d_{\perp}/|r|) \ll \theta_1$ . Second, spin control may require certain body torques to be applied according to (3.10). However correction of body pitch errors may require that other torques be applied. Priority is given to control of spin. Correction of the body angle can be deferred to a later time.



**Figure 3-6:** Path control. The 3D model was made to follow a square path. It started at (1,-1), lower right, and progressed clockwise through (-1,-1), (-1,1), and (1,1), finally returning to the starting point. (Grid spacing is 0.2 m. Center is (0,0).) The upper trace marks the path of the center of gravity. The lower trace marks the path of the foot. Total time around the square was 24 sec.

### 3.4.5 Path control

The control algorithms just described can be used to get a simple form of path control. If a desired path is decomposed into a set of straight line segments, then the path can be followed by stopping the machine at each vertex and changing its direction of travel. The plane of motion is not uniquely defined when there is no forward travel, so the control system is free to choose the plane that includes the next straight path segment. Figure 3-6 shows a cartoon of the one-legged machine, and the trajectory it took in traversing a square path. The settling time at each vertex made progress quite slow, about 24 sec for the circuit, but the accuracy of the path was reasonably good.

Even for the simple case of a one-legged system, the algorithms presented here are not yet complete solutions to the 3D locomotion control problem. First, we do not yet know how to change heading while running. In order to change the direction of travel, the existing control system brings the machine to a halt, selects a new direction, and then accelerates. It would be very tedious to follow a winding contour using this approach. Second, choosing the plane of motion to incorporate lateral velocity errors permits the system to balance using the planar algorithms, but errors in heading cannot be corrected once travel starts. Yaw, roll, and lateral velocity errors will all contribute to heading drift. Third, these algorithms depend on a system that can travel equally well in all directions. Although it is possible to change heading, the algorithms provide no way to change the machine's facing direction.

Another consideration is that these algorithms have only been tested in simulation. We are in the process of testing them on a physical 3D one-legged system.

### 3.5 Conclusion

Legged locomotion is a largely planar activity that takes place in 3D space. We argue that such behavior can be accomplished by providing one set of control algorithms that balance and generate travel within a plane, and a second set of control algorithms that eliminate motions that deviate from that plane. Control within the plane of motion can be further decomposed. The entire system consists of four control algorithms:

- Height: The springy leg is driven to cause hopping oscillations of the machine. Hopping height is regulated by using a measurement of the system's vertical energy to determine the correct amount of thrust.
- Forward velocity: The CG-print is the locus of points over which the machine's center of gravity will travel during the next stance period. The control system regulates forward velocity by manipulating placement of the foot relative to the center of the CG-print.
- Attitude: During stance when friction holds the foot in place, hip torque is used to erect the body. Pitch and roll angles are both corrected with a linear PD servo.
- Spin: The foot is placed outside of the plane of motion and a torque is generated at the hip. This produces a torque about the yaw axis that retards spin motion.

Simulation data showing effective forward velocity control, spin suppression, and straight segment path control encourage us to further test the feasibility of these ideas with a set of physical experiments.

### 3.6 Appendix II. Description of 3D Model

#### Dimensions of 3D one-legged model:

Link	leg	cylinder	ring	body	Units
Description	Cylinder	Cylinder	Ring	Ring	
Mass	.8626	0.5902	0.1	14.755	Kg
Length	0.8	0.15	0.01		Meters
Radius	0.01	0.02	0.03	0.3	Meters
Moments of Inertia:					
$J_{xx}$	0.0474	0.00674	0.00009	1.152	$\text{Kg}\cdot\text{m}^2$
$J_{yy}$	0.0474	0.0004	0.000046	0.807	$\text{Kg}\cdot\text{m}^2$
$J_{zz}$	0.0001	0.00674	0.000046	0.115	$\text{Kg}\cdot\text{m}^2$
$J_{xy}$	0	0	0	0	$\text{Kg}\cdot\text{m}^2$
$J_{yz}$	0	0	0	0	$\text{Kg}\cdot\text{m}^2$
$J_{xz}$	0	0	0	0	$\text{Kg}\cdot\text{m}^2$

#### Denavit-Hartenberg description of the model:

Joint #	$\theta$	d	a	$\alpha$	Description
1	$\pi/2$	$Q_1$	0	$\pi/2$	External degree of freedom. X displacement of foot.
2	$\pi/2$	$Q_2$	0	$\pi/2$	External degree of freedom. Y displacement of foot
3	$\pi/2$	$Q_3$	0	$\pi/2$	External degree of freedom. Z displacement of foot.
4	$Q_4$	0	0	$\pi/2$	External degree of freedom. Orientation of leg.
5	$Q_5$	0	0	$\pi/2$	External degree of freedom. Orientation of leg.
6	$Q_6$	0	0	0	External degree of freedom. Orientation of leg.
7	$\pi/2$	$Q_7$	0	$\pi/2$	Length of leg.
8	$Q_8$	0	0	$\pi/2$	Orientation of leg with respect to hip.
9	$Q_9$	0	0	$\pi/2$	Orientation of leg with respect to hip.

## 4. Design and Construction of 3D One-Legged Machine

### 4.1 Introduction

We have designed and built a 3D one-legged hopping machine to enable experiments on legged systems that balance in 3-space. Figure 4-1 is a diagram of the machine, and a photograph is shown in Fig. 1-3. The machine is largely a generalization of the 2D hopper described in chapter 2. It includes a leg that changes length, a body that carries sensors and interface electronics, and an actuated 2-axis hip. The machine has an overall height of 43.5 inches (1.10 m) and a mass of 38 lbs. (17.3 kg). Appendices III and IV give a detailed specification of the machine along with comparable data for the 2D hopper.

The leg consists of a double ended air cylinder with a foot at one end and a length sensor at the other end. Air pressure applied to the top of the cylinder causes the piston and rod to extend downward against the floor providing an upward thrust to the body of the machine. When the valves seal off the cylinder, trapped air makes the leg springy along it's long axis. A cushioned foot at the lower end of the cylinder rod softens impacts of the foot with the floor, and provides good traction. Two hydraulic actuators, oriented at  $90^\circ$  to one another, drive motion of the leg with respect to the body. They attach to the center portion of the leg just below the hip.

Three major design decisions were made early:

- The machine would not carry its own power supplies nor its own computing.
- The machine would have only one leg.
- The leg would be similar to the one used on the 2D hopping machine.
- The machine would have no preferred direction of travel.

We decided early on not to build a self contained machine. Therefore the hydraulic and pneumatic power supplies are mounted off-board and connected to the machine through a flexible umbilical cable. The control computer is located in the next room, and communicates digitally through a ribbon cable. The design effort required to mount power sources and computing on board would have distracted us from our main objective of studying balance and dynamic control.

There were four reasons why we decided to build a 3D machine with only one leg. First, it is simpler to study balance in machines with one leg, because coupling between legs does not have to be understood and controlled. It is also easier to focus on balance, because it is such an important problem for a one-legged machine that cannot provide itself with a tripod of static support. Second, we wanted to build as little equipment as possible. More equipment means more construction time, more down time, and less reliable

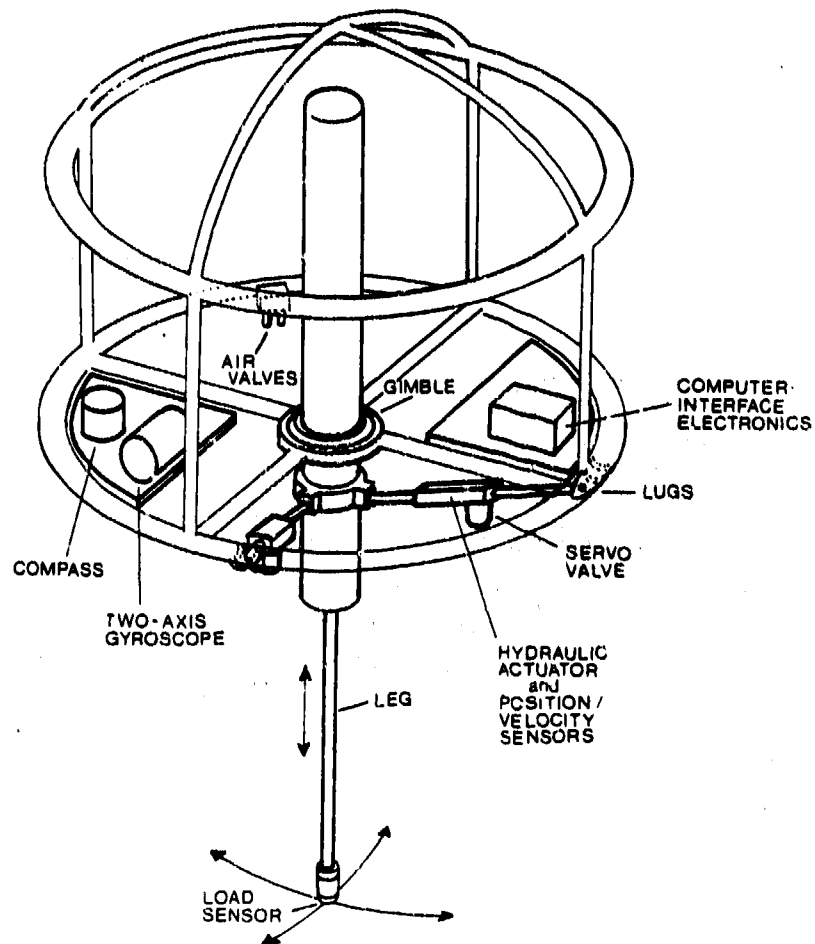


**Figure 4-1:** Diagram of 3D one-legged machine that was built. The leg is connected to the body by a two axis gimble hip. Two hydraulic actuators control the orientation of the leg with respect to the body. The leg is a pneumatic cylinder with a padded load-sensing foot at one end, and a linear potentiometer at the other end. The foot measures 3 forces acting between it and the ground. The body is made of an aluminum frame, within which are mounted computer interface electronics, valves, a gyroscope, and an electronic compass.

operation. The machine described here has only three actuators, one leg, one foot, and about a dozen sensors. Third, the behavior of a one-legged device is fundamentally similar to the behavior of each leg in multi-legged systems. Therefore study of a one-legged machine provides knowledge that helps to understand all sorts of dynamic legged systems. Fourth, we wanted to apply what we learned in the 2D case to the 3D case, generalizing the designs, the algorithms, and the concepts as needed.

We see the need to turn and to control motions during turning as very complicated activities which we wanted to avoid. A machine without a preferred axis does not have to change its heading to change its direction of travel. It is also less encumbered by uncontrolled spin, since the machine can continue making progress in the desired direction, even if the machine changes its heading on each hop. A symmetrical machine should be easier to control.

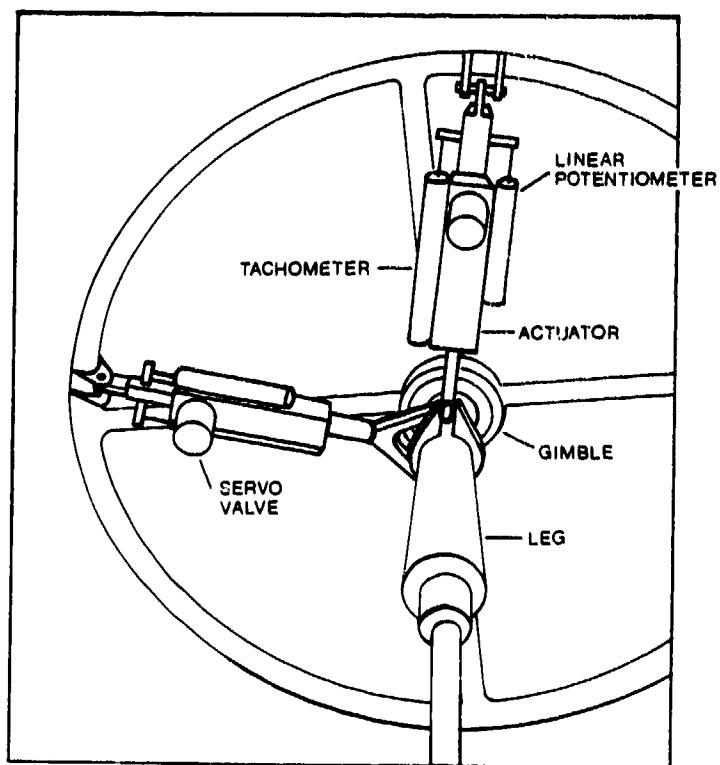


Figure 4-2: A bottom view of the hip. The two hydraulic actuators position the leg with respect to the body. Each actuator is provided with a position sensor, a velocity sensor, and a flow control servo valve. The arrangement of actuators and linkages provides  $\pm 30^\circ$  leg motion about one axis, and  $\pm 20^\circ$  about the other.

## 4.2 Design Details

The leg is very similar in design to that used on the 2D hopper. The choice of leg equipment was an act of conservatism: there was no reason to improve on the leg used in the 2D machine, since it worked very well. The air cylinder is identical to that of the 2D hopper, except that the bore was increased from 1-1/8 inch (28.6 mm) to 1-1/2 inch (38.1 mm) while the stroke remains the same at 10 inches (254 mm). The full actuator stroke will not be used during normal hopping, but will permit retracting the leg to prevent damage in crash situations.

The system is designed to operate on 90 psig (620 kPa) compressed air, which is available in our laboratory. The 77% increase in cross-sectional area of the cylinder should make the vertical hopping performance close to that of the 2D hopper, with the weight increase from 19 to 38 lb. (88 to 170 N). The cylinder rod diameter was increased from 3/8 to 1/2 in. (9.5 to 12.7 mm), which should make the rod much less vulnerable to bending. The double-ended rod configuration provides two widely spaced rod bearings to minimize binding and wear. Control of the vertical thrust is by means of four normally-closed solenoid driven air valves. They

permit each end of the air actuator to be connected to supply pressure, room pressure, or to be sealed. A linear potentiometer, housed at the top end of the vertical air cylinder, senses the position of a wiper attached to the top end of the actuator rod. It provides a measurement of the length of the leg.

We chose hydraulic power to drive motions of the hip, rejecting pneumatic and electric power. A design goal was that the hip actuators should be able to swing the leg through a full  $60^\circ$  motion in about 100 msec. Calculations were based upon a constant acceleration/deceleration trajectory, the theoretical optimum for force-limited actuators. For high-performance electric servo motors, reasonable power-to-weight ratios can be obtained only at high rotational speeds. Thus the power delivered to the load was limited by the inertia of the motor and gearing. We concluded that our application would require an excessively heavy actuator package. Electric actuators become even less attractive as a legged system scales to larger sizes.

We also decided not to use pneumatic power, even though it had worked reasonably well in the 2D machine. Air power has two sets of limitations, one involving servo compliance, the other involving energy efficiency. Since air is compressible, air servos cannot be made very stiff without operating at high pressure. However, high pressure compressed air is not readily available, even at moderate flow rates. Pneumatic servo valves also have limitations: Single stage valves consume large amounts of compressed air, much of which is dumped to atmosphere when no motion is required. Two-stage pneumatic servo valves, although more efficient, are generally vulnerable to contaminants in the air and provide relatively poor frequency response. Of course, pneumatics has the advantage that it is easy to clean up after leaks.

On the basis of the design target, a hydraulic actuator displacement of  $0.2 \text{ in}^3 @ 1000 \text{ psi}$  ( $3.3 \text{ cm}^3 @ 7.0 \text{ mPa}$ ) was needed. With a servo valve rated for  $0.5 \text{ gpm} @ 1000 \text{ psi}$  ( $32 \text{ cm}^3/\text{sec} @ 7.0 \text{ mPa}$ ) pressure drop, the specified performance could be obtained at a supply pressure of 2000 psi (14 mPa). We selected a double-ended actuator with  $0.2 \text{ in}^2$  ( $1.3 \text{ cm}^2$ ) cross-sectional area,  $5/8 \text{ in.}$  (14.9 mm) bore,  $3/8 \text{ in.}$  (9.5 mm) rod, a  $1 \text{ 7/8 in.}$  (47.6 mm) stroke. The choice allowed us to use available actuators, and to minimize the bearing load at the hip by keeping the attachment point of the actuator to the leg a reasonable radius from the hip joint. It provides approximately twice the desired displacement. The double-ended rod configuration provides equal areas on both sides of the piston for symmetrical performance. The extra rod is used to operate position and velocity transducers. A two-stage servo valve with a rating of  $1 \text{ gpm} @ 1000 \text{ psi}$  ( $63 \text{ cm}^3/\text{sec} @ 7.0 \text{ mPa}$ ) was selected to match the actuator characteristics. The hydraulic power supply and all system components are rated  $@ 3000 \text{ psi}$  (21 mPa).

The two actuators that drive the hip are built as complete, modular units. See Fig. 4-3. Each actuator is equipped with a linear potentiometer and a linear tachometer, to provide position and velocity measurements on both axes. The body of each transducer attaches directly to the body of each hydraulic actuator, with the sensor rods connected to the unused rod of the actuator. The servo valves are mounted directly on the cylinders for maximum response.

The original goal was to design a machine that was symmetrical about the vertical axis. However, design

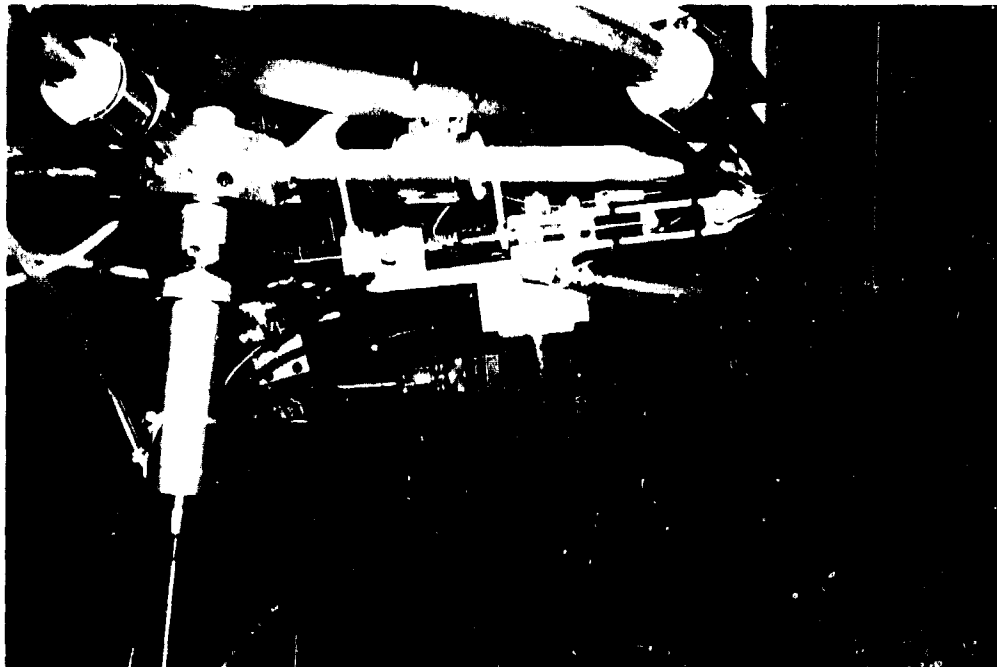
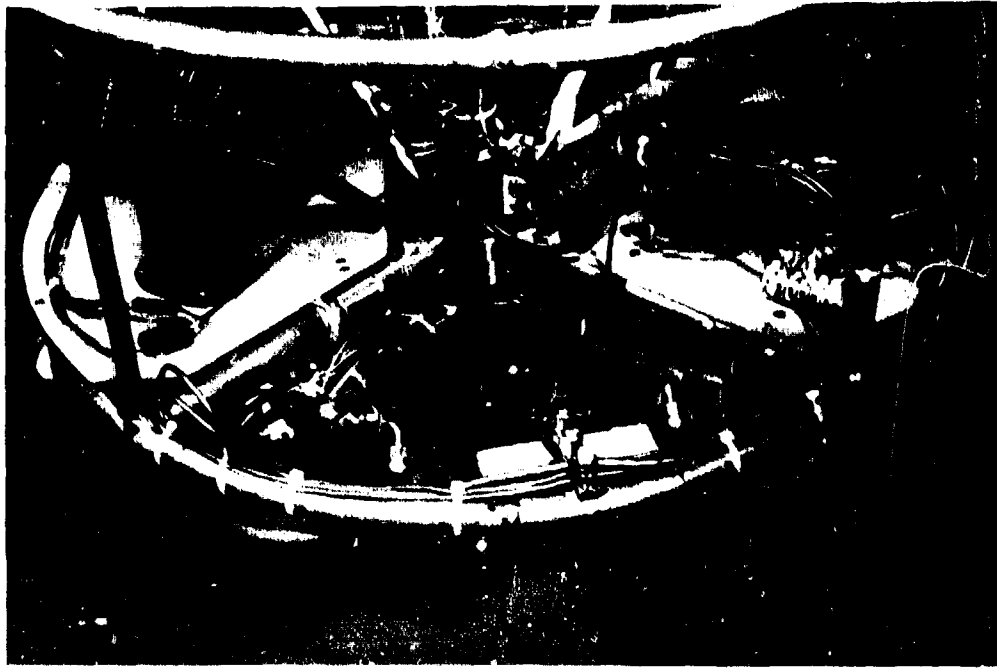


Figure 4-3: Photographs showing the hip joint and hydraulic actuators. The hydraulic servo valves are mounted directly on the actuators, and hang below them. Position and velocity sensors are attached to the sides of the actuators. See Fig. 1-3 for a photograph of the entire device.

considerations dictated a compromise in this plan. Ideally, the two actuators would act nominally at right angles to the lever arm from the hip joint, and the body pivot of each actuator would be in the plane of the hip joint. To meet these requirements, the rod-end pivot points of the horizontal cylinders must pass through the body of the leg cylinder. A rather complex mechanism is required to satisfy this requirement, if it is to accommodate the full motion of the leg when actuated about both axes simultaneously. The problem is aggravated when both pivot points must be at the same radius from the hip. The design was greatly simplified by placing the fore-aft actuator in the preferred configuration, while the attachment of the other actuator was moved outside of the body of the leg, and below the pivot point of the other actuator. Because of the hip gimbal geometry, leg rotation was seen only by the side-to-side actuator; this was accommodated by a spherical rod-end bearing. This design allows the desired  $\pm 30^\circ$  swing in the fore-aft direction, with  $\pm 20^\circ$  movement side-to-side.

Several hip designs were considered to provide the required two degrees of freedom. Ruggedness, minimum weight, and friction were primary considerations. The need for the structure of the leg to pass through the hip joint precluded the use of a through shaft at the pivots, and necessitated a relatively large mechanism. We considered placing the body of the leg cylinder below the hip, but decided this was not consistent with the desired stroke length and a hip height of 23 inches (0.58 m). A ball-and-socket joint encircling the leg cylinder was considered, but rejected due to large size, weight, high friction, and difficulty in manufacturing. No reasonable flexure arrangement using metals, plastics, or elastomers was evident which would meet the required range of motions and provide the rigidity and strength needed for precise control. Based on these considerations, a gimbal arrangement was selected. This mechanism uses two sets of pivots arranged at  $90^\circ$ , and an intermediate floating ring to connect the two.

The body frame of the machine was designed as a cage that encloses and protects the machine components. Light weight aluminum tubing was formed, machined, and held in a jig while all joints were welded. The overall diameter of 30 inches (0.76 m) was dictated by the required radius for the hip actuators. The frame must be strong and rigid enough to withstand horizontal actuator forces of 400 lbs. (1800 N) without substantial deflection. While the frame is relatively large and rugged, it comprises only about 15% of the machine's total weight. The cage will protect the machine when it falls over, and provide handling points. It also permits the addition of weights to adjust the center of mass and moments of inertia as desired. Finally, the frame tubing provides a space for storage of compressed air, supplied through the umbilical, to maximize the leg's responsiveness.

### 4.3 Sensors

Roll, pitch and yaw angles must be known throughout the hopping cycle in order to control the machine. A 2-axis vertical gyro measures roll and pitch angles of the body. A magnetic flux sensor provides information that indicates yaw angle. These instruments are relatively fragile and will have to be properly mounted and protected from the shock of normal hopping, and the shock of a crash. It is uncertain how these instruments will behave under the continual vertical accelerations that occur during hopping. We anticipate that the attitude measurement problem will be one of the most challenging problems in achieving 3D control.

Force sensing is incorporated in the design of the foot. Force sensing will be useful in the measurement and control of the foot thrust and side forces, and may enable detection of foot slippage or impending loss of traction. A single-axis load cell (in the thrust direction) has been built using a four-strain-gauge bridge at the foot. Preliminary tests indicate that this load cell will provide reasonable measurements of the foot thrust as well as a clear indication of the time of touch-down. A 3-axis load cell is being built using 12 strain gauges. It will have integral instrumentation amplifiers in the foot to provide a high-level, low-noise signal. The force-sensing foot may be supplemented by pressure sensors on the three actuators.

All communications between the 3D hopper and the control computer are digital. Onboard interface electronics provides analog to digital conversion for sensors, digital to analog conversion for actuators, digital outputs for the air valves, and appropriate multiplexing.

#### 4.4 Auxiliary Equipment

In addition to the hopping machine itself, we have designed and constructed a tether boom, similar to that used with the 2D hopper. The tether constrains the machine to move on an circle of 8 foot (2.5 m) radius. The arm itself is constructed as a space frame of light-weight aluminum tubing, and adds only about 1.7 lb (0.75 kg) to the effective mass of the hopper. The fixed end of the tether boom attaches to a pivot post that provides three degrees of freedom: pitching about the axis of the arm, vertical translation of the machine, and horizontal translation. Individual degrees of freedom can be selectively locked at the pivot end of the arm to permit various operating modes. Initially the machine will operate only in the vertical mode, to permit testing and refinement of the vertical control algorithms. Then the machine will operate as a 2D hopper to allow individual testing and tuning of the two horizontal control systems. Ultimately, the machine will be released from the tether and operate in 3D. Use of this tether mechanism will make it easier to isolate control problems systematically, and to refine control.

The umbilical cable will be large, and may cause problems when operating in 3D. It will include two hydraulic lines, one air-hose, wires for computer signals, and an electrical power cable. During 3D operation, the umbilical must permit the machine to move substantial distances in both horizontal directions without applying large torques about roll, pitch, or yaw axes. Engineering of suitable support mechanisms for the umbilical is a challenge that awaits experience with the operational machine.

#### 4.5 Appendix III. Specifications for 3D and 2D One-Legged Machines, Metric Units

Parameter	3D Hopper	2D Hopper
Overall Height	1.10 m	0.69m
Overall Width	0.76 m	0.97 m
Hip Height	0.58 m	0.50 m
Total Mass (Body & Leg)	17 kg	8.6 kg
Unsprung Leg Mass	0.91 kg	0.45 kg
Ratio: Body Mass to Unsprung Leg Mass	18:1	19:1
Body Moment of Inertia	0.709 kg-m <sup>2</sup>	0.520 kg-m <sup>2</sup>
Leg Moment of Inertia	0.111 kg-m <sup>2</sup>	0.037 kg-m <sup>2</sup>
Ratio: Body Moment of Inertia to Leg Moment of Inertia	6.4:1	14:1
<u>Leg Vertical Motion</u>		
Stroke	0.25 m	0.25 m
Ideal No-Load Stroke Time	0.031 s @620 kPa	0.040 s @620 kPa
Static Force	630 N @620 kPa	360 N @620 kPa
Ratio: Static Force to Weight	3.7:1	4.2:1
Theoretical Max. Work per Stroke	160 N-m	90 N-m
<u>Leg Sweep Motion</u>		
Sweep Angle	1.00 rad/0.71 rad	0.66 rad
Ideal No-Load Sweep Time	0.069 s @14 mPa	0.010 s @620 kPa
Static Torque	90 N-m/136 N-m @ 14 mPa	27 N-m @620 kPa
Theoretical Max. Work per Stroke	83 N-m	15 N-m

#### 4.6 Appendix IV. Specifications for 3D and 2D One-Legged Machines, English Units

Parameter	3D Hopper	2D Hopper
Overall Height	43.5 in	27.3 in
Overall Width	30.0 in	38.0 in
Hip Height	23.0 in	19.5 in
Total Mass (Body & Leg)	38 lbm	19 lbm
Unsprung Leg Mass	2.0 lbm	1.0 lbm
Ratio: Body Mass to Unsprung Leg Mass	18:1	19:1
Body Moment of Inertia	2420 lbm-in <sup>2</sup>	1770 lbm-in <sup>2</sup>
Leg Moment of Inertia	380 lbm-in <sup>2</sup>	125 lbm-in <sup>2</sup>
Ratio: Body Moment of Inertia to Leg Moment of Inertia	6.4:1	14:1
<u>Leg Vertical Motion</u>		
Stroke	10.0 in	10.0 in
Ideal No-Load Stroke Time	0.031 s @90 psig	0.040 s @90 psig
Static Force	140 lb @90 psig	80 lb @90 psig
Ratio: Static Force to Weight	3.7:1	4.2:1
Theoretical Max. Work per Stroke	1400 lb-in	800 lb-in
<u>Leg Sweep Motion</u>		
Sweep Angle	57°/41°	38°
Ideal No-Load Sweep Time	0.069 s @2000 psig	0.010 s @90 psig
Static Torque	800 lb-in/1200 lb-in @2000 psig	240 lb-in @90 psig
Theoretical Max. Work per Stroke	740 lb-in	130 lb-in

## 5. Using Tables for Dynamic Stability in a One-Legged System

### 5.1 Abstract

A legged system that balances as it runs must choose a place to plant each foot in order to control tipping and forward motion. In this paper we describe a method for computing a suitable location for the foot that uses a large table of pre-computed data. The table was organized around a subset of the system state and control variables, and the stored data were computed by numerically simulating a dynamic model of the legged system as it progressed through the stance portion of the running cycle. Repeated simulations were used to characterize the non-linear dynamics of the system for different landing conditions. The approach takes advantage of the very regular, cyclic character of legged behavior. Because the size of the table may be prohibitively large for some problems, polynomial surfaces were used to approximate the tabular data. Simulations verified the feasibility of using the tabular and polynomial methods to control balance and forward travel in a planar one-legged system.

### 5.2 Introduction

Control algorithms that use well organized tabular data offer the promise of providing good control for systems with complicated dynamics. Tabular techniques are powerful because they use the results of arbitrarily complicated calculations for control, but the time penalty of actually doing the calculation is incurred off-line. Therefore, tabular methods typically involve very simple run-time computations that execute with high speed. In a comparison of techniques for computing manipulator dynamics, Hollerbach showed that a tabular method developed by Raibert and Horn required the fewest run-time operations when applied to a manipulator with fewer than nine joints [150].

Another advantage of tabular control methods is that tables make it easy to implement simple forms of learning and adaptation. A tabular controller typically performs a very simple computation on the state variables to determine appropriate control values. The computation is based on some sort of representation of the dynamics of the system to be controlled. Because the computations are simple, it is usually easy to determine values for the coefficients of the computation, provided the form of the control computation is already known. Learning occurs when coefficient values are calculated from data obtained by observing the behavior of the system to be controlled [3], [4], [282], [230].

The main problem with tabular control methods is that the size of the tables they use grows exponentially with the number of state and control variables needed to characterize the dynamic system [281]. This problem has been attacked in a number of ways. Albus used a hashing function that mapped tables of astronomical size into the available memory of his computer in order to control a robot manipulator [3], [4]. His hashing

functions were designed to use knowledge of the manipulator's dynamics in order to minimize hashing collisions. Hashing could work in that case because the controller, rather than having the potential of producing all possible motions, dealt only with the subset of manipulator motions that had been learned. Raibert and Horn reduced the size of the tables needed to control a manipulator by striking a balance between computation and tabularization [283]. They found that for most manipulators with  $n$  joints, an  $n-1$  dimensional *configuration space* table would do. Simons et. al. reduced the size of the tables they use to do manipulator force control by finding an optimum quantization of the state inputs [310].

In this chapter we describe a tabular controller that maintains balance and regulates forward running speed in a walking system that hops on one leg. The task of finding a useful table of moderate size is accomplished, not by manipulating the form of the table, but by partitioning the problem into parts that can be solved separately. Once the problem is partitioned, the table is required to deal with only a subset of the state variables. We use the stereotyped cyclic motion of the legged system to find a simple partitioning. In this chapter we also show that multivariate polynomials of low degree can effectively approximate the tabular data. Evaluating the polynomial requires fewer data than the table, but somewhat more computation. Both methods are used to control the one-legged hopping system in simulation.

### 5.3 The Problem

During hopping in place, placement of the foot on each step determines how a legged system will balance and it influences the system's translational velocity. Consider the planar one-legged system shown in Fig. 5-1. It has a rigid body, a springy leg, a hip driven by torque source,  $\tau$ , and a small foot. The system is described in detail in [286]. If the foot is placed to the left, then the system will tip and accelerate to the right. If the foot is placed to the right, then the vice versa. If the foot is placed directly under the body, then the system will neither tip nor accelerate. A corresponding set of rules applies when the system is travelling with a forward velocity. For each forward velocity there is a forward position for the foot that will neither tip the system, nor change the rate of forward travel.

The effects of foot placement are important because the foot's position can be directly controlled by torquing the hip during flight, because the foot cannot be moved once placed, and because the foot's position strongly affects balance. For the present problem we think of the foot's position when the system first touches the ground, not as a state variable, but as a control variable.

Once a cycle of stepping activity has been established, the problem of controlling balance and forward velocity is one of choosing a place to put the foot on each cycle that will take the system to the desired state. More specifically the control task is to find a position for the foot before *touch-down*, the moment there is contact between the foot and the ground, so as to minimize state errors at *lift-off*, the moment the foot next leaves the ground. The state errors of interest are those in forward velocity,  $\dot{x}_2$ , body angle,  $\theta_2$ , and body angular rate,  $\dot{\theta}_2$ .

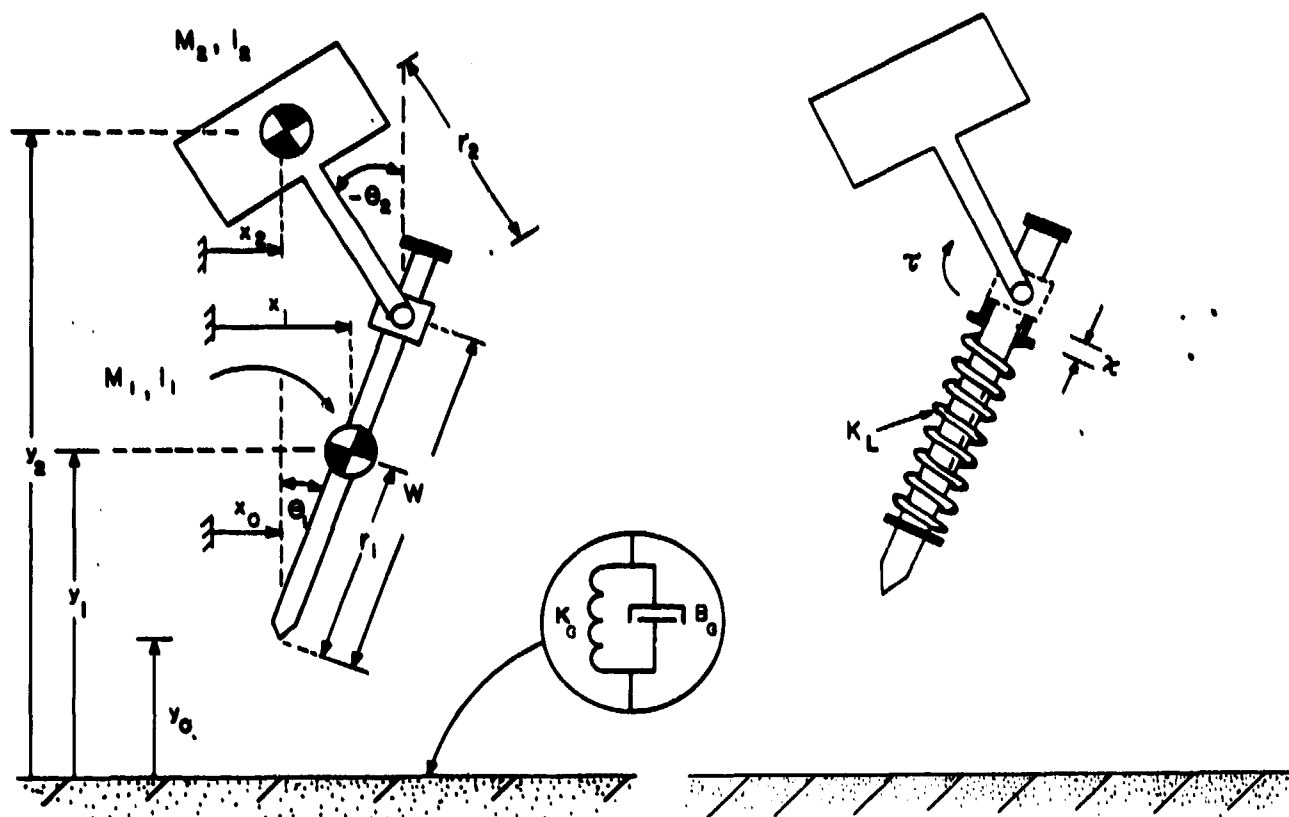


Figure 5-1: Schematic diagram of planar one-legged system used to test tabular control. The body and leg, each having mass and moment of inertia, are connected by a hinge joint at which torques,  $\tau$ , are generated. The leg consists of a spring in series with a position actuator of length  $x$ . Center of mass of the leg is located a distance  $r_1$  from the lower tip of the leg, which is the foot. The body is represented by a rigid mass, with the center of mass located a distance  $r_2$  above the hip. The angle of the leg,  $\theta_1$ , determines the relative position of the foot with respect to the system's center of gravity. Rhythmic activation of the leg actuator,  $x$ , causes the system to leave the ground in a hopping motion. Motion of the entire system is restricted to the plane. For more details and equations of motion see [286].

Assume that during flight the leg angle will be adjusted by a linear servo of the form:

$$\tau(t) = K_p(\theta_1 - \theta_{1,d}) + K_v(\dot{\theta}_1) \quad (5.1)$$

where

$\theta_{1,d}$  is the desired leg angle, and  
 $K_p, K_v$  are feedback gains.

Further assume that during stance the angle between body and leg,  $(\theta_1 - \theta_2)$ , is held constant by a linear servo similar to (5.1). We designate the value of a variable at touch-down by the subscript TD, and the value of a variable at lift-off by subscript LO. The problem to be solved is, given the state at touch-down,  $X_{TD}$ , find  $\theta_{1,TD}$  to minimize:

$$PI = Q_1(\dot{x}_{2,LO} - \dot{x}_{2,d})^2 + Q_2(\theta_{2,LO} - \theta_{2,d})^2 + Q_3(\dot{\theta}_{2,LO} - \dot{\theta}_{2,d})^2 \quad (5.2)$$

where:

$Q_1, Q_2, Q_3$  are weights, and

$\theta_{2,d}, \dot{\theta}_{2,d}, \dot{x}_{2,d}$  are desired values.

#### 5.4 Tabular Method

In order to minimize (5.2), a relationship,  $\Gamma$ , is needed that relates the state of the system at lift-off to the state at touch-down:

$$(\dot{x}_{2,LO}, \theta_{2,LO}, \dot{\theta}_{2,LO}) = \Gamma(X_{TD}) \quad (5.3)$$

In general, behavior of the system during stance is influenced by the entire state vector at touch-down,

$$X_{TD} = (x_2, \dot{x}_2, y_2, \dot{y}_2, \theta_2, \dot{\theta}_2, w, \dot{w}) \quad (5.4)$$

The regular nature of the stepping cycle permits us to partition the state variables into two groups, those that vary from one stepping cycle to the next, and those that do not. We assume that the values of  $y_2, \dot{y}_2, w,$  and  $\dot{w}$  vary along the same trajectory from one cycle to the next. The values of these variables are important to the relationship expressed in (5.3), but their effect is constant from hop to hop. Therefore, (5.3) can be expressed as a function of a subset of the state variables:

$$(\dot{x}_{2,LO}, \theta_{2,LO}, \dot{\theta}_{2,LO}) = \Gamma(\dot{x}_{2,TD}, \theta_{2,TD}, \dot{\theta}_{2,TD}, \theta_{1,TD}) \quad (5.5)$$

We call the vector  $x_{TD} = [\dot{x}_{2,TD}, \theta_{2,TD}, \dot{\theta}_{2,TD}]$  the touch-down state vector,  $x'_{TD} = [\dot{x}_{2,TD}, \theta_{2,TD}, \dot{\theta}_{2,TD} \mid \theta_{1,TD}]$  the augmented state vector, and  $x_{LO} = [\dot{x}_{2,LO}, \theta_{2,LO}, \dot{\theta}_{2,LO}]$  the lift-off state vector. We define a vector field  $\Lambda$ , such that there is a dimension of  $\Lambda$  that corresponds to each component of  $x'_{TD}$ , and for each point in  $\Lambda$  there is a unique value of  $x_{LO}$ .

For this problem we think of  $\theta_1$  as a control variable since it can be changed during flight at will, and the remaining components of  $x'_{TD}$  as state. In general there are  $i$  control variables and  $n$  state variables.

The vector field  $\Lambda$  is approximated by a multidimensional table. One dimension of the table corresponds to each dimension of  $\Lambda$ , and all dimensions are quantized to  $M$  levels. For  $n$  variables and  $i$  control variables, each quantized to  $M$  values, there are  $M^{n+i}$  hyper-regions in the table, each storing an  $n$ -vector.  $M$  must be chosen to quantize the table finely enough level to capture the variations in  $x_{LO}$ .

We have used such a table to control the planar hopper in simulation. Forward velocity  $\dot{x}_2$ , body angle  $\theta_2$ , and body angular rate  $\dot{\theta}_2$ , are the state variables used to access the table,  $n=3$ . Leg angle  $\theta_1$  is a control

variable,  $i=1$ . These variables index a 4 dimensional space. Each dimension of the memory is quantized to nine levels,  $M=9$ , requiring that  $M^{i+n}=19,683$  values be stored. To compensate for such a coarse quantization, the function that accesses the tabular data,  $T(x'_{TD})$ , performs a linear interpolation among the  $2^{n+i}$  stored values that bracket the desired value.

Tabular data were obtained by simulating a large set of locomotion cycles, with systematically varied initial conditions. For these simulations, the angle between leg and body was held constant by (5.1) during stance, just as it would be when controlled. In order to minimize (5.2) the table was searched along a path determined by varying  $\theta_1$  through its entire range, with  $x=x_{TD}$ . The details of the search are given in Appendix V. The leg was then moved just before touch-down to the minimizing value of  $\theta_1$ .

This tabular controller was tested in a simple simulated balance problem. The task was to return the one-legged system to a balanced posture, after starting with the body in an inclined position. Figure 5-2 plots the body angle and horizontal position of the hopper for the test in which the hopper was dropped from a height of 0.3 m with an initial body angle error of 0.8 radians. Setpoints were  $\dot{x}_{2,d} = 0$ ,  $\theta_{2,d} = 0$ ,  $\theta_{2,d} = 0$ . A vertical posture with no horizontal motion was attained in about 6 sec. In this test no attempt was made to control  $x_2$ , horizontal position.

The same algorithm was used to control forward velocity while the system traveled from one point to another. Figure 5-3 shows data from the resulting translation in which  $x_2$  was controlled indirectly through rate control. Forward velocity was very slow, but precisely controlled with no limit cycles like those caused by linear control. The low rate of forward travel was an artifact of the restricted motion of the hip during stance, as required by the simple foot placement algorithm. It is not an inherent attribute of the tabular control method.

In the example given here, the control variable,  $\theta_1$ , was not explicitly varied during the interval between touch-down and lift-off. Hip angle was fixed during stance. In general it is not necessary that the control variables be constant, only that they do not vary with more degrees of freedom than are represented in the table. This means that variations in the control signals are perfectly acceptable, provided that their variation is completely determined by the augmented state vector that is available when (5.3) is used.

The table just described is used to evaluate (5.3). Control is actually served by evaluating:

$$\theta_{1,TD} = \Gamma^{-1}(\dot{x}_{2,LO}, \theta_{2,LO}, \dot{\theta}_{2,LO} | \dot{x}_{2,TD}, \theta_{2,TD}, \dot{\theta}_{2,TD}) \quad (5.6)$$

Eq. (5.6) was effectively implemented by searching the table. It is possible to create a table that implements (5.6) directly, provided specific values are provided for  $\dot{x}_2$ ,  $\theta_{2,d}$ ,  $\dot{\theta}_{2,d}$ , and  $Q_1$ ,  $Q_2$ ,  $Q_3$ . Then control can proceed without search.

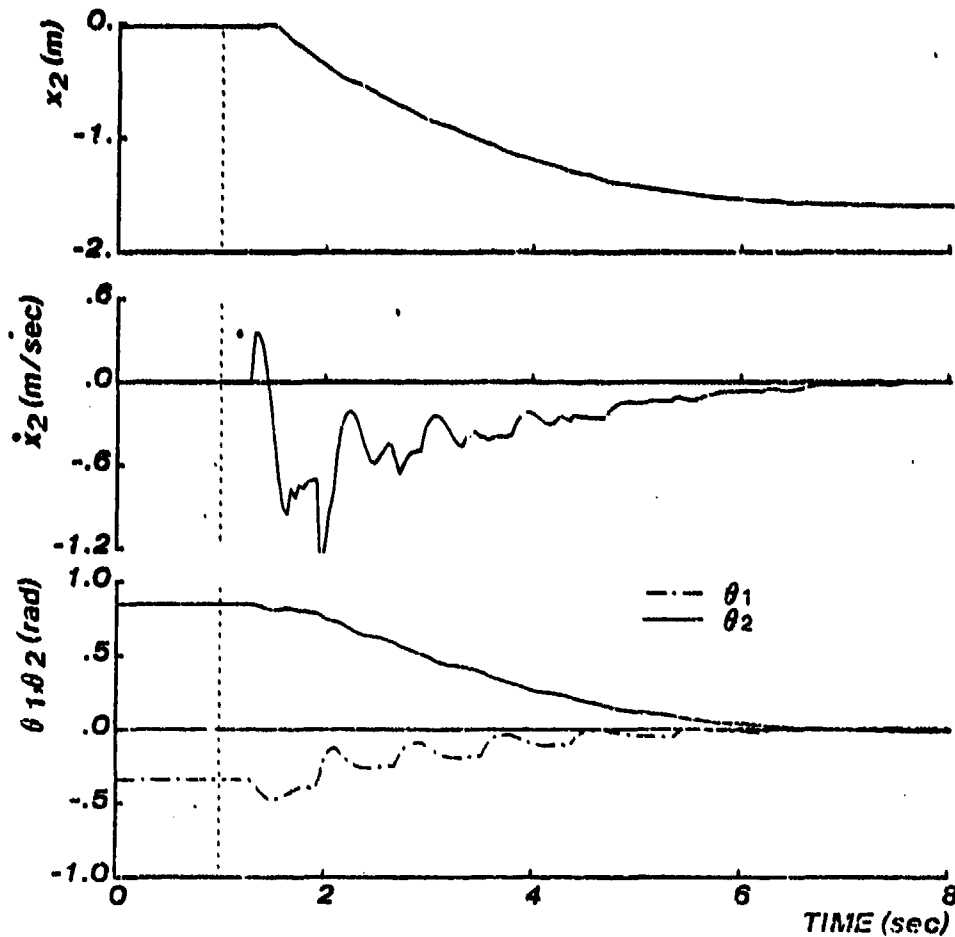


Figure 5-2: Orientation of the body is corrected using tabular method. At  $t=0$  initial error in body attitude was 0.8 radians. At  $t=1$  gravity is turned on and hopping begins. State errors approached zero about 6 sec later. Horizontal position is not controlled, so position changes without correction. ( $Q_1=1.5, Q_2=5.0, Q_3=1.0$ )

## 5.5 Polynomial Approximation to Tabular Data

The data of the last section show that the tabular method can effectively control a non-linear dynamic system with few state and control variables. However, even when the problem is partitioned, the memory requirements for this approach become severe in larger applications. In this section we show that the tabular data can be approximated by polynomials in the state variables. The polynomials can have many fewer coefficients than entries in the original table, at the expense of additional run-time computation.

Given  $N=n+i$  state and control variables, polynomials were constructed that map touch-down state vectors into estimates of lift-off state vectors. Each of  $n$  polynomials minimizes the total square error for the variable it approximates across all data points in the table.

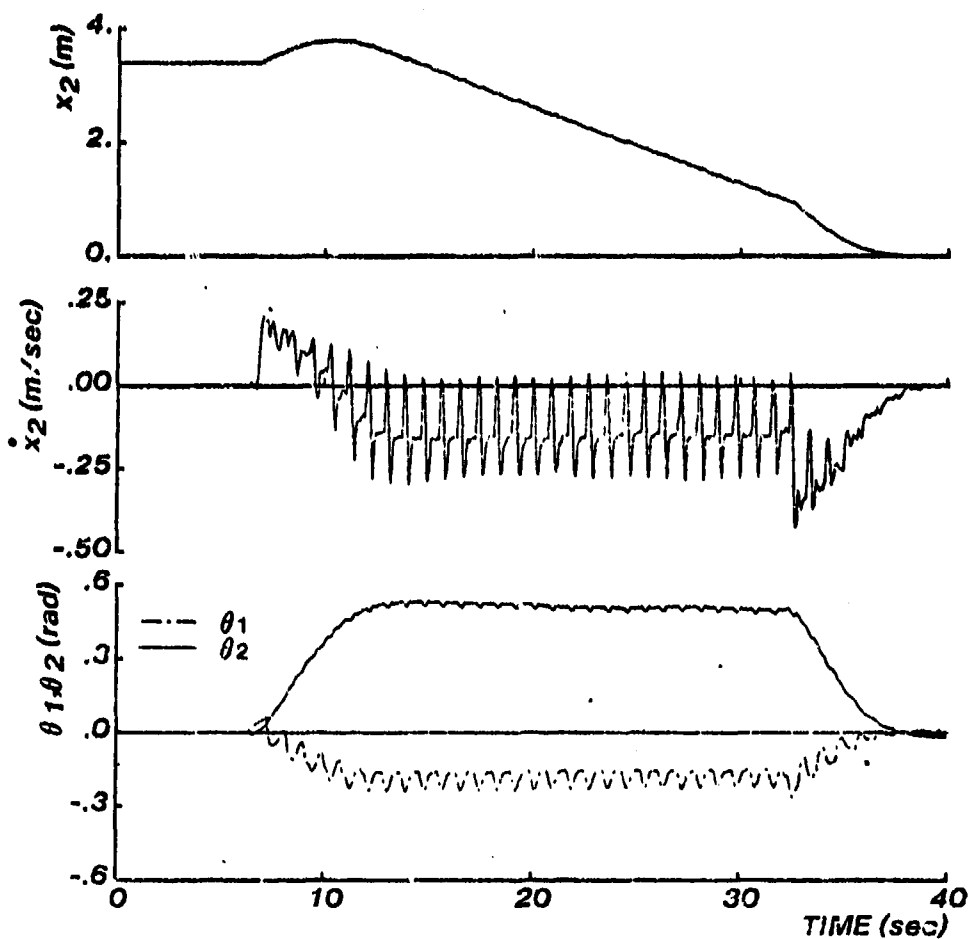


Figure 5-3: Lateral step controlled by tabular method. ( $Q_1 = 1.0$ ,  $Q_2 = 5.0$ ,  $Q_3 = 1.0$ )

Let  $A$  be a matrix in which each row contains values of the  $N$  state and control variables; let  $B$  be the matrix that contains future values of the state variables in corresponding rows. The matrices  $A$  and  $B$  then form a data structure for the predictive state space memory. Given a sequence of distinct terms of the form:

$$\langle x_1^{\alpha_{11}} x_2^{\alpha_{12}} x_3^{\alpha_{13}} x_4^{\alpha_{14}} \dots x_1^{\alpha_{M1}} x_2^{\alpha_{M2}} x_3^{\alpha_{M3}} x_4^{\alpha_{M4}} \rangle \quad (5.7)$$

determine a row of the  $M$ -column matrix  $C$  by evaluating these terms at the values defined by the same row of  $A$ . Then

$$(C^T C X = C^T B) \quad (5.8)$$

is a linear system whose solution  $X$  contains, in each column, the coefficients of a least squares polynomial that estimates the values in the corresponding column of  $B$  [317]. The polynomial is, of course, determined by the choice of the exponents in the above sequence, including many set to zero.

Using the polynomial, (5.2) can be minimized in closed form. The details of the procedure are given in Appendix Vi. For the case of the one-legged machine,  $\dot{x}_2$ ,  $\theta_2$ ,  $\dot{\theta}_2$ , and  $\theta_1$ , are the independent variables and  $\theta_2$ ,  $\dot{\theta}_2$ , and  $x_2$  are the variables to be approximated.

Several polynomials have been generated and tested using the same procedure described earlier for Fig. 5-2, as well as other similar tests. In each case, the resulting behavior is compared to that obtained with the tabular data:

- 24 term polynomial consists of all odd terms of degree 3 or less. The body angle did not reach the setpoint after 20 seconds.
- 40 term polynomial consists of all terms of degree 1 and 3, with 16 terms of degree 5. Behavior was similar to the table, with slightly less rapid convergence.
- 68 term polynomial consists of all terms of degree 1, 3, and 5. Convergence is slightly faster than for the 40 term polynomial.
- 625 term polynomial consists of all terms such that the exponents of each of the independent variables is less than or equal to 4. Behavior is very similar to the original tabulated data.

The approximation error for each polynomial is listed in the following table:

No. of Terms	Mean Square Error		
	$\dot{x}_2$	$\dot{\theta}_2$	$\theta_2$
24	16.6	0.602	4.53
40	13.6	0.527	4.39
68	10.5	0.359	4.25
625	9.55	0.308	3.94

To use the table we must search it at run-time to find the entry that minimizes (5.2). Specifically this is a search where  $\theta_2$ ,  $\dot{\theta}_2$  and  $\dot{x}_2$  are fixed and  $\theta_1$  may vary. The table is quantized with respect to  $\theta_1$  at nine equally spaced points in the interval  $-1 < \theta_1 < 1$ . In each subinterval we derive a linear interpolation formula for each element of  $x_{LO}$ . Since  $\theta_1$  is the only free variable, we substitute the interpolation expressions for  $\theta_2$ ,  $\dot{\theta}_2$  and  $\dot{x}_2$  into MINIMIZE, differentiate with respect to  $\theta_1$ , set the result equal to zero, and solve for  $\theta_1$ . Eight candidates are obtained. We select the one that minimizes globally.

A similar approach is used in applying the polynomial. Since  $\theta_2$ ,  $\dot{\theta}_2$  and  $\dot{x}_2$  are fixed during the search for  $\theta_1$ , multivariate polynomials in four variables are made simpler polynomials in one variable. For instance, consider the 68 term polynomials discussed above. The highest power of  $\theta_1$  occurring in each of the three polynomials is  $\theta_1^5$ . When computing a control signal, we evaluate six coefficients for each of the three polynomials; these are determined by the given values of  $\theta_2$ ,  $\dot{\theta}_2$  and  $\dot{x}_2$  as well as by the 68 original coefficients. The six term polynomials are algebraically substituted into (5.2), and the resulting polynomial of degree 10 is differentiated with respect to  $\theta_1$ . The result is a single polynomial of degree 9 in  $\theta_1$ . Its zeros are found by using Laguerre's method [DAH74]. The PI is explicitly evaluated for each real zero in the interval  $-1 < \theta_1 < 1$ , and the smallest of these values determines the globally optimum  $\theta_1$ .

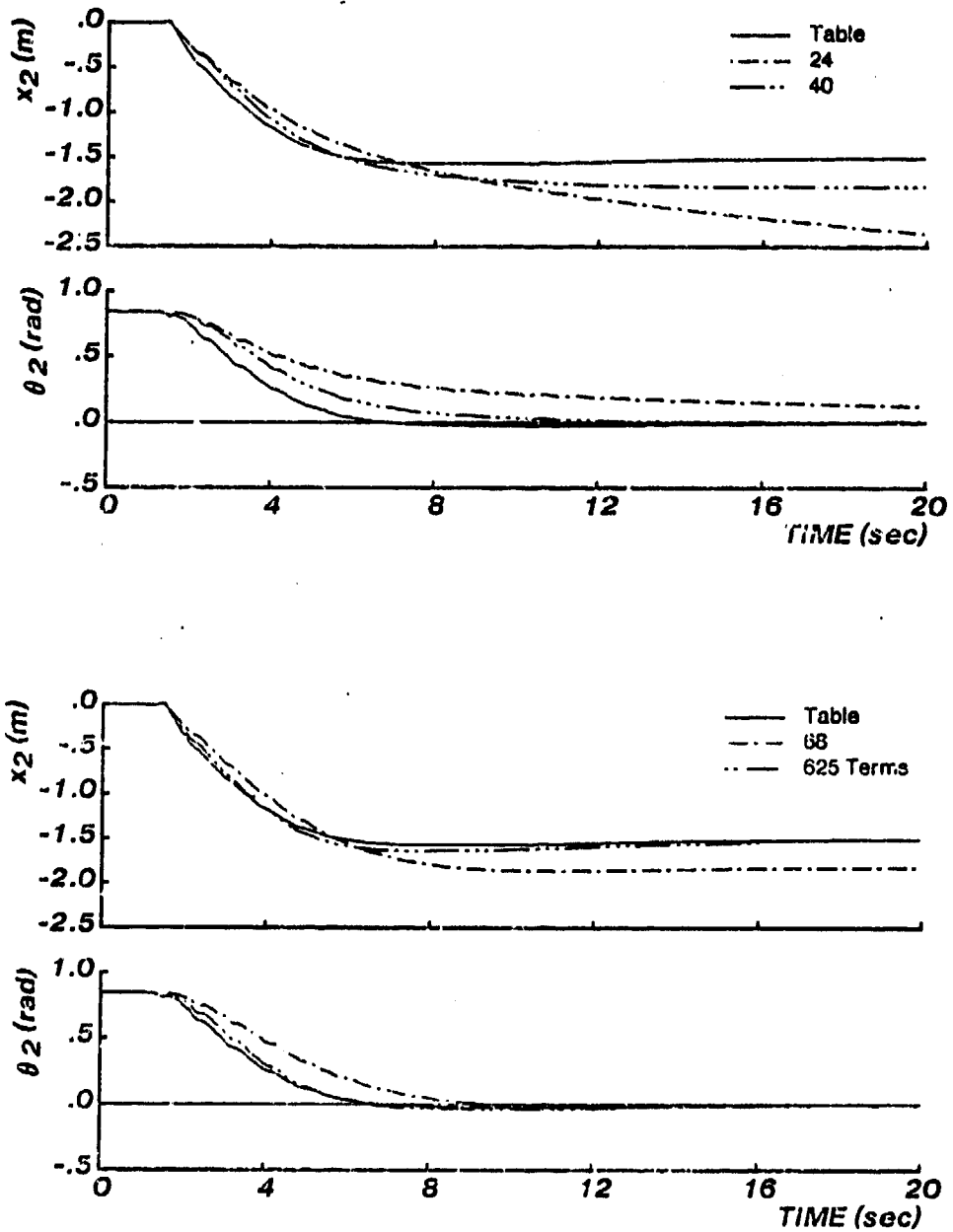


Figure 5-4: Polynomial approximations are compared to tabular data in test that corrects orientation of body, using same procedure as in Fig. 5-2. The responses for the tabular data and four different polynomial approximations are plotted. See text for description of how terms were chosen.

This procedure for minimizing (5.2) does not require finding the zeros of a large polynomial in four variables. For example, the 625 term polynomials with all possible terms of degree four and less requires zeros of a single ninth degree polynomial in  $\theta_1$ .

## 5.6 Appendix V. Algorithm that Minimizes Performance Index for Tabular Data.

Given a state vector at touchdown  $[\theta_2, \dot{\theta}_2, \dot{x}_2]$  it is required to find the value of  $\theta_1$  that minimizes the performance index  $PI([\theta_{2L}, \dot{\theta}_{2L}, \dot{x}_{2L}])$  where  $[\theta_{2L}, \dot{\theta}_{2L}, \dot{x}_{2L}] = T([\theta_1, \theta_2, \dot{\theta}_2, \dot{x}_2])$  is the state vector at next lift-off;  $T$  denotes the function that implements the interpolated table lookup. Recall that

$$PI([\theta_{2L}, \dot{\theta}_{2L}, \dot{x}_{2L}]) = Q_1(\theta_{2L} - \theta_{2,d})^2 + Q_2(\dot{\theta}_{2L} - \dot{\theta}_{2,d})^2 + Q_3(\dot{x}_{2L} - \dot{x}_{2,d})^2 \quad (5.9)$$

where  $Q_1, Q_2$  and  $Q_3$  are weights and  $\theta_{2,d}, \dot{\theta}_{2,d}$  and  $\dot{x}_{2,d}$  are desired values.

Assume that  $\theta_{2A} \leq \theta_2 \leq \theta_{2B}, \dot{\theta}_{2A} \leq \dot{\theta}_2 \leq \dot{\theta}_{2B}$  and  $\dot{x}_{2A} \leq \dot{x}_2 \leq \dot{x}_{2B}$  where the A and B subscripts indicate adjacent values stored at quantized locations in the table. Also, assume that:  $\theta_{1A} \leq \theta_1 \leq \theta_{1B}$ . Consider as an example the first term of (5.9) which can be written in terms of the tabulated data:

$$Q_1(\theta_{2L} - \theta_{2SP})^2 = Q_1 \left[ \frac{(\theta_1 - \theta_{1A})\theta_{2B} - (\theta_{1B} - \theta_1)\theta_{2A}}{(\theta_{1B} - \theta_{1A})} - \theta_{2,d} \right]^2 \quad (5.10)$$

where  $\theta_{2A} = T([\theta_{1A}, \theta_2, \dot{\theta}_2, \dot{x}_2])$  and  $\theta_{2B} = T([\theta_{1B}, \theta_2, \dot{\theta}_2, \dot{x}_2])$ . In other words, once interpolation has been completed for the three state variables, two adjacent values in the table that bracket  $\theta_1, \theta_{1A}$  and  $\theta_{1B}$  are substituted in the linear interpolation formula.

Now the right hand side of (5.10) can be rewritten:

$$Q_1(\theta_{2L} - \theta_{2,d})^2 = Q_1(\theta_1 Q_A + Q_B)^2 \quad (5.11)$$

where  $Q_A = \frac{(\theta_{2B} - \theta_{2A})}{(\theta_{1B} - \theta_{1A})}$  and  $Q_B = \frac{\theta_{2A}\theta_{1B} - \theta_{2B}\theta_{1A}}{\theta_{1B} - \theta_{1A}} - \theta_{2,d}$ . An identical treatment of the other two terms of (5.9) yields

$$PI = Q_1[Q_A\theta_1 + Q_B]^2 + Q_2[Q_C\theta_1 + Q_D]^2 + Q_3[Q_E\theta_1 + Q_F]^2 \quad (5.12)$$

Upon differentiation with respect to  $\theta_1$ , setting the result equal to zero, and solving for  $\theta_1$  we have a closed expression for that value of  $\theta_1$  that minimizes the PI in the interval  $\theta_{1A} \leq \theta_1 \leq \theta_{1B}$ :

$$\theta_1 = - \frac{Q_1 Q_A Q_B + Q_2 Q_C Q_D + Q_3 Q_E Q_F}{Q_1 Q_A^2 + Q_2 Q_C^2 + Q_3 Q_E^2} \quad (5.13)$$

To obtain the *global* minimum this computation is performed for each of the  $M$  subintervals determined by the quantization of  $\theta_1$ .

### 5.7 Appendix VI. Algorithm that Minimizes Performance Index for Polynomial.

The general form of the  $K$ -term polynomials that approximate the tabulated data is:

$$\begin{aligned}\theta_{2L} &= f_{1,1}\theta_1^{\alpha_{11}}\theta_2^{\alpha_{12}}\dot{\theta}_2^{\alpha_{13}}x_2^{\alpha_{14}} + \dots + f_{1,K}\theta_1^{\alpha_{K1}}\theta_2^{\alpha_{K2}}\dot{\theta}_2^{\alpha_{K3}}x_2^{\alpha_{K4}} \\ \dot{\theta}_{2L} &= f_{2,1}\theta_1^{\alpha_{21}}\theta_2^{\alpha_{22}}\dot{\theta}_2^{\alpha_{23}}x_2^{\alpha_{24}} + \dots + f_{2,K}\theta_1^{\alpha_{K1}}\theta_2^{\alpha_{K2}}\dot{\theta}_2^{\alpha_{K3}}x_2^{\alpha_{K4}} \\ \dot{x}_{2L} &= f_{3,1}\theta_1^{\alpha_{31}}\theta_2^{\alpha_{32}}\dot{\theta}_2^{\alpha_{33}}x_2^{\alpha_{34}} + \dots + f_{3,K}\theta_1^{\alpha_{K1}}\theta_2^{\alpha_{K2}}\dot{\theta}_2^{\alpha_{K3}}x_2^{\alpha_{K4}}\end{aligned}\quad (5.14)$$

where, again, the  $L$  subscript denotes values at next lift-off and  $[\theta_2, \dot{\theta}_2, x_2]$  is a state vector at touch-down. Since  $\theta_1$  is the only free variable, (5.14) can be recast as:

$$\begin{aligned}\theta_{2L} &= F_{1,1}\theta_1^{\beta_0} + \dots + F_{1,N}\theta_1^{\beta_N} \\ \dot{\theta}_{2L} &= F_{2,1}\theta_1^{\beta_0} + \dots + F_{2,N}\theta_1^{\beta_N} \\ \dot{x}_{2L} &= F_{3,1}\theta_1^{\beta_0} + \dots + F_{3,N}\theta_1^{\beta_N}\end{aligned}\quad (5.15)$$

where  $\beta_0 > 0$  and  $\beta_N$  is the highest power of  $\theta_1$  in (5.14). Substituting these equations into (5.9) yields a polynomial of degree  $2\beta_N$  which expresses the PI as a function of  $\theta_1$ :

$$PI = G_0 + \theta_{2,d}^2 + \dot{\theta}_{2,d}^2 + \dot{x}_{2,d}^2 + G_1\theta_1^{2\beta_0} + \dots + G_{2N}\theta_1^{2\beta_N}\quad (5.16)$$

The real zeros of the derivative of this polynomial are found using Laguerre's method. The global minimum is found by evaluating (5.15) for each zero and substituting the results into (5.9).

## 6. Control of Balance in 2D -- Modeling and Simulation for the One-Legged Case

### 6.1 Abstract

In this chapter we model and simulate a 2D one-legged hopping machine in order to better understand legged systems that hop and run. The analysis focuses on balance, dynamic stability, and resonant oscillation for the planar case. The model incorporates a springy leg with non-zero mass, a simple body, and an actuated hinge-type hip. We decompose control of the model into a vertical hopping part, a horizontal velocity part, and a body attitude part. Estimates of total system energy are used in regulating hopping height in order to initiate hopping, to maintain level hopping, to change from one hopping height to another, and to terminate hopping. Balance and control of forward velocity are explored with three algorithms: First we study the role of foot placement in balance through a linear algorithm that stabilizes the system and generates low velocity translations from point to point. Second, we improve control of forward velocity by considering constraints that arise in constant velocity forward travel, and we introduce the *CG-print*. The improved algorithm places the foot forward with respect to the center of the *CG-print* during flight, and sweeps the leg backward during stance. Third we improve control of body attitude by using the hip actuator to correct pitch errors during stance. Simulations verify the feasibility of decomposing control of running into a height control part, a forward velocity control part, and an attitude control part.

### 6.2 Introduction

Substantial study has been devoted to understanding legged systems that crawl and walk, but little attention has been given to systems that run and hop. During crawling and walking, support is provided by at least one leg at all times, but in running and hopping support is provided only intermittently, with intervening periods of ballistic flight. One consequence of intermittent support is the vertical bouncing motion that characterizes running. A second consequence of intermittent support is the intermittent opportunity for the system to change its angular momentum to maintain balance and control attitude. Because angular momentum is conserved when there are no external forces on the system, torques can be applied to the body to change angular momentum only when the system is in contact with the ground. A further consequence of intermittent support is that leg dynamics play an important role in determining a system's behavior -- both the pattern and efficiency of a running system's motion are influenced by leg dynamics.

In this chapter we model a hopping system with just one leg, and simulate its behavior as controlled by algorithms that manipulate hopping height and running speed, while maintaining balance and attitude. The purpose is to understand the principles of balance and dynamic stability as they apply to legged systems, while ignoring the problem of coupling many legs. Since each leg in multi-legged running systems does roughly the same thing as every other leg, the hopping of a one-legged model can be viewed as a fundamental activity through which running and certain types of walking can be better understood.

Hopping is actually a special case of running, in which all legs provide support at the same time. For a system with one leg, running and hopping are the same. The part of the stepping cycle in which the leg is unloaded, called *transfer*, is also the part of the cycle in which no legs give support, called *flight*. During flight motion of the center of gravity of the system is ballistic. The period when the leg provides support is called *stance*, during which behavior of the system is like that of an inverted pendulum.

The model developed here incorporates a springy leg, in imitation of legs found in nature. While rigid massless leg models have sufficed to study walking [338], [128], leg models that include mass and springs are important for understanding running and hopping. The stiffness of the leg influences the vertical oscillatory behavior of the hopping system and governs the details of landing on the ground and of taking off. The resonant interaction between body mass and springy legs in the vertical direction has a profound impact on the behavior of a running system. This has been shown by McMahon and Green [218] in the human, and by Dawson and Taylor [64] and Alexander and Vernon [7] in the hopping kangaroo.

Previous work on balance began with Cannon's control of inverted pendulums that rode on a small powered truck [141]. His experiments included balance of a single pendulum, two pendulums one atop the other, two pendulums side by side, and a long limber pendulum. Hemami and his co-workers [99], [129], [128], [131], [50], [135], Vukobratovic and his co-workers [164], [338], [342], and others [87], [31], [26], [211], [169] have studied the dynamic characteristics of a variety of multi-link legged models that walk. These models range from a fully static walking biped described by Juricic [164] to the dynamically stabilized five link model of Hemami and Farnsworth [128]. Each of these models relies on continuous contact with the support surface. Additional references to work on walking can be found in the bibliography.

Balance in hopping has also been studied; In 1967 Seifert explored the concept of a hopping vehicle for lunar exploration [302]. Many interesting ideas came from his aerospace approach to that problem. Matsuoka [196] analyzed hopping in humans with a one-legged model. He derived a time-optimal state feedback controller that stabilized his system, assuming that the leg could be massless, and that the stance period could be of very short duration. In fact, legs comprise a substantial fraction of a human's mass, and the duration of stance during running for each leg of a biped is about 40% of the total duration of a stride [196]. Therefore the model used here includes non-zero leg mass, and a ratio of leg stiffness to body mass that makes it operate in a regime where support time is about 40% of stride time.

In this paper control of hopping is presented as two parts, a vertical control part that uses energy measures to regulate hopping height, and a horizontal control part that maintains balance and generates forward travel. Although there are interactions between these activities, their dynamics are not strongly coupled. The section that follows develops the one-legged hopping model and characterizes its behavior. Section III presents an analysis of hopping and the control algorithm used to regulate hopping height. Section IV describes three algorithms that provide balance while hopping in place and running.

### 6.3 The Model

The basic components of legged systems are a set of legs and a body to which the legs are attached. For humans and other animals the body has many actuated degrees of freedom whose actions enhance performance and versatility. For instance, stretching of the back efficiently increases stride length for the running quadrupeds. The body also carries the payload and sensors. The most important characteristic of the body is that it forms an elevated mass that must be balanced atop the legs, and that it forms a structure from which torques can be applied to the legs.

Legs typically do two things during locomotion: they change length and they change orientation with respect to the body. This is true for organisms that crawl, walk, run, and hop, and for organisms with two legs, four legs, six legs, and many legs. A leg changes length to propel the body upward and forward, to cushion landings, and to reduce its own moment of inertia and increase its clearance when swung forward. The lengthening and shortening of a leg during these activities is not merely a kinematic action, but a dynamic action governed by the resonant interaction of leg compliance, body mass, and gravity [46]. Energy is stored in springy muscle and tendon when the leg is shortened, and energy is retrieved when the leg is lengthened. Legs swing back and forth to propel, to permit feet to be precisely positioned with respect to the system's center of gravity, and to change angular momentum.

The model used in this paper, shown in Fig. 6-1, has a single springy leg that articulates with respect to a body about a simple hinge-type hip. The body is represented by a rigid mass, to which the leg is connected. The leg has mass  $M_1$ , moment of inertia  $I_1$ , and the body has mass  $M_2$ , moment of inertia  $I_2$ . The center of mass of the leg is located a distance  $r_1$  from the lower tip of the leg, which is the foot. The center of mass of the body is located a distance  $r_2$  above the hip.

A control torque,  $\tau$ , is generated between the body and the leg at the hip. A simple linear servo is closed around this actuator to position the leg or body. It is of the form:

$$\tau(t) = K_p(\theta_1 - \theta_{1,d}) + K_v(\dot{\theta}_1) \quad (6.1)$$

where

$\theta_{1,d}$  is the desired leg angle, and  
 $K_p, K_v$  are feedback gains.

The same feedback rule is used during stance and during flight, but with different values for  $K_p$  and  $K_v$ , as listed in Appendix VIII.

The leg is composed of a spring in series with a position actuator. The spring is soft in compression and stiff in extension. The soft region of the leg spring represents the ability of the leg to absorb energy when it shortens. The purpose of the stiff region of the spring is to model the effect of a mechanical stop that limits extension of the leg to a maximum length. Modeling the mechanical stop as a spring alone would lead to vibration whenever the spring was fully extended, so damping was added to its stiff region. The damping

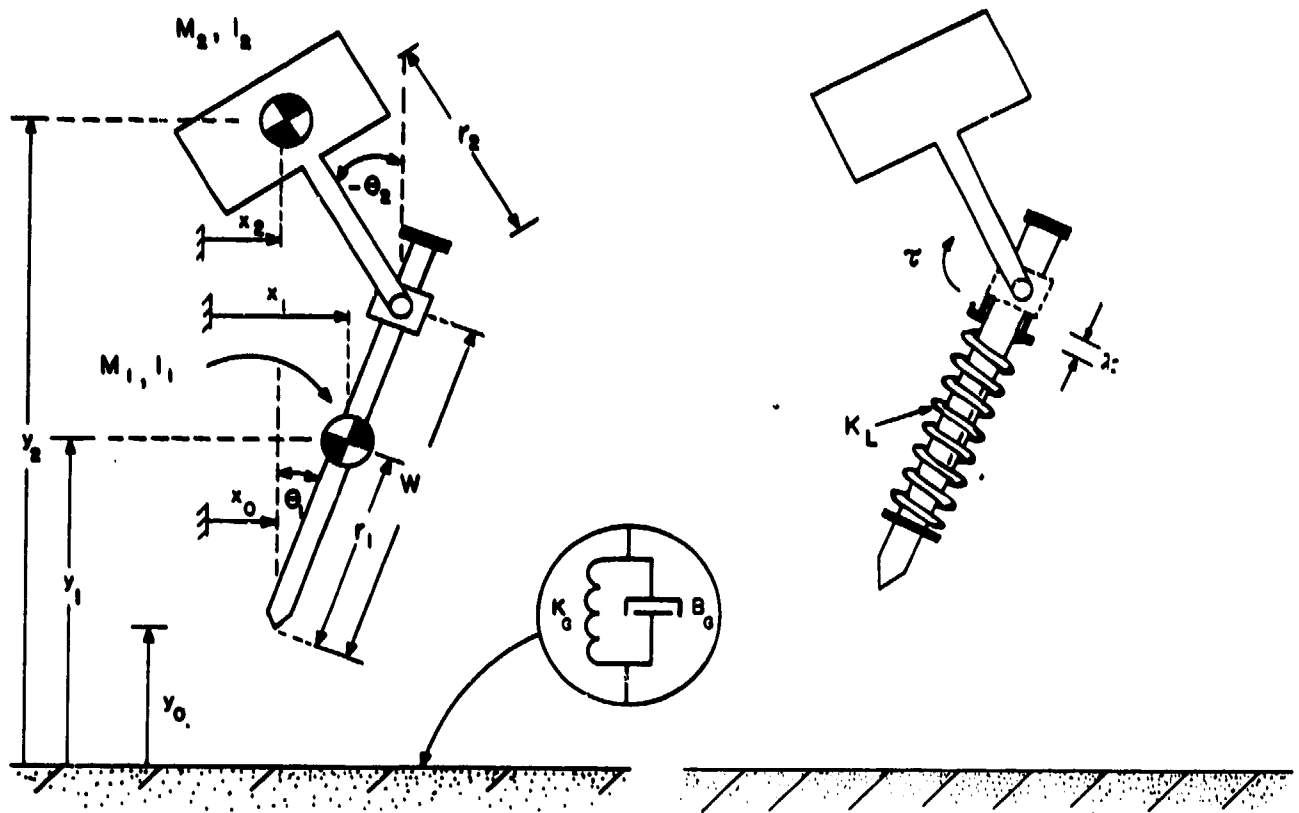


Figure 6-f: Planar one-legged model used for analysis and simulation. The body and leg, each having mass and moment of inertia, are connected by a hinge joint at which torques are generated. The leg consists of a spring in series with a position actuator. The support surface is springy itself in two dimensions. The model is restricted to motion in the plane. See Appendix VII for equations of motion and Appendix VIII for model parameters used in simulations.

coefficient,  $B_{L2}$ , is chosen so that vibrations that occur between body and leg when the stop is hit decay within a few cycles. The length of the position actuator,  $\chi$ , determines the rest length of the leg. While the position actuator is represented as an ideal source, the finite response time of a physical actuator is taken into consideration by requiring that  $\chi$  increase and decrease with a quadratic trajectory:

$$\chi = \chi_0 + k t^2 \quad (6.2)$$

where

- $\chi_0$  is the initial length of position actuator, and
- $k$  is a timing constant

Stroke of the position actuator is limited to  $\chi_{\min} < \chi < \chi_{\max}$ . The importance of this arrangement of actuator, spring, and mechanical stop is that during support, rhythmic activation of the actuator can excite resonant oscillations in the spring-mass system formed by body and leg. As these oscillations build in amplitude, the system will leave the ground and hop.

The support surface is modeled as a two dimensional spring,  $K_G$ , and damper,  $B_G$ . One dimension of the spring acts vertically, the other horizontally, with no interaction between the two. The spring and damper influence the hopper only when the foot is in contact with the ground,  $y_0 < 0$ . During flight the coefficients of spring and damper are zero. Each time the foot touches the ground, the rest position of the horizontal ground spring is reset to the point at which the foot first touches. The damping coefficient is chosen to make vibrations between the foot and ground negligible, while the coefficient of friction between the foot and ground is assumed to be so large that slipping never occurs.

The leg actuator acts between the body and leg spring. Lengthening the actuator when the leg is providing support and the spring is in its soft region does positive work on the system by compressing the spring and accelerating the body mass upward. Shortening the actuator during support does negative work on the system. Changing the length of the position actuator during flight results in no net change in system energy, since this produces oscillations of the leg spring that are rapidly damped by the mechanical stop. Energy is injected into the system over a number of hopping cycles by lengthening the position actuator during support and shortening it during flight. By changing the phase of these actions it is possible to remove energy from the system.

The leg mass,  $M_1$ , represents that portion of the leg below the spring, the rest being included in  $M_2$ . We also assumed that the stiffness of the ground is much greater than the stiffness of the leg,  $K_G \gg K_L$ . When the leg provides support the model is a spring-mass oscillator with natural frequency:

$$\omega_n = \sqrt{\frac{K_L}{M_2}} \quad (6.3)$$

Each stance interval has duration:

$$T_{ST} = \frac{\pi}{\omega_n} = \pi \sqrt{\frac{M_2}{K_L}} \quad (6.4)$$

During flight the model is a gravity-mass oscillator. A full hopping cycle has period:

$$T = \pi \sqrt{\frac{M_2}{K_L}} + \sqrt{\frac{8H_0}{g}} \quad (6.5)$$

where

- $K_L$  is the stiffness of leg spring,
- $H_0$  is the hopping height measured at the foot and
- $g$  is the acceleration of gravity.

For the duration of support to equal the duration of flight, hopping height must be:

$$H_0 = \frac{\pi^2 M_2 g}{8K_L} \quad (6.5)$$

A parameter that is important to the mechanical design of a legged system is how much the spring must compress and the leg shorten during the stance portion of the hopping cycle. The maximum compression of the leg spring during stance is a function of body mass, leg stiffness, and hopping height:

$$\Delta w = \frac{2M_2 g}{K_L} + \sqrt{\frac{M_2^2 g^2}{K_L^2} + \frac{2M_2 g H_0}{K_L}} \quad (6.7)$$

Equations of motion for the model with respect to a ground-centered coordinate system were derived using d'Alembert's principle. The resulting system of non-linear coupled differential equations are given in Appendix VII. These equations describe the system's behavior for both stance and flight, with the characteristic equation of the ground spring responsible for introducing the multi-phase nature of the model. Computer simulations used standard digital numerical integration techniques to determine system behavior as a function of time. The numerical constants used for simulation are given in Appendix VIII.

The simple nature of this model captures the important aspects of dynamic locomotion while keeping complications to a minimum: Since there is only one leg, active balance is studied directly while avoiding the problems of coupling between legs and of multiple support phases. At the same time, vertical oscillations are easily studied by using a leg model that includes mass, spring, and position actuator. Three dimensional dynamics are avoided by considering the planar case.

## 6.4 Vertical Control

The task of synthesizing a system that will control behavior of the one-legged model was broken into two sets of algorithms. One set of algorithms controls forward running velocity, allowing the system to translate from place to place while maintaining the body in an upright posture. This is called horizontal control, about which more is said in the next section. This section discusses a separate control algorithm that controls vertical motion. It generates stable resonant oscillations that cause the locomotion system to hop off the ground, and it controls the height of each hop.

An important function of this hopping motion is to establish a regular cycle of activity within which horizontal and attitude control can take place. A wheel changes its point of support continuously and gradually while bearing weight. Unlike a wheel, a leg changes its point of support all at once and must be unloaded to do so. Therefore, in order for a legged system to balance and to make forward progress there must be periods of support when the leg bears weight making the foot immobile, and there must be other periods when the leg is unloaded and the foot free to move. Such an alternation between a loaded phase and an unloaded phase is observed in the legs of all legged systems. For the present system this alternation is the hopping cycle.

There are four well defined events in the hopping cycle:

- LIFT-OFF: The moment at which the foot loses contact with the ground.
- TOP: The moment in flight when the body has peak altitude and vertical motion changes from upward to downward.
- TOUCH-DOWN: The moment the foot makes contact with the ground.
- BOTTOM: The moment in stance when the body has minimum altitude and vertical motion of body changes from downward to upward.

These events are each detected from behavior of the state variables, and are used to determine four distinct states. The regular cyclic progression among these states suggests use of a finite state sequencer to organize control of the system.

Vertical control must initiate hopping, control hopping height, change between different hopping heights, and terminate hopping. These tasks can be accomplished by regulating the energy in the oscillating spring-mass system formed by the springy leg and the mass of the body. Hopping is initiated by exciting the spring/mass oscillator with the position actuator until hopping velocity is reached -- when the inertial forces are sufficiently large to overcome gravity, the foot leaves the ground and hopping begins. At this point the system becomes a spring/mass, gravity/mass oscillator.

The height of a hop can be controlled by measuring and manipulating the system's energy. For the simplified case in which motion is primarily vertical, angles and angular rates of the leg and body,  $\theta_1$ ,  $\dot{\theta}_1$ ,  $\theta_2$ , and  $\dot{\theta}_2$  are negligible. The total vertical energy during stance:

$$E_{\text{STANCE}} = PE_g(M_1) + PE_g(M_2) + KE(M_1) + KE(M_2) + PE_e(M_1) + PE_e(M_2) \quad (6.8)$$

$$= M_1 g y_1 + M_2 g y_2 + .5 M_1 \dot{y}_1^2 + .5 M_2 \dot{y}_2^2 + .5 K_L (k_0 - w + \chi)^2 + .5 K_G y_0^2$$

where

- $PE_g$  is gravitational potential energy,
- $PE_e$  is elastic potential energy,
- $KE$  is kinetic energy,
- $g$  is the acceleration of gravity, and
- $k_0$  is the rest length of the leg spring.

Additional variables are defined in Fig. 6-1. The expressions for potential energy were chosen so that they are zero when the hopper is standing vertically with the leg spring extended to its rest length and with the foot just touching the ground. As (6.8) shows, energy may be stored in the leg spring, in the ground spring, and in the motion of the body and leg masses.

Energy is lost to the ground damping throughout stance and to air resistance throughout the hopping cycle, but such losses are generally small [280] and are disregarded. Significant energy losses occur at two events in the hopping cycle, TOUCH-DOWN and LIFT-OFF. At TOUCH-DOWN the leg is very suddenly brought to rest by dissipating its kinetic energy in ground damping:

$$E_{TD-LOSS} = KE(M_1) = .5 M_1 \dot{y}_{1,TD-}^2 \quad (6.9)$$

where

$\dot{y}_{1,TD-}^2$  is the vertical velocity just before TOUCH-DOWN.

At LIFT-OFF damping in the stiff region of the leg spring dissipates a fraction of the system's kinetic energy. This fraction can be calculated by equating the system's linear momentum just before and after LIFT-OFF. Since the leg is stationary during stance it's vertical velocity is zero. When the leg extends fully during stance the hopper leaves the ground, accelerating the leg from rest to  $\dot{y}_{1,LO+}$ . After LIFT-OFF the leg and body move at the same rate. Equating linear momentum before and after LIFT-OFF:

$$M_2 \dot{y}_{2,LO-} = (M_1 + M_2) \dot{y}_{2,LO+} \quad (6.10)$$

$$\dot{y}_{2,LO+} = \frac{M_2}{(M_1 + M_2)} \dot{y}_{2,LO-} \quad (6.11)$$

Substituting (6.11) back into (6.8), the kinetic energies before and after LIFT-OFF, and the loss associated with accelerating the leg upward are:

$$KE_{LO-} = \frac{1}{2} M_2 \dot{y}_{2,LO-}^2 \quad (6.12)$$

$$KE_{LO+} = \frac{M_2^2}{2(M_1 + M_2)} \dot{y}_{2,LO-}^2 \quad (6.13)$$

$$E_{LO-LOSS} = \frac{M_1}{M_1 + M_2} KE_{LO-}(M_2) = \frac{M_1 M_2}{2(M_1 + M_2)} \dot{y}_{2,LO-}^2 \quad (6.14)$$

where

$KE_{LO-}(M_2)$  is the total kinetic energy just before LIFT-OFF,  
 $\dot{y}_{2,LO-}^2$  is the vertical velocity of the body just before LIFT-OFF and  
 Subscript LO- means just before LIFT-OFF.

The fraction  $M_2/(M_1 + M_2)$  represents a fundamental efficiency of the leg. It is maximized when the ratio of leg mass to body mass is minimized. This can be done by minimizing the unprung mass of the leg.

To compensate for losses the vertical controller operates the position actuator to increase the vertical energy. When  $\chi$  changes from  $\chi_i$  to  $\chi_i + \Delta\chi$  with  $w < k_0$ , then there is an energy change:

$$\Delta E_{\chi} = K_L [.5 \Delta\chi^2 + \Delta\chi (k_0 - w + \chi_i)] \quad (6.15)$$

Energy is removed when  $\Delta\chi$  is negative. For a given  $\Delta\chi$  the magnitude of  $\Delta E$  depends on the length of the leg and the position actuator. More work is done when the spring is compressed than when it is relaxed. Lengthening the actuator at BOTTOM and shortening during flight causes the total hopping energy to increase. Shortening the actuator at BOTTOM and lengthening during flight causes the total hopping energy to decrease, eventually to zero.

The task of the vertical control algorithm is to manipulate the altitude to which the system will bounce. If the leg spring assumes its rest length during flight, all energy takes the form of gravitational potential when  $\dot{y}_2 = 0$  at the top of each hop. It is possible, therefore, to predict the height of the next hop at any time during stance. All energy is in the form of kinetic energy at LIFT-OFF:

$$E_{LO-} = KE_{LO-} = E_{STANCE} \quad (6.16)$$

The fractional loss of kinetic energy at LIFT-OFF is known from (6.14). Neglecting ground damping and air resistance losses, the total energy during flight is obtained in terms of variables available during stance by combining (6.14) and (6.8):

$$E_{FLIGHT} = KE_{LO+} \quad (6.17)$$

$$\begin{aligned} &= \frac{M_2}{M_1 + M_2} KE_{LO-} \\ &= \frac{M_2}{M_1 + M_2} [M_1 g y_1 + M_2 g y_2 + .5 M_1 \dot{y}_1^2 + .5 M_2 \dot{y}_2^2 + .5 K_L (k_0 - w + \chi)^2 + .5 K_G y_0^2] \end{aligned}$$

For the body to hop to height H the total vertical energy must be:

$$E_H = M_1 g [H - r_2 - (k_0 - r_1)] + M_2 g H \quad (6.18)$$

During stance the energy change needed to produce a hop of height H:

$$\Delta E_H = E_H - E_{LO+} \quad (6.19)$$

$$= \frac{M_2}{M_1 + M_2} E_{STANCE}$$

This energy can be supplied or removed by the vertical actuator. From (6.15) and (6.19) the linear actuator must extend by:

$$\Delta\chi = -(\chi - w + k_0) + \sqrt{(\chi - k_0 + w)^2 + \frac{2\Delta E_H}{K_L}} \quad (6.20)$$

Simulations were used to evaluate application of this vertical control algorithm to the model. Each time BOTTOM occurred, indicated by  $\dot{y}_0$  changing sign from negative to positive, (6.8) and (6.17) were used to predict hopping height. The length of the leg actuator,  $\chi$ , was then increased or decreased accordingly. Figure 6-2 plots the vertical position of the foot and body, and the actuator length during a period of increasing hopping height, and during stable-hopping. Starting at rest, the system executed a positive work cycle on each hop until the vertical energy increased to the specified value. This level was then maintained. Since the stroke of the position actuator was limited to  $\chi_{\max}$ , the energy that could be injected on a single cycle was limited. A number of cycles therefore were required to achieve the desired hopping height.

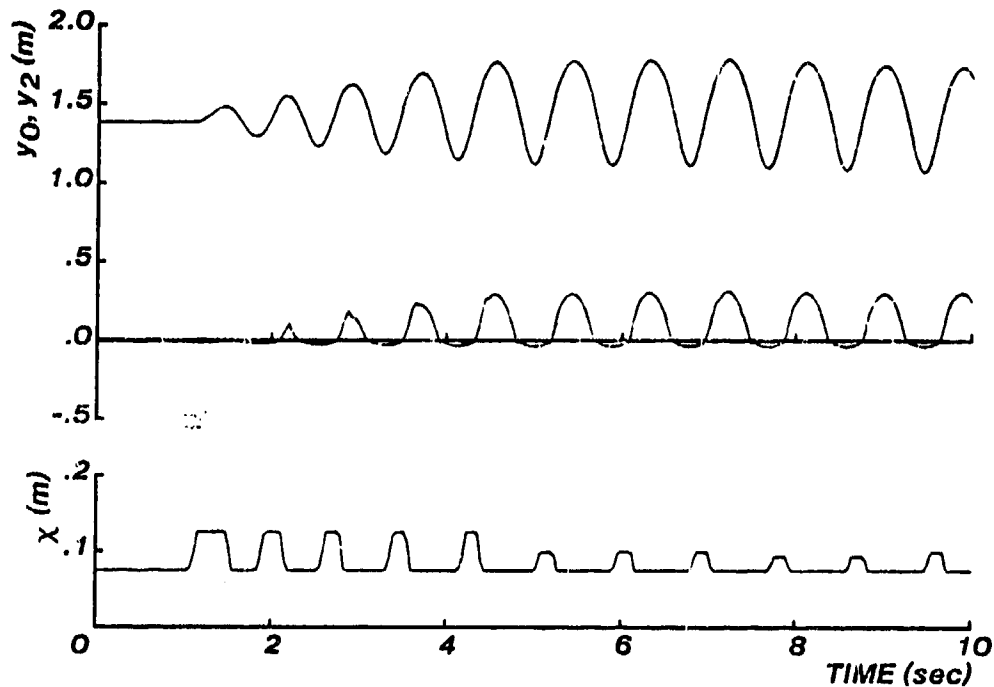


Figure 6-2: Vertical hopping. Starting from rest, vertical energy was increased until desired hopping height was attained. Hopping height was regulated through the position actuator that acts in series with the leg spring. Note different vertical scales. Top curve: elevation of hip. Middle curve: elevation of foot.

The last 2 seconds of data from Fig. 6-2 are replotted in the phase plane in Fig. 6-3. The body velocity is plotted on the abscissa and body altitude is plotted on the ordinate. The parabolic trajectory during flight was caused by constant gravitational acceleration, and the harmonic trajectory during stance was due to the spring. The four events that synchronized actions of the controller to behavior of the hopping system, LIFT-OFF, TOP, TOUCH-DOWN, and BOTTOM are indicated in the figure.

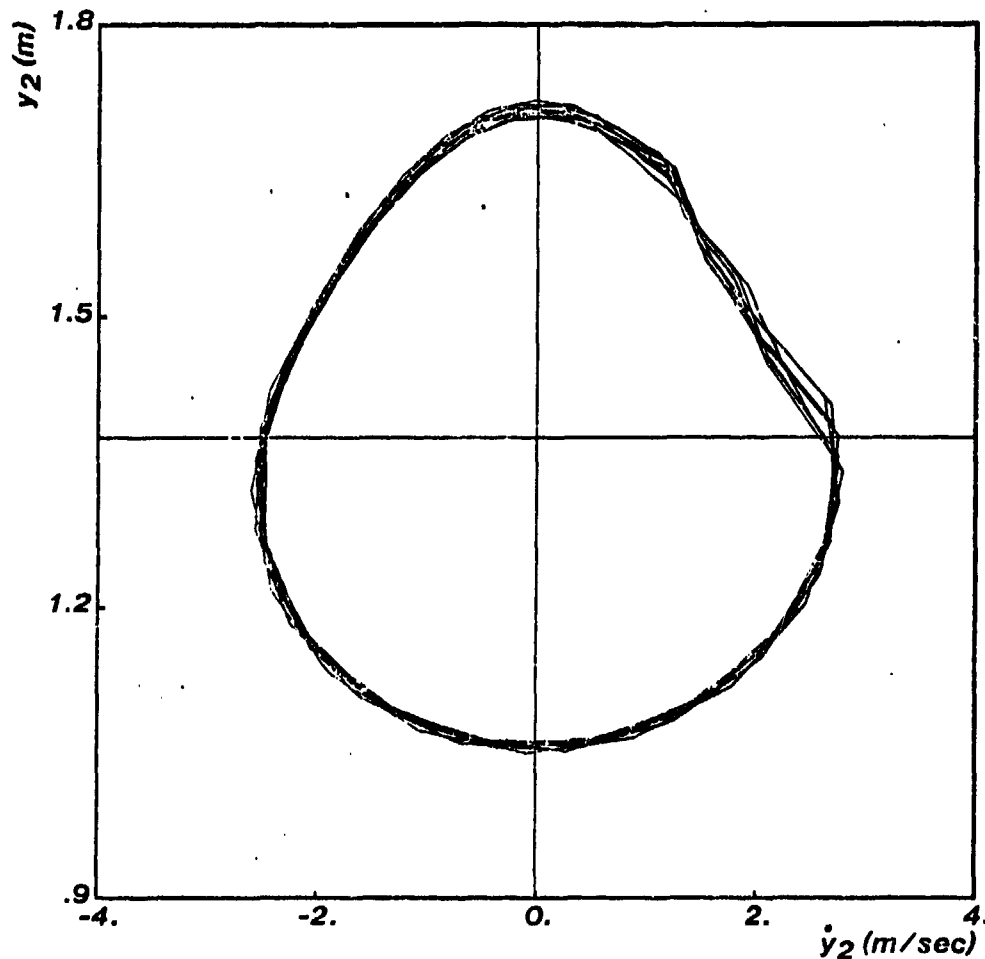


Figure 6-3: Phase plot for vertical hopping. Four synchronization events are indicated where curve crosses axes. Data are from stable part of Figure 6-2. The rough part of the curves between LIFT OFF and TOP indicate the damped vibration that occurred when the mechanical stop was hit. Note that position is plotted on the ordinate, velocity is on the abscissa, and the action advances in a counterclockwise direction.

Figure 6-4 is a plot of vertical energy during two cycles of fixed height hopping. A lossless system would produce a perfectly flat total energy line. The primary losses occur when the foot strikes the ground, and when it leaves the ground, as indicated by (6.9) and (6.14). Energy increases during the latter part of stance, when the actuator lengthens. These data are similar in qualitative detail, to those obtained for the kangaroo by Alexander and Vernon [7].

Figure 6-5 shows an 80 second simulation sequence of vertical hopping in which desired height was adjusted a number of times. It was mentioned earlier that the leg actuator could be used to remove energy from the

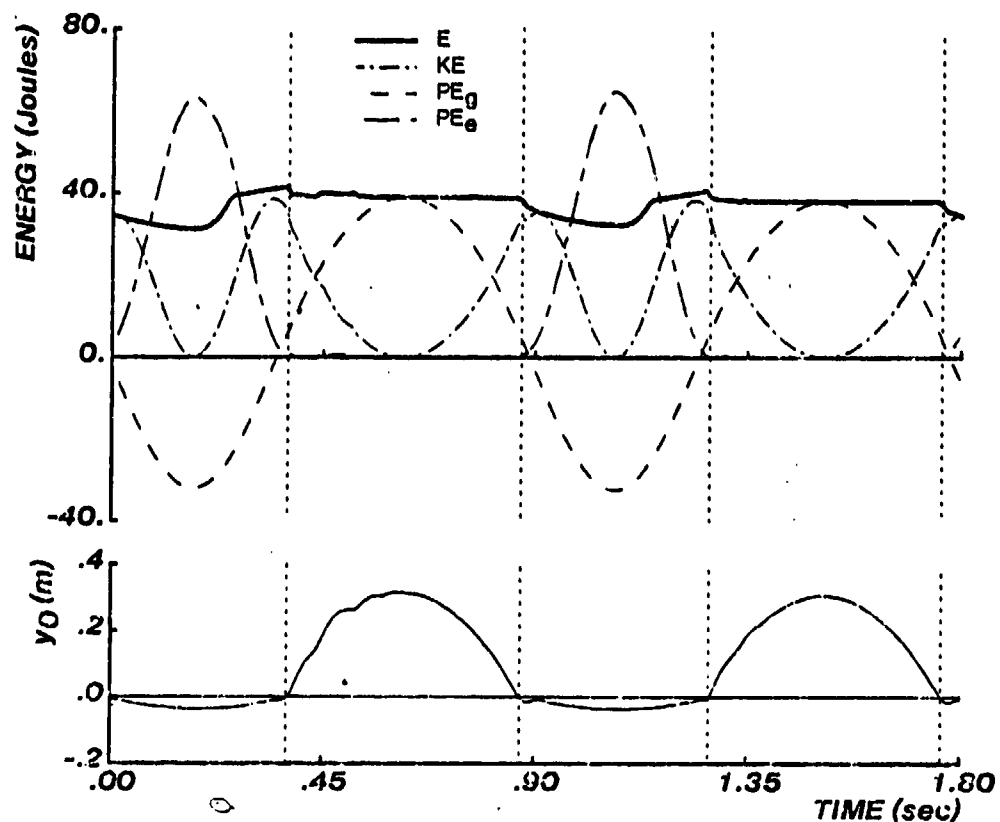


Figure 6-4: Vertical energy for two hopping cycles at constant hopping height. Total energy, kinetic energy, gravitational potential, and elastic potential are shown. Primary losses of energy occur at TOUCH-DOWN and LIFT-OFF, indicated by the vertical dotted lines. Data are from Fig. 6-2,  $t = 7.5$  to  $9.3$  sec.

system, to reduce hopping height. The figure shows that a descent employing active damping ( $t=45$ ) was more rapid than one relying on passive system losses ( $t=65$ ). In general, the algorithm obtained good control of hopping height.

The time at which the leg is shortened during a steady state hop cycle can be manipulated to optimize hopping according to a variety of criteria:

- When the leg is shortened at LIFT-OFF, ground clearance of the foot during flight is optimized. This is important when terrain is uneven or when large horizontal swinging motions of the leg occur during flight, as when the model translates at high speed. If the leg is not short during swing it may become difficult to avoid *stopping the toe*. Shortening at LIFT-OFF also minimizes the leg's moment of inertia during flight, so the leg can be swung forward faster and with less angular effect on the body.
- When the leg is shortened at TOP, the time between vertical actuations is maximized. This strategy could permit use of an actuator of lower bandwidth.

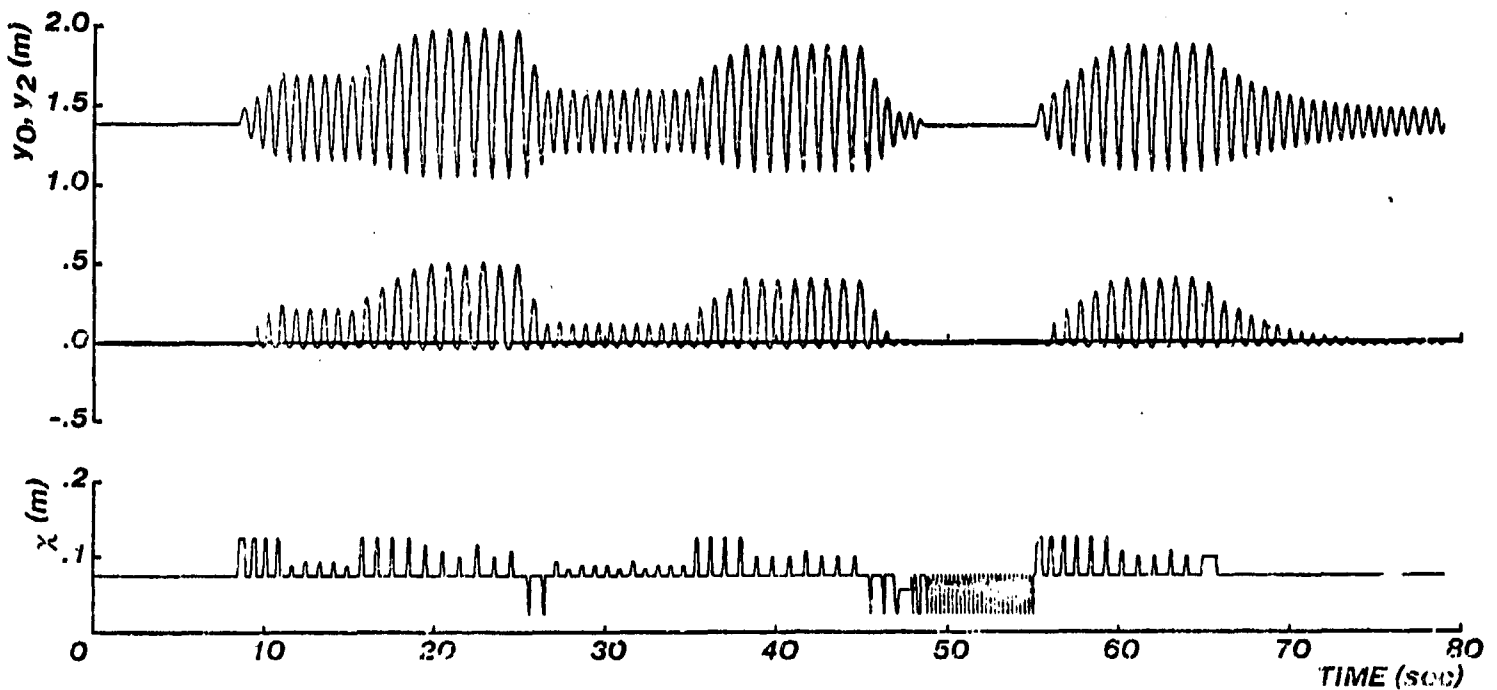


Figure 6-5: Vertical hopping sequence. At times  $t = 9, 15, 25, 35, 45, 55, 65$  desired hopping height  $H = 1.7, 2.0, 1.6, 1.9, 1.4, 1.9, 1.4$ . The descent beginning at  $t=45$  was actively damped, while the descent at  $t=65$  was passive. Top curve: elevation of hip. Middle curve: elevation of foot.

- When the leg is shortened occurs upon TOUCH-DOWN, then the ground impact forces on the foot are minimized. This strategy is normally used by humans when they are asked to hop in place on a flat floor.

It is also possible to shorten the leg at LIFT-OFF, lengthen it again just before the next TOUCH-DOWN, and let it shorten during the landing. This strategy, apparently used by humans when running, maximizes ground clearance and simultaneously minimizes impact forces on the foot. However this is accomplished at the expense of additional actuator bandwidth. Although more energy is required for these extra lengthening and shortening motions, the leg can be swung forward more efficiently with a lower moment of inertia.

## 6.5 IV. Horizontal Control

The preceding section discusses the vertical hopping behavior of the model, and a method for controlling hopping height. We now turn to the question of balance, and control of travel from place to place. These two phenomena are intimately related. The tasks of a balance algorithm are to ensure that there are no unwanted horizontal motions, that horizontal motions of adequate velocity are generated when necessary, and that the locomotion system does not tip over.

An important characteristic of dynamically stabilized legged systems is that they are always tipping, but their control system ensures that the tipping motions are controlled and orderly. Two mechanisms can be used to control balance and horizontal travel: foot placement and hip motion. Placement of the foot with respect to the center of gravity of a locomotion system has a powerful influence on the tipping and horizontal motion of the system. Gravity generates a moment about the foot proportional to the horizontal displacement of the foot from the center of gravity. Foot placement can be adjusted during the flight part of each hop to influence attitude and translation during the next stance interval. The pattern of hip motion between the body and leg during stance influences the angular momentum. Such motions change the momentum of the system only during stance when there is adequate friction to hold the foot firmly in place on the ground.

Actually, there is a third mechanism that can influence the balance and horizontal travel of a legged system. Since a leg is not always vertical, it is possible to influence the system's horizontal behavior by modulating the forces generated along the leg's axis. Effective use of this mechanism, however, requires intimate coordination between vertical and horizontal control. In order to keep the vertical control mechanisms separate from the horizontal control mechanisms, and thereby obtain simplicity in the control, this mechanism is not used. Rather, we assume that the pattern of axial leg forces is dictated solely by the requirements of regulating resonant vertical hopping.

The remainder of this section explores three algorithms for controlling balance and travel. The first method relies solely on foot placement as a means for effecting horizontal control, with no hip motion during stance. The second method uses an improved foot placement algorithm that is developed by considering the kinematic constraints imposed by constant velocity locomotion. The improved foot placement is combined with hip motion that sweeps the leg backwards during stance. The third method uses the same foot placement as method two, but gets better control of body attitude by servoing the body angle during stance.

### 6.5.1 Method 1: Foot Placement

Each time a hopping system touches the ground the foot can be positioned horizontally to influence the translation and tipping of the system. When hopping upright in place, ( $\theta_2 = 0$ ,  $\dot{\theta}_2 = 0$ ,  $\dot{x}_2 = 0$ ), movement of the foot to one side during flight causes the body to tip and translate toward the other side during stance. Similar rules hold when the system is not upright and stationary. Therefore, if the hip angle is kept fixed during stance, i.e.  $(\theta_2 - \theta_1)_{LO} = (\theta_2 - \theta_1)_{TD}$ , then the model behaves qualitatively like a one link inverted pendulum. It is not precisely an inverted pendulum because the leg shortens during stance.

A simple algorithm to balance the model uses linear feedback to place the foot. Two factors determine where the foot should be placed: the projection of center of gravity and an error function of state variables. First, the projection of the center of gravity,  $x_{CG}$ , is calculated. Then a linear function of errors in state,  $x_{ERR}$ , is added. Model kinematics are then used to calculate a leg angle that places the foot. Since the leg has mass, movement of the leg changes the projection of the center of gravity -- simultaneous equations are solved. The following analysis is done in a coordinate system that translates with the hip.

Find horizontal position of center of gravity:

$$x_{CG} = \frac{(r_1 - w)M_1 \sin(\theta_1) + r_2 M_2 \sin(\theta_2)}{M_1 + M_2} \quad (6.21)$$

Calculate linear combination of state errors to provide corrective feedback:

$$x_{ERR} = K_1(\dot{x}_2 - \dot{x}_{2,d}) + K_2(\theta_2 - \theta_{2,d}) + K_3(\dot{\theta}_2) \quad (6.22)$$

where

$\dot{x}_{2,d}$ ,  $\theta_{2,d}$  are desired values for  $\dot{x}_2$  and  $\theta_2$ , and  
 $K_1$ ,  $K_2$ ,  $K_3$  are feedback gains.

Place foot at TOUCH-DOWN:

$$x_{TD} = x_{CG} + x_{ERR} \quad (6.23)$$

Take kinematics of model into account:

$$w \sin(\theta_1) = -x \quad (6.24)$$

Substitute (6.21), (6.22), and (6.23) into (6.24) and solve for foot placement with respect to hip:

$$x_{TD} = w \frac{r_2 M_2 \sin(\theta_2) - (M_1 + M_2) x_{ERR}}{r_1 M_1 + w M_2} \quad (6.25)$$

Apply leg kinematics again to obtain corresponding leg angle:

$$\theta_1 = -\text{Arcsin} \left[ \frac{r_2 M_2 \sin(\theta_2) - (M_1 + M_2) x_{ERR}}{r_1 M_1 + w M_2} \right] \quad (6.26)$$

The servo given in (6.1) is used to move the leg to this angle.

Figures 6-6 and 6-7 show results from simulation using the foot placement algorithm. The data of Fig. 6-6 show correction of a large error in body attitude that was introduced through the initial conditions. The 0.5 radian initial error in body attitude,  $\theta_2$ , was corrected in about 6 hops. In this simulation horizontal position was not controlled, so the transient error in horizontal velocity causes the system to come to rest some distance from the origin. Figure 6-7 shows the response of the same foot placement algorithm to a pair of step changes in desired horizontal position. Control of  $x_2$  is accomplished by implementing a position controller of the form:

$$\dot{x}_{2,d} = \min\{K(x_2 - x_{2,d}), \dot{x}_{2,d,max}\} \quad (6.27)$$

Desired body angle,  $\theta_{2,d}$ , is also manipulated during translations. Balance using this method was stable with a variety of initial conditions and body attitudes.

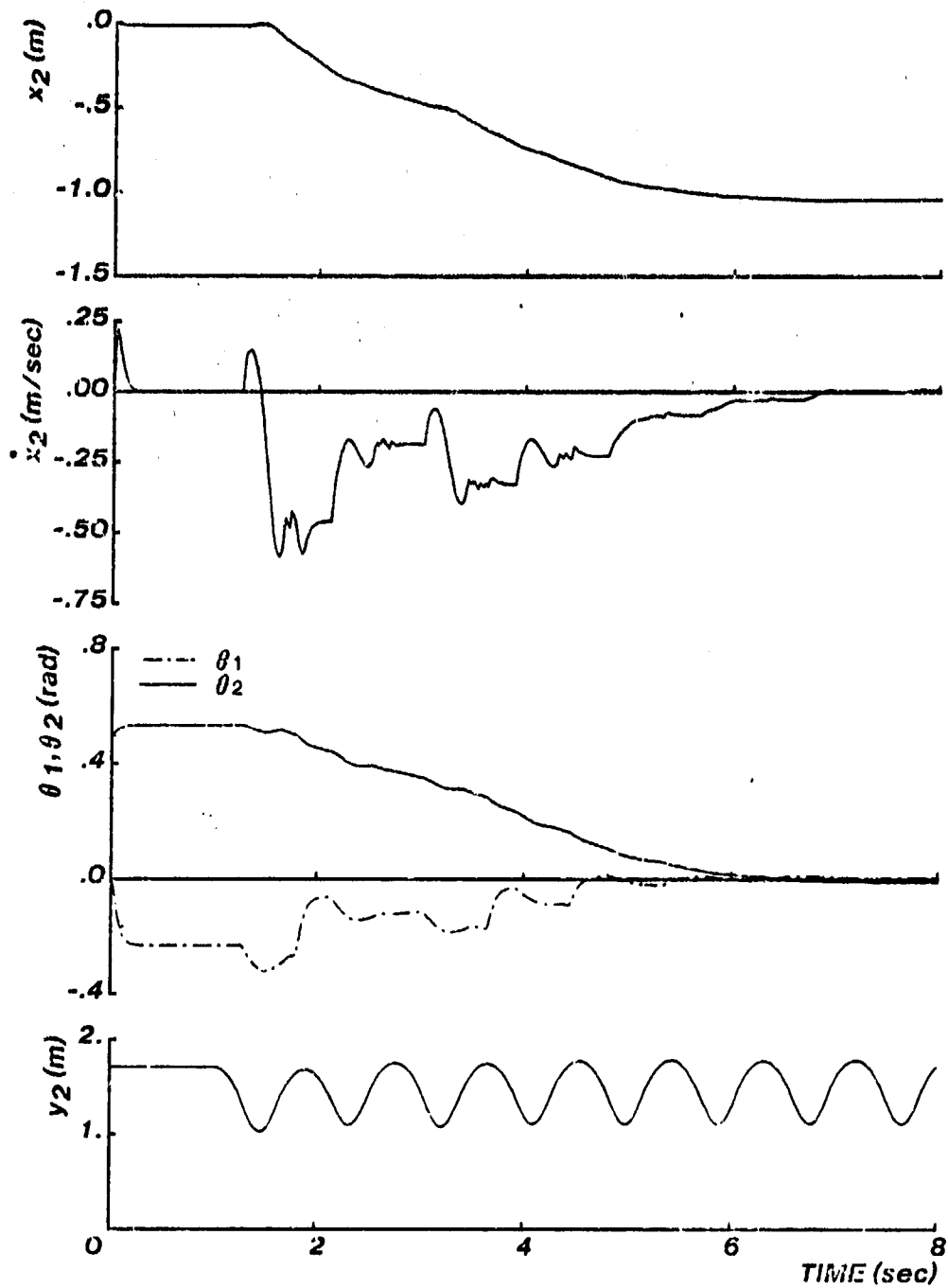


Figure 6-6: Test of foot placement controller. At  $t=0$  initial error in body attitude was 0.5 radians. At  $t=1$  gravity is turned on and hopping begins. State errors approached zero in about 7 sec.  $K_1=0.05$ ,  $K_2=0.3$ ,  $K_3=0.1$ .

Limit cycle oscillations in horizontal velocity were observed in the data, especially at forward velocities greater than about .25 m/sec. Maximum rate is limited because motion of the leg is restricted during stance by the fixed hip angle. Another consequence of the fixed hip is the *hunched* posture assumed by the body and leg during travel.

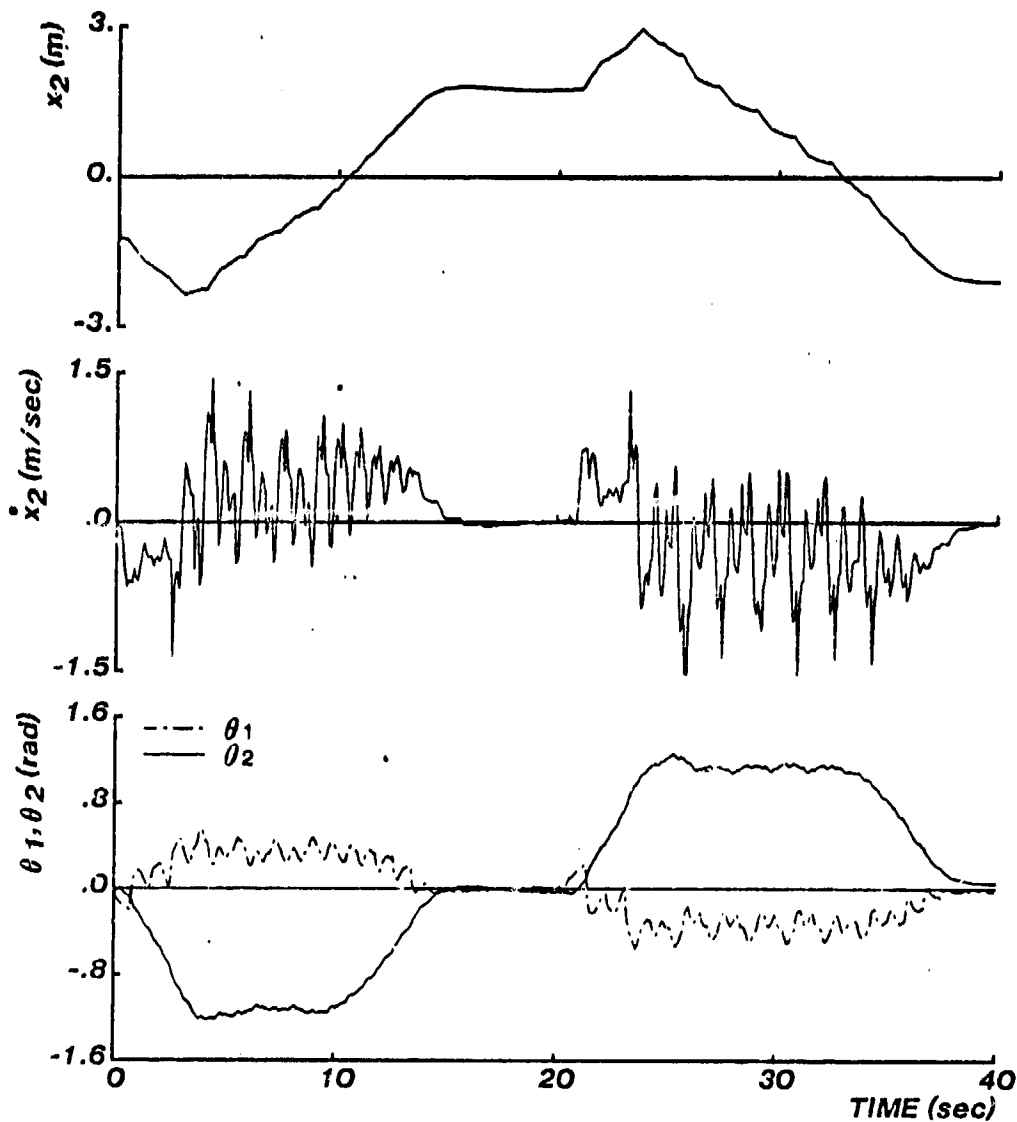


Figure 6-7: Response of model to step in  $x_{2,d}$  using foot placement algorithm. Horizontal position errors generated rate setpoints as described in text.  $K_1=0.18$ ,  $K_2=0.3$ ,  $K_3=0.4$ .

### 6.5.2 Method 2: Leg Sweeping

The leg sweeping algorithm is based on a generalization of the foot placement approach just described. It arises when one thinks about the constraints imposed by constant velocity travel, the legged system's kinematics, the forces generated between the foot and the ground, and the need to balance. We start by finding the nominal motion that will maintain constant forward velocity with no tipping, and then modify this motion to eliminate deviations from the desired state. The resulting algorithm has two parts; one part that places the foot to control balance and tipping, and another part that moves the hip during stance to control forward velocity.

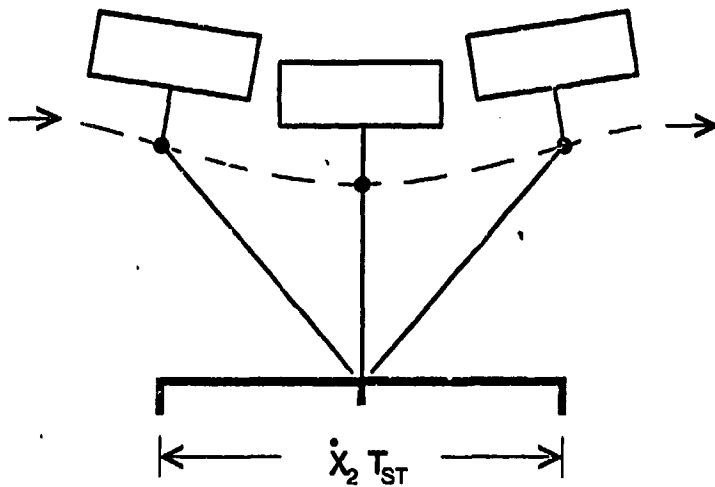


Figure 6-8: When the foot is placed in the center of the CG-print, there is symmetry in the model's motion. Running from left to right, the left-most drawing shows model's configuration just before TOUCH-DOWN, the center drawing shows configuration at BOTTOM, and right-most drawing shows configuration just after LIFT-OFF.

In natural biped running each leg extends forward during flight so that the foot first touches the ground some distance in front of the body. During stance the leg sweeps backward with respect to the body. The foot then leaves the ground some distance behind the body and the other foot extends forward. There is a symmetry in this motion about the point half way through stance, when the leg is directly under the center of gravity. Figure 6-8 diagrams the symmetry. This symmetrical motion causes no tipping because the center of gravity spends about an equal time in front of the point of support, and an equal time behind it. The gravitational tipping moments average to zero throughout stance.

In order to achieve symmetry of this sort for the one-legged model, the control system must determine the locus of points over which the center of gravity will travel during the next stance period. We call this locus a *CG-print*, in analogy to a footprint. The length of the CG-print is just the product of the forward velocity and the duration of stance. In the steady state the control system places the foot in the center of the CG-print.

When the attitude of the body deviates from its desired value, the control system moves the foot from the center of the CG-print to correct the error. Placing the foot forward of the center of the CG-print will create a net backward tipping moment during stance, while placing it behind the center of the CG-print will create forward tipping. Figure 6-9 illustrates the three cases. A linear combination of state errors to determine how far to move the foot from the center of the CG-print. The method uses the same rule for placing the foot with respect to the center of the CG-print as the last method used for placing the foot with respect to the projection of the center of gravity.

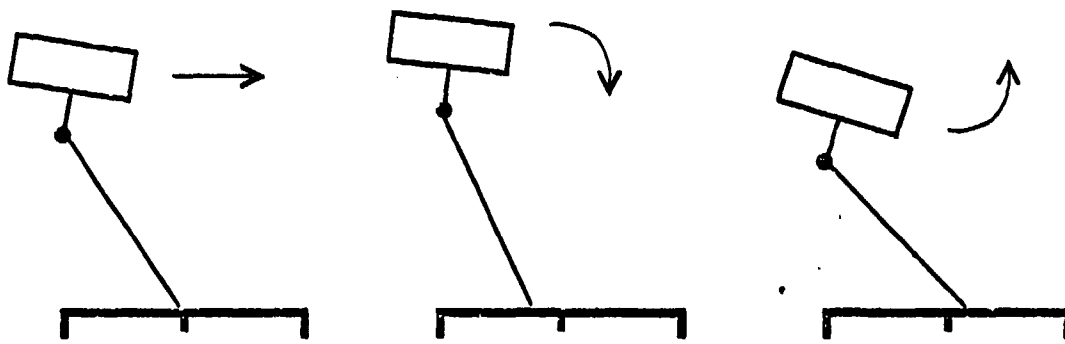


Figure 6-9: Three types of behavior when foot is placed in CG-print. a) Foot is placed in center of the CG-print. No angular change in model, horizontal velocity is unmodified. b) Foot is placed toward rear of CG-print, causing body to tip forward during stance interval. c) Foot is placed toward front of CG-print, causing body to tip rearward during stance interval. Horizontal lines indicate CG-print, locus of projection of center of gravity during stance.

Motion of the hip during stance generates forces between the ground and the foot that determine how the system's forward velocity will change. If the system is to progress at a constant forward rate with no forward acceleration, then the horizontal component of all forces acting on the system must be zero. Viewing the problem in a coordinate system that moves forward with the hip, the task is to make the foot sweep backward at the same rate as the ground. The leg sweeping algorithm accomplishes this task by calculating a target angle for the hip at each moment during stance. The target angle is based on the rate of forward travel, the instantaneous length of the leg, the time that passed since TOUCH-DOWN, and the placement of the foot relative to the hip at TOUCH-DOWN. Under nominal conditions this motion will cause the resultant force acting on the foot to be vertical.

When the forward velocity deviates from the desired value, the sweeping motion of the leg no longer results in a match between the speed of the foot and the ground. The result will be an accelerating or retarding force that corrects the velocity error. Faster leg sweeping will accelerate forward velocity, and slower sweeping will retard it.

If the duration of stance, the horizontal velocity of the body, and the geometry of the vehicle are known, then an appropriate leg angle for TOUCH-DOWN and a sweeping function for the leg can be calculated. The duration of stance can be recorded from the previous hop. When the horizontal velocity is  $\dot{x}_2$ , the horizontal distance traversed during stance, the length of the CG-print, is:

$$\Delta x_{\text{STANCE}} = \dot{x}_2 T_{\text{ST}} \quad (6.28)$$

Combining (6.28) with (6.25) a new equation for foot placement is obtained:

$$x_{\text{TD}} = w \frac{r_2 M_1 \sin(\theta_2) - (M_1 + M_2) x_{\text{ERR}}}{r_1 M_1 + w M_2} + \frac{\Delta x_{\text{STANCE}}}{2} \quad (6.29)$$

For vertical hopping in place, where  $\dot{x}_2 = 0$ , (6.29) reduces to (6.25) of the last section. During stance leg angle must change in a specified way in order to satisfy the symmetry argument for zero net ground force and moment. At time  $t$  during stance:

$$x(t) = \lambda_{FD} + \frac{(t - t_{FD})}{T_{ST}} \Delta x_{STANCE} \quad (6.30)$$

Once again, taking the kinematics of the model into account, a leg sweeping function can be found:

$$\theta_1(t) = -\text{Arcsin}\left(\frac{x(t)}{w}\right) \quad (6.31)$$

Though the leg is vertical only momentarily during each stride, a sweeping serve employing (6.30) and (6.31) resolves leg springiness into the vertical direction. Horizontal foot motion is rigid.

Figures 6-10, 6-11, 6-12, and 6-13 show the results of simulating this algorithm. Figure 6-10 shows a constant velocity translation at 0.75 m/sec. These data show that horizontal velocity was well controlled, with only small variations within each cycle. The leg swung forward during flight to place the foot, and swept backward during stance to minimize horizontal ground forces. The leg and the body counter-oscillated. Body attitude was kept to within 0.1 radians of vertical, with a distinct 0.3 hz oscillation superimposed on the stepping oscillation.

To accommodate forward acceleration a compromise between actual and desired velocity was used to calculate the length of the CG-print.

$$\Delta x_{STANCE} = \begin{cases} (\dot{x}_2 - \Delta \dot{x}_{MAX}) T_{ST} & \text{for } \dot{x}_{2,d} < (\dot{x}_2 - \Delta \dot{x}_{MAX}) \\ (\dot{x}_2 + \Delta \dot{x}_{MAX}) T_{ST} & \text{for } \dot{x}_{2,d} > (\dot{x}_2 + \Delta \dot{x}_{MAX}) \\ \dot{x}_{2,d} T_{ST} & \text{otherwise.} \end{cases} \quad (6.32)$$

$\Delta \dot{x}_{MAX}$  limits the magnitude of sudden changes in desired velocity. Eq. (6.32) replaces (6.28). The controller employing this algorithm stretches the leg forward and lengthens the stride in order to accelerate the model.

Figure 6-12 demonstrates regulation of forward velocity as the system accelerates smoothly. The same data are shown in cartoon form in Fig. 6-13 where the pattern of motion can be more easily visualized. The paths of the body and foot are indicated by a string of dots that correspond to equal time intervals. After about 10 seconds the rate of travel is 2.2 m/sec. The rightmost strides in this cartoon show that clearance of the foot above the ground was reduced as stride and speed increased. The model's tendency to stub its toe as clearance is reduced is the factor that limits maximum speed.

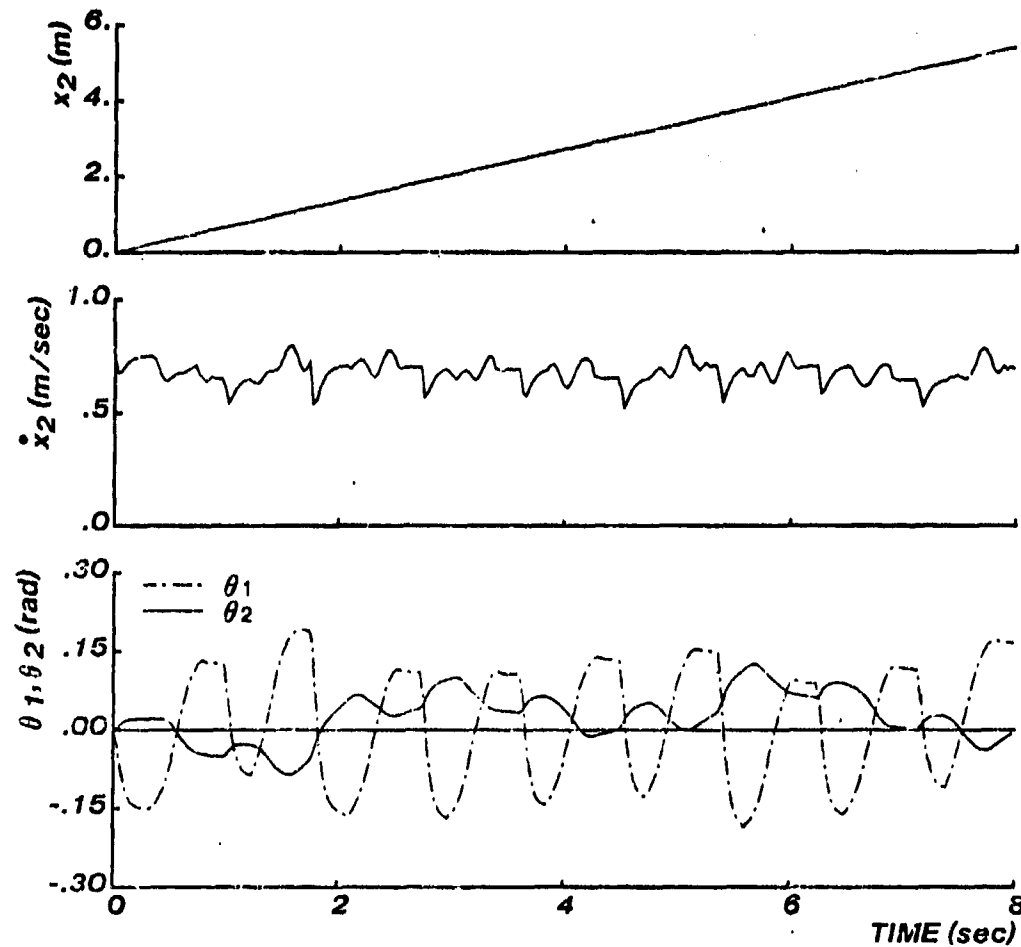


Figure 6-10: Running at constant horizontal rate is generated by algorithm that places the foot in the center of the CG-print, and then sweeps the leg backward during stance. Rate of travel is .75 m/sec. ( $K_1=0.2$ ,  $K_2=0.1$ ,  $K_3=0.1$ )

Figure 6-11 demonstrates the algorithm's ability to respond to changes in velocity setpoint. The model starts hopping in place, then accelerates to 1 m/sec, then to 2 m/sec, and then slows to a stop. Velocity control is reasonably good once the model has accelerated up to speed. Control of body attitude is not particularly good. At 2 m/sec the body deviates from vertical by about .3 m/sec.

### 6.5.3 Method 3: Servo Attitude

The leg sweeping algorithm maintained an even forward velocity, but it did not control the attitude of the body with any precision. In Fig. 6-12 the body deviates from its erect position by about 0.3 radians when running at full speed. Instead of using the hip actuator to sweep the leg according to the running rate, method 3 uses the hip actuator to erect the body during stance. Placement of the foot in the CG-print is as before using (6.22), (6.28), and (6.29):

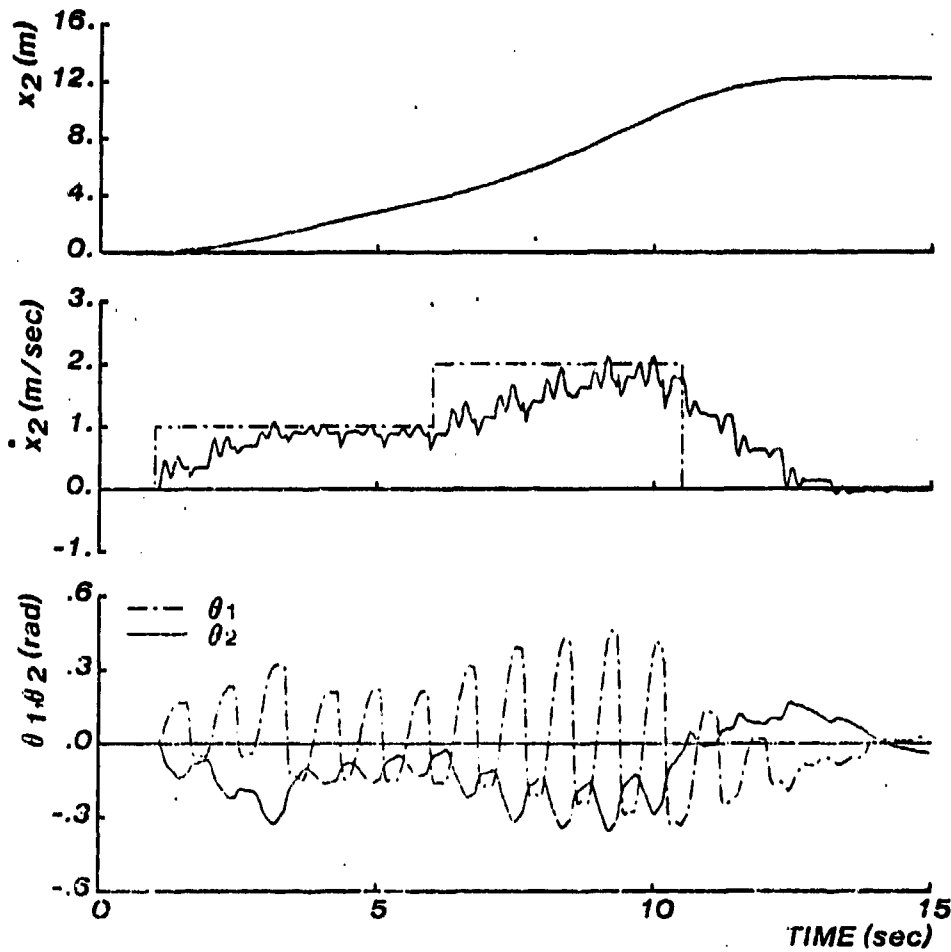


Figure 6-11: Leg sweeping algorithm controls running as desired velocity,  $\dot{x}_{2,d}$  (shown stippled in second plot), changed in steps. ( $K_1=0.2$ ,  $K_2=0.1$ ,  $K_3=0.1$ ,  $\Delta x_{\max}=0.45$ )

$$\tau(t) = K_p(\theta_2 - \theta_{2,d}) + K_v(\dot{\theta}_1) \quad (6.33)$$

where  $\theta_{2,d}$  is selected on each hop to make the average body angle zero.

This algorithm controls forward velocity through placement of the foot, and the accelerations that result from tipping. Since the hip servo erects the body during stance, placement of the foot with respect to the center of the CG-print exclusively controls forward velocity,  $K_2 = K_2 = 0$ . Figure 6-14 shows the behavior of this algorithm when executing the same sequence of steps in forward velocity that were used to produce Fig.6-12.

Method 3 is simpler to implement than the leg sweeping algorithm. It is not necessary to servo a hip trajectory during stance, as required by (6.30). A setpoint for desired body angle is specified once during stance, and another setpoint for leg angle is specified during flight. The fore and aft swinging motions of the leg that characterize running are not explicitly programmed, but the result of interactions between the servos that alternate satisfying these two setpoints.

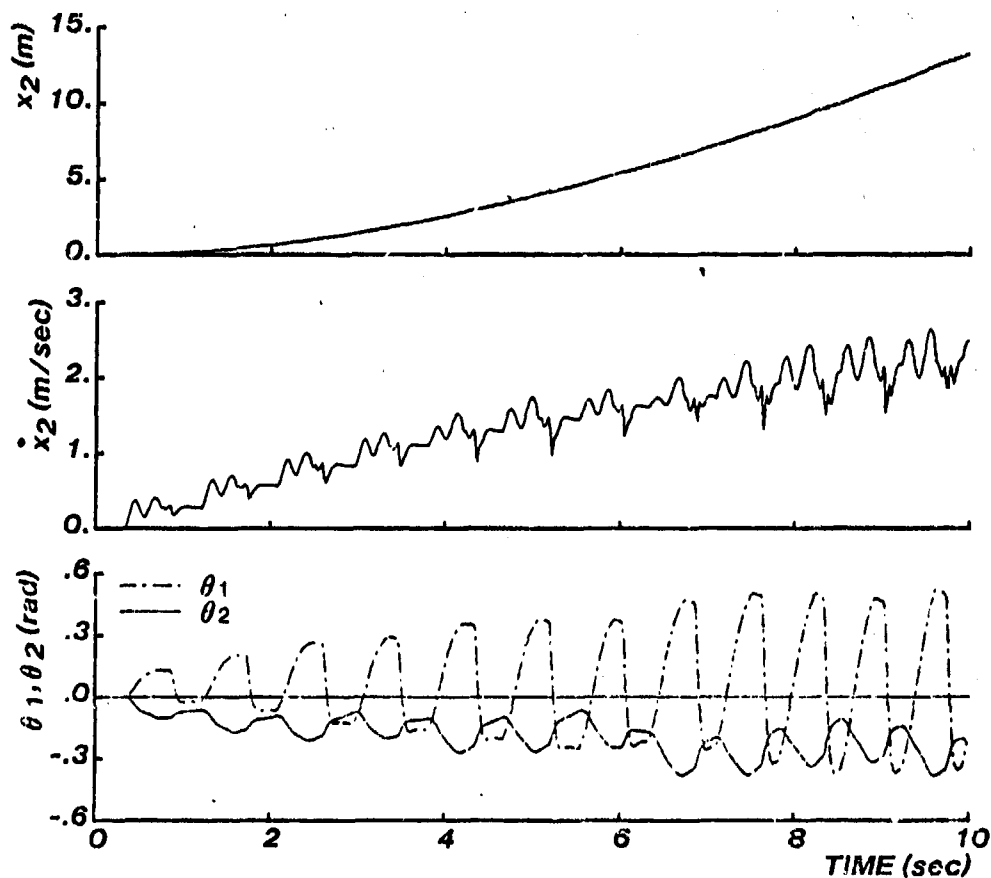


Figure 6-12: Sweep control algorithm was extended to generate horizontal acceleration. Starting from rest the model increases its rate of travel up to about 2.2 m/sec. These data are replotted in cartoon form in Fig. 6-13. ( $K_1=0.2$ ,  $K_2=0.1$ ,  $K_3=0.1$ )

Method 3 is also simple because it allows control of running to be decomposed into three separate parts. One part controls hopping height by regulating the amount of thrust delivered on each hop. A second part controls forward velocity by placing the foot with respect to the center of the CG-print. The third part controls attitude of the body by servoing the hip joint during stance. No explicit coupling between these parts is required.

## 6.6 V. Conclusion

The long range goal of this work is to develop an understanding of balance and dynamics in legged locomotion that will help to explain behavior observed in biological legged systems, and to lay the groundwork needed to construct useful legged vehicles. The purpose of this paper is to describe results obtained from modeling and simulating a legged system that hops on one leg. Such a model encourages focus on the problem of balance, without attending to the coordination of many legs.

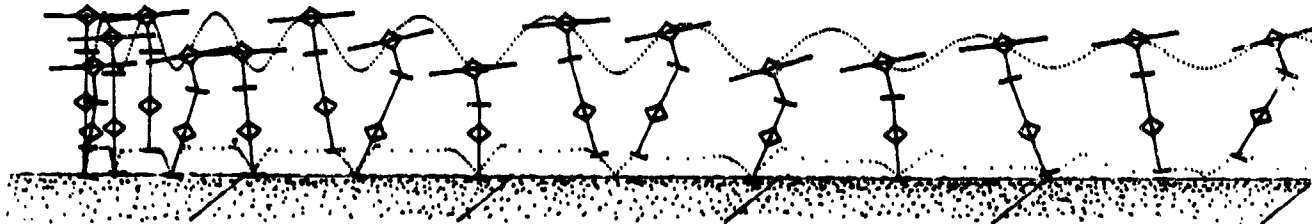


Figure 6-13: Cartoon of running controlled by leg sweeping algorithm. Model accelerates from standing start to about 2.2 m/sec in 10 sec. The dotted lines represent the paths of hip and foot. (20 msec/dot, .6 sec/stick figure.) Maximum speed is limited by clearance between foot and ground. When the stride becomes too long the model *stubs its toe*.

The model consists of a body, an actuated hinge-type hip, and a leg. The leg is massful, it is springy, and its length can be controlled by a position actuator. We separate control of the model into a vertical hopping part and a horizontal balance part. Vertical control takes advantage of the springy leg to achieve resonant hopping motion. The control system regulated hopping height using a measure of vertical energy to control the thrust delivered on each hop.

Horizontal control ensures that the body is maintained in an upright posture, and that the rate of forward travel is well controlled. We explored three algorithms for horizontal control; method 1, the foot placement algorithm, method 2, the leg sweeping algorithm, and method 3, the attitude control algorithm.

- Method 1: The foot placement algorithm places the foot with respect to the projection of the center of gravity, and holds the hip fixed during stance. It maintained balance when hopping in place, but could move forward only slowly.
- Method 2: The leg sweeping algorithm uses the CG-print to calculate a where to put the foot on each step, and a hip trajectory that will control forward travel. It controlled forward velocity with good precision, but control of body angle was poor.
- Method 3: The attitude control algorithm also uses the CG-print to place the foot, but hip torque during stance controls body attitude. This simpler algorithm control forward velocity and attitude with good precision.

Control of running in the one-legged model can be decomposed into height control, a forward velocity control, and attitude control.

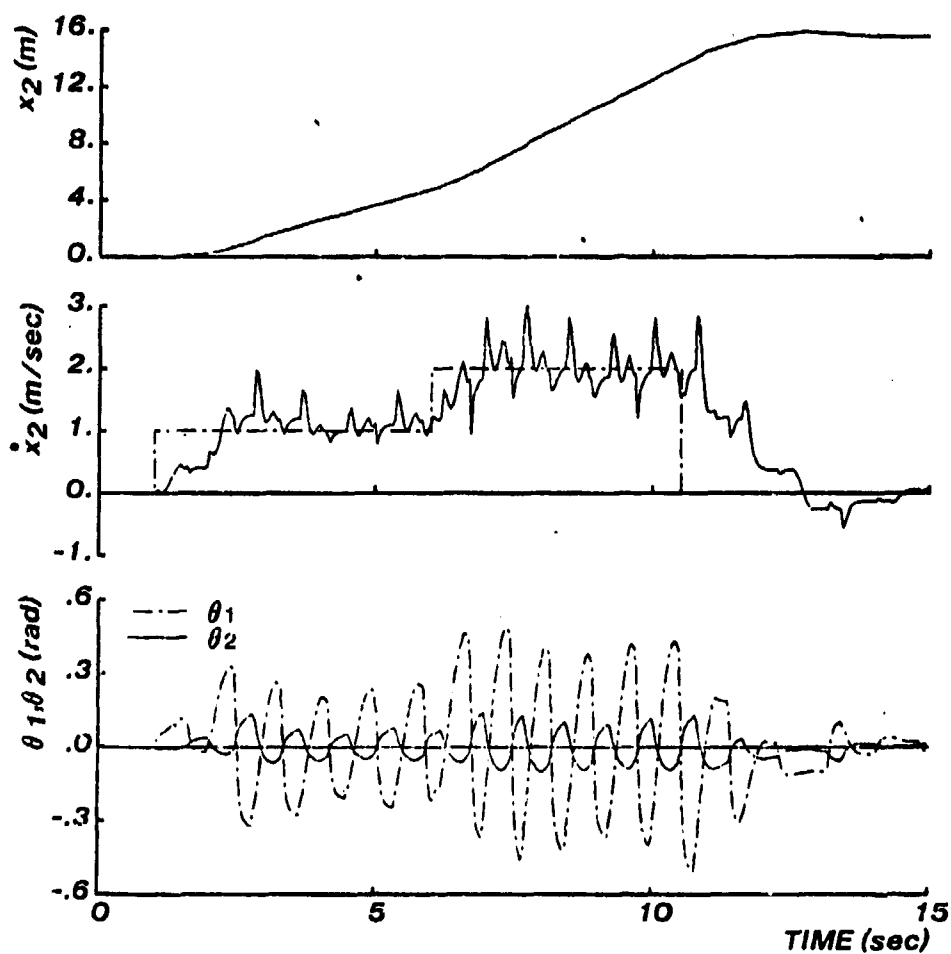


Figure 6-14: Method 3 algorithm shown responding to step changes in desired velocity,  $x_{2,d}$  (shown stippled). The algorithm generates hip torque during stance to control attitude of body. ( $K_1=0.15$ ,  $K_2=0.0$ ,  $K_3=0.0$ ,  $\Delta x_{MAX}=0.5$ )

## 6.7 Appendix VII. Equations of Motion for Model

These equations were derived from free body diagrams of the leg and body using d'Alembert's principle.

$$\ddot{y}_1 = \ddot{y}_0 - r_1(\ddot{\theta}_1 \sin(\theta_1) + \dot{\theta}_1^2 \cos(\theta_1)) \quad (6.34)$$

$$\ddot{x}_1 = \ddot{x}_0 + r_1(\ddot{\theta}_1 \cos(\theta_1) - \dot{\theta}_1^2 \sin(\theta_1)) \quad (6.35)$$

$$\begin{aligned} \ddot{y}_2 = \ddot{y}_0 + \ddot{w} \cos(\theta_1) - w\ddot{\theta}_1 \sin(\theta_1) - w\dot{\theta}_1^2 \cos(\theta_1) \\ - r_2(\ddot{\theta}_2 \sin(\theta_2) + \dot{\theta}_2^2 \cos(\theta_2)) - 2\dot{w}\dot{\theta}_1 \sin(\theta_1) \end{aligned} \quad (6.36)$$

$$\begin{aligned} \ddot{x}_2 = \ddot{x}_0 + \ddot{w} \sin(\theta_1) + w\ddot{\theta}_1 \cos(\theta_1) - w\dot{\theta}_1^2 \sin(\theta_1) \\ + r_2(\ddot{\theta}_2 \cos(\theta_2) - \dot{\theta}_2^2 \sin(\theta_2)) + 2\dot{w}\dot{\theta}_1 \cos(\theta_1) \end{aligned} \quad (6.37)$$

$$M_1 \ddot{y}_1 = F_y - F_T \cos(\theta_1) + F_N \sin(\theta_1) - M_1 g \quad (6.38)$$

$$M_1 \ddot{x}_1 = F_x - F_T \sin(\theta_1) - F_N \cos(\theta_1) \quad (6.39)$$

$$I_1 \ddot{\theta}_1 = -F_x r_1 \cos(\theta_1) + F_y r_1 \sin(\theta_1) - F_N (w - r_1) - \tau(t) \quad (6.40)$$

$$M_2 \ddot{y}_2 = F_T \cos(\theta_1) - F_N \sin(\theta_1) - M_2 g \quad (6.41)$$

$$M_2 \ddot{x}_2 = F_T \sin(\theta_1) + F_N \cos(\theta_1) \quad (6.42)$$

$$I_2 \ddot{\theta}_2 = F_T r_2 \sin(\theta_2 - \theta_1) - F_N r_2 \cos(\theta_2 - \theta_1) + \tau(t) \quad (6.43)$$

where

- $(x_0, y_0)$  are coordinates of the foot,
- $(x_1, y_1)$  are coordinates of the leg's CG,
- $(x_2, y_2)$  are coordinates of the body's CG,

$F_x, F_y$  are the vertical and horizontal forces on the foot, and  
 $F_T, F_N$  are the tangent and normal forces between the leg and body.

These equations are expressed in terms of the state variables  $\theta_1, \theta_2, x_0, y_0, w$  by eliminating  $x_1, y_1, x_2, y_2, F_N,$  and  $F_T$ :

$$\cos(\theta_1)(M_2 W w + I_1) \ddot{\theta}_1 + M_2 r_2 W \cos(\theta_2) \ddot{\theta}_2 + M_2 W \ddot{x}_0 + M_2 W \sin(\theta_1) \ddot{w} = \quad (6.44)$$

$$\begin{aligned}
 & WM_2(\dot{\theta}_1^2 W \sin(\theta_1) - 2\dot{\theta}_1 \dot{w} \cos(\theta_1) + r_2 \dot{\theta}_2^2 \sin(\theta_2) + r_1 \dot{\theta}_1^2 \sin(\theta_1)) \\
 & - {}_1 F_x \cos^2(\theta_1) + \cos(\theta_1)(r_1 F_y \sin(\theta_1) - \tau(t)) + F_k W \sin(\theta_1)
 \end{aligned}$$

$$-\sin(\theta_1)(M_2 W w + I_1) \ddot{\theta}_1 - M_2 r_2 W \sin(\theta_2) \ddot{\theta}_2 + M_2 W \ddot{y}_0 + M_2 W \cos(\theta_1) \ddot{w} = \quad (6.45)$$

$$\begin{aligned}
 & WM_2(\dot{\theta}_1^2 W \cos(\theta_1) + 2\dot{\theta}_1 \dot{w} \sin(\theta_1) + r_2 \dot{\theta}_2^2 \cos(\theta_2) + r_1 \dot{\theta}_1^2 \cos(\theta_1) - g) \\
 & + r_1 F_x \cos(\theta_1) \sin(\theta_1) - \sin(\theta_1)(r_1 F_y \sin(\theta_1) - \tau(t)) + F_k W \cos(\theta_1)
 \end{aligned}$$

$$\cos(\theta_1)(M_1 r_1 W - I_1) \ddot{\theta}_1 + M_1 W \ddot{x}_0 = \quad (6.46)$$

$$\begin{aligned}
 & W(M_1 r_1 \dot{\theta}_1^2 \sin(\theta_1) - F_k \sin(\theta_1) + F_x) - \\
 & \cos(\theta_1)(F_y r_1 \sin(\theta_1) - F_x r_1 \cos(\theta_1) - \tau(t))
 \end{aligned}$$

$$-\sin(\theta_1)(M_1 r_1 W - I_1) \ddot{\theta}_1 + M_1 W \ddot{y}_0 = \quad (6.47)$$

$$\begin{aligned}
 & W(M_1 r_1 \dot{\theta}_1^2 \cos(\theta_1) - F_k \cos(\theta_1) + F_y - M_1 g) - \\
 & \sin(\theta_1)(F_y r_1 \sin(\theta_1) - F_x r_1 \cos(\theta_1) - \tau(t))
 \end{aligned}$$

$$-\cos(\theta_2 - \theta_1) I_1 r_2 \ddot{\theta}_1 + I_2 w \ddot{\theta}_2 = \quad (6.48)$$

$$W(F_k r_2 \sin(\theta_2 - \theta_1) + \tau(t)) - r_2 \cos(\theta_2 - \theta_1)(r_1 F_y \sin(\theta_1) - r_1 F_x \cos(\theta_1) - \tau(t))$$

where

$$W = w - r_1$$

$$F_k = \begin{cases} K_L(k_0 - w + \chi) & \text{for } (k_0 - w + \chi) > 0 \\ K_{L2}(k_0 - w + \chi) - B_{L2}w & \text{otherwise} \end{cases} \quad (6.49)$$

$$F_x = \begin{cases} -K_G(x_0 - x_{TD}) - B_Gx_0 & \text{for } y_0 < 0 \\ 0 & \text{otherwise} \end{cases} \quad (6.50)$$

$$F_y = \begin{cases} -K_Gy_0 - B_Gy_0 & \text{for } y_0 < 0 \\ 0 & \text{otherwise} \end{cases} \quad (6.51)$$

### 6.8 Appendix VIII. Simulation Parameters

$$M_1 = 1 \text{ kg}$$

$$I_1 = 1 \text{ kg}\cdot\text{m}^2$$

$$r_1 = .5 \text{ m}$$

$$k_0 = 1 \text{ m}$$

$$K_L = 10^3 \text{ Nt/m}$$

$$K_{L'} = 10^5 \text{ Nt/m}$$

$$K_G = 10^4 \text{ Nt/m}$$

$$M_2 = 10 \text{ kg}$$

$$I_2 = 10 \text{ kg}\cdot\text{m}^2$$

$$r_2 = .4 \text{ m}$$

$$B_{1,2} = 125 \text{ Nt}\cdot\text{sec/m}$$

$$B_G = 75 \text{ Nt}\cdot\text{sec/m}$$

$$H = 1.8 \text{ m}$$

$$K_p = \begin{array}{l} 1800 \text{ Nt}\cdot\text{m/rad} \\ 1200 \text{ Nt}\cdot\text{m/rad} \end{array}$$

$$\begin{array}{l} \text{for } y_0 \leq 0 \\ \text{otherwise} \end{array}$$

$$K_v = \begin{array}{l} 200 \text{ Nt}\cdot\text{m}\cdot\text{sec/rad} \\ 60 \text{ Nt}\cdot\text{m}\cdot\text{sec/rad} \end{array}$$

$$\begin{array}{l} \text{for } y_0 \leq 0 \\ \text{otherwise} \end{array}$$

## Bibliography

1. Agarwal, G.C., Berman, B.M., Stark, L., Lohnberg, P., Gottlieb, G.L. "Studies in postural control systems: Parts I, II, and III." *IEEE t. on Systems Science and Cybernetics ssc-6*, 2 (1970), 116-132.
2. Albus, J.S. *Theoretical and experimental aspects of a cerebellar model*. Ph.D. Th., Biomedical Engineering, University of Maryland, 1972.
3. Albus, J.S. "A new approach to manipulator control: the Cerebellar Model Articulation Controller (CMAC)." *J. Dynamic Systems, Measurement, and Control, Series G 97*, 3 (1975), 220-227.
4. Albus, J.S. "Data storage in the Cerebellar Model Articulation Controller (CMAC)." *J. Dynamic Systems, Measurement, and Control, Series G 97*, 3 (1975), 228-233.
5. Aleshinsky, Zatsiorsky. "Human locomotion." *J. Biomechanics 11* (1978), 101-108.
6. Alexander, R. McN. "The mechanics of jumping by a dog." *J. Zoology, Lond. 173* (1974), 549-573.
7. Alexander, R. McN., Vernon, A. "The mechanics of hopping by kangaroos (Macropodidae)." *J. Zool., Lond. 177* (1975), 265-303.
8. Alexander, R. McN., Goldspink, G.. *Mechanics and energetics of animal locomotion*. Chapman and Hall, London, 1977.
9. Alexander, R. McN., Jayes, A.S. "Fourier analysis of forces exerted in walking & running." *J. Biomechanics 13* (1980), 383-390.
10. Alexander, R. McN. Mechanics of bipedal locomotion. In *Perspectives in Experimental Biology*, Spencer-Davies, P., Ed., Pergamon, Oxford, , pp. 493-504.
11. Alexander, McN. R.; Langman, V.A.; and Jayes, A.S. "Fast locomotion of some African ungulates." *J. Zool., London 183* (1977), 291-300. Univ. of Leeds and Univ. of Nairobi
12. Anderson, F.. *Registration of the pressure power (the force) of the body on the floor during movements, especially vertical jumps*. , 1st Int. Seminar, Surich, 1967.
13. Andriacchi, Ogle, Galante. "Walking speed as a basis for normal & abnormal gait measurements." *J. Biomechanics 10* (1977), 195-200.
14. Arutyunyan, G.A., Gurfinkel, V.S., Mirskii, M.L. "Organization of movements on execution by man of an exact postural task." *Biofizika 14*, 6 (1969), 1103-1107.

15. Asatryan, D.G.; Fel'dman, A.G. "Functional tuning of nervous system with control of movement or maintenance of a steady posture..." *Biofizika* 10, 5 (1965), 837-846. Inst. of Biol. Physics, USSR, Acad. of Sc., Moscow
16. Badler, N.I.; Sinoliar, S.W. The representation of human movements using a digital computer. Tech. Rept. Movement Proj. Report No.9, MS-CIS-78-4, 1977.
17. Bair, I.R.. *Patent No. 2918738. Volume : Amphibious walking vehicle. . 1959.*
18. Bassmajian, J. V., Tuttle, R. Engineering of locomotion in gorilla and man. In *Control of Posture and Locomotion*. R.B. Stein, K.G. Pearson, R.S. Smith, J.B. Redford, Eds., Plenum Press, New York, N.Y., 1973, pp. 500-609.
19. Beckett, R., Chang, K. "An evaluation of the kinematics of gait by minimum energy." *J. Biomech.* 1 (1968), 147-159.
20. Bekker, M.G.. *The evolution of locomotion: A conjecture into the future of vehicles. , 1961.*
21. Bekker, M.G. "Is the wheel the last word in land locomotion?" *New Scientist* 17, 248 (1961), 406-410.
22. Bekker, M.G.. *Theory of land locomotion*. University of Michigan Press, 1962.
23. Bekker, M.G.. *Introduction to terrain-vehicle systems*. University of Michigan Press, Ann Arbor, 1969.
24. Belerskii, V.V. "Biped locomotion dynamics I." *Izv. AN SSSR. Mekhanika Tverdogo Tela* 10, 3 (1975), 3-14.
25. Beletskii, V.V. "Dynamics of two-legged walking, II." *Izv. AN SSSR. Mekhanika Tverdogo Tela* 10, 4 (1975), 3-13.
26. Beletskii, V.V., Kirsanova, T.S. "Plane linear models of biped locomotion." *Izv. AN SSSR. Mekhanika Tverdogo Tela* 11, 4 (1976), 51-62.
27. Beletskii, V.V., Chudinov, P.S. "Parametric optimization in the problem of biped locomotion." *Izv. AN SSSR. Mekhanika Tverdogo Tela* 12, 1 (1977), 25-35.
28. Beletskii, V.V. "Walking Control and Dynamics of a System with Two Legs." (), 1-11.
29. Beletskii, V.V.; Chudinov, P.S. "Control of motion of a bipedal walking robot." *Izv. AN SSSR. Mekhanika Tverdogo Tela* 15, 3 (1980), 30-38. UDC 531.8
30. Bennet-Clark, H.C. "The energetics of the jump of the locust *schistocerca gregaria*." *J.Exp.Biol.* 63 (1975), 53-83.

31. Bessonov, A.P., Umnov, N.V.. *The analysis of gaits in six-legged vehicles according to their static stability.* Proc. Symposium on Theory and Practice of Robots and Manipulators, Udine, Italy, 1973.
32. Bishop, Jerry E. Why Do Kangaroos Say to Their Friends, 'Let's Go to the Hop'? 1980 Wall Street Journal.
33. Bresler, B. and Frankel, J.P. "The forces and moments in the leg during level walking." *t. Amer. Soc. Mech. Eng.* 27 (1950).
34. Brown, L.S.. *The right way to walk four-legged.* . .
35. Buckett, J. *Design of an on-board electronic joint control system for a six-legged vehicle.* Ph.D. Th., The Ohio State University, Columbus, Ohio, 1977.
36. Burnett, C.N., Johnson, E.W. "Development of gait in childhood, Parts I and II." *Developmental Medicine in Child Neurology* 13, 2 (1971), 196-215.
37. Burns, M.D.. *The control of walking in Orthoptera. I --leg movements in normal walking.* J. Exp. Biol., 1973.
38. Camana, P.C. *A study of physiologically motivated mathematical models for human postural control.* Ph.D. Th., The Ohio State University, Columbus, Ohio, 1977.
39. Camana, P.C., Hemami, H., Stockwell, C.W. "Determination of feedback for human posture control without physical intervention." 7 (1977).
40. Cannon, R.H., Jr. "Some basic response relations for reaction-wheel attitude control." *ARS Journal* (1962), 61-74.
41. Cappozzo, Maini, Marchetti, Pedotti. *Analysis of hybrid computer of ground reaction in walking.* Proc. IV Int. Seminar on Biomechanics, Philadelphia, Pa., 1973.
42. Cappozzo, Aurelio, et.al. "A General computing method for the analysis of human locomotion." *J. Biomechanics* 8 (1975), 307-320.
43. Cappozzo, et.al. "Interplay of muscular & external forces in human ambulation." *J. Biomechanics* 9 (1976), 35-43.
44. Carson, P.F.. *Walking tractor.* , 1958.
45. Cavagna, G.A., Margaria, R. "Mechanics of walking." *J. Applied Physiology* 21 (1966), 271-278.

46. Cavagna, G.A. "Elastic bounce of the body." *J. Applied Physiology* 29 (1970), 279-282.
47. Cavagna, G.A. "Force platforms as ergometers." *J. Applied Physiology* 39 (1975), 174-179.
48. Cavanagh, P.R. " " *J. Biomechanics* 13 (1979), 397-406.
49. Ceranowicz, A.Z. Decoupling and finite state control of a five link planar biped model standing on one leg. Master Th., The Ohio State University, Columbus, Ohio, 1979.
50. Ceranowicz, A.Z. *Planar biped dynamics and control*. Ph.D. Th., Department of Electrical Engineering, The Ohio State University, Columbus, Ohio, 1979.
51. Ceranowicz, A.Z., Syman, B.F., Hemami, H. "Control of constrained systems of controllability index two." *IEEE t. on Automatic Control AC-25* (1980).
52. Chand, S.; Doty, K.L. A unique table-lookup scheme for open-loop control of a robotic manipulator. , S.E. Conf. on System Theory, Orlando, FL, 1981, pp. vi-36 to vi-37.
53. Cheng, I.S. *Computer-television analysis of biped locomotion*. Ph.D. Th., The Ohio State University, Columbus, Ohio, 1974.
54. Chow, C.K., Jacobson, D.H. "Studies of human locomotion via optimal programming." *Mathematical Biosciences* 10 (1971), 239-306.
55. Chow, C.K., Jacobson, D.H. "Further studies of Human Locomotion: Postural stability and Control." *Mathematical Biosciences* 15 (1972), 93-108.
56. Cook, T., Cozzens, B. The initiation of gait. In *Neural control of locomotion*, R.N. Herman, S. Grillner, P.S. Stein, D.G. Stuart, Eds., Plenum Press, New York, 1976.
57. Corliss, W.R., Johnson, E.G.. *Teleoperator controls*. NASA SP-5070, 1968.
58. Cotes, J.E., and Meade, F. "The energy expenditure and mechanical energy demand in walking." *Ergonomics* (1960).
59. Cox, W.. *Big muskie*. New in Engineering, The Ohio State University, Columbus, Ohio, 1970.
60. Cruse, H.. *A new model describing the coordination pattern of the legs of a walking stick insect*. Biol. Cybernetics, 1979.
61. Cutting, J.F. "Generation of synthetic male and female walkers through manipulation of a biomechanical invariant." *Perception* 7 (1978), 393-405.

62. Dahlquist, G., Bjorck, A., Anderson N. *Numerical Methods*. Prentice-Hall, Englewood Cliffs, NJ, 1974.
63. Dawson, T.J. "Kangaroos." *Scientific American* 237, 2 (1977), 78-89.
64. Dawson, T.J.; Taylor, C.R. "Energetic cost of locomotion in kangaroos." *Nature* 246 (1973), 313-314.
65. Dawson, T.J.; Taylor, C.R. "Energetic cost of locomotion in kangaroos." *Nature* 246 (1973), 313-314.  
School of Zool., Univ. of New S. Wales, Australia
66. Dawson, T.J. "Energetic cost of locomotion in Australian hopping mice." *Nature* 259 (1976), 305-307.  
School of Zool., Univ. of New S. Wales, Australia
67. Dougan, S. "The angle of gait." *American J. Physiological Anthropology* 7 (1924), 275-279.
68. Drillis, R., Contini, R. Body Segment Parameters. Tech. Rept. Technical Report No. 1166.03, New York University, New York, 1966.
69. Ehrlich, A. *Patent No. 1691233*. Volume : *Vehicle propelled by Steppers*, 1928.
70. Ekrot, C.F., Larson, B., Oscarsson, O. Information carried by the spinocerebellar paths. In *Reflex Control of Posture and Movement*, Granit, R., Pompeiano, O., Eds., Elsevier/North-Holland Biomedical, New York, 1979, pp. 79-90.
71. Elftman, H. "A cinematic study of the distribution of pressure in the human foot." *Anat. Rec.* 59 (1934), 481-490.
72. Elftman, H. "Forces and energy changes in the leg during walking." *Amer. J. Physiol.* 125 (1939), 339-356.
73. Elftman, H. "The basic pattern of human locomotion." *Ann. New York Acad. of Sci. Rec.* 51 (1951), 1207-1212.
74. Elftman, H. "Basic function of the lower limbs." *Biomedical Engineering* (1967), 342-345.
75. Engin, A.E. Experimental determination of the patello femoral joint forces. , 29th ACEMB, Boston, Mass., 1976.
76. Ewald, B.A., Lucas, D.B., Ralston, H.J.. *Effect of immobilization of the hip on energy expenditure during level walking*, UCSF Berkeley, 1961.
77. Farnsworth, R. Gait stability and control of a five link model of biped locomotion. Master Th., The Ohio State University, Columbus, Ohio, 1975.

78. Fedak, M.A.; Plashow, B.; Schmidt-Nielsen, K. "Energy cost of bipedal running." *Amer. J. of Physiol.* 227, 5 (1977), 1038-1044. Dept. of Zool., Duke Univ., NC
79. Fenn, W.O. "Work against gravity and work due to velocity changes in running." *Amer. J. Physiol.* 93 (1930).
80. Fitch, J.M., Templer, J., Corcoran, P. "The dimensions of stairs." *Scientific American* 231, 42 (1974).
81. Foley, et.al. "Kinematics of normal child locomotion." *J. Biomechanics* 12 (1979), 1-6.
82. Fomin, S.V., Shtilkind, T.I. "The concept of equilibrium of systems having legs." *Biofizika* 17, 1 (1972), 131-134.
83. Fomin, S.V., Gurfinkel, V.S., Feldman, A.G., Shtilkind, T.I. "Movements of the joints of human legs during walking." *Biophysics* 21 (1976), 572-577.
84. Frank, A.A. *Automatic control systems for legged locomotion machines*. Ph.D. Th., Univ. of Southern California, Los Angeles, California, 1968.
85. Frank, A.A., McGhee, R.B. "Some considerations relating to the design of autopilots for legged vehicles." *Journal of Terramechanics* 6, 1 (1969), 23-25.
86. Frank, A.A., Vukobratovic, M. On the synthesis of biped locomotion machines. In *8th International Convrence on Medical and Biological Engineering*, , Evanston, Illinois, 1969.
87. Frank, A.A. "An approach to the dynamic analysis and synthesis of biped locomotion machines." *Medical & Biological Engineering* 8 (1970), 465-476.
88. Frank, A.A. "On the stability of an algorithmic biped locomotion machine." *J. of Terramechanics* 8, 1 (1971), 41-50.
89. Frank, A.A. "A method of coordinating the legs of the General Electric walking truck." , ECE-73-3 (1973).
90. Franklin, R.; Bell, W.J.; Jander, R. "Rotational locomotion by the cockroach *blattella germanica*." *J. Insect Physiol.* 27, 4 (1981), 249-255. Printed in G.B., Pergamon Press Ltd.
91. Friedman, M.B. "Visual control of head movements during avian locomotion." *Nature* 255, 5503 (1975), 67-69.
92. Gage, H. "Accelerographic analysis of human gait." *ASME Winter Annual Meeting WA/HU*, 64 (1964), 137-152.

93. Galiana, H.L., Milsum, J.H.. *A mathematical model for the walking human leg*. 21<sup>st</sup> ACEMB, Houston, Texas, 1968.
94. Gannett, W.R.. *The peripod*, U.S. Army Weapons Command, Rock Island, Illinois, 1967.
95. Garg, D.P. "Vertical mode human body vibration transmissibility." *IEEE t. Systems SMC-6*, 2 (1976).
96. Giralt, G.. *Multi-level planning & navigation system for a mobile robot*, August 1979.
97. Golliday, C.L., Jr. *Toward development of biped locomotion control: planar motion of the kneeless biped standing and walking gaits*. Ph.D. Th., The Ohio State University, Columbus, Ohio, 1975.
98. Golliday, C.L., Jr., Hemami, H. "Postural stability of the two degree-of-freedom biped by general linear feedback." *IEEE t. on Automatic Control AC-21*, 1 (1976), 74-79.
99. Golliday, C.L., Jr., Hemami, H. "An approach to analyzing biped locomotion dynamics and designing robot locomotion controls." *IEEE t. Automatic Control AC-22*, 6 (1977), 963-972.
100. Graham, D. "Effects of circum-oesophageal lesion on the behavior of the stick insect *Carausius morosus*; I. Cyclic behaviour patterns." *Biol. Cybernetics* 32 (1979), 139-145.
101. Graham, D. "Effects of circum-oesophageal lesion on the behavior of the stick insect *Carausius morosus*; II. Changes in walking co-ordination." *Biol. Cybernetics* 32 (1979), 147-152.
102. Greene, P.H. Problems of organization of motor systems. Quarterly report 29, U. of Chicago Inst. for Comp. Research, 1971. Section II C
103. Greene, P.R.; McMahon, T.A. "Reflex stiffness of man's anti-gravity muscles during knee bends while carrying extra weights." *J. Biomechanics* 12 (1979), 881-891. Pergamon Press
104. Greene, P.R.; McMahon, T.A. "Running in circles." *The Physiologist* 22, 6 (1979), S-35 & S-36. Harvard Univ., BioMechanics Lab.
105. Grillner, S. "The role of muscle stiffness in meeting the changing postural and locomotor requirements of force development by the ankle extensors." *Acta physiol. scand.* 86 (1972), 92-108.
106. Grillner, S. "Locomotion in vertebrates: central mechanisms and reflex interaction." *Physiol. Rev.* 55 (1975), 247-304.
107. Grillner, S. Some aspects on the descending control of the spinal circuits generating locomotor movements. In *Neural control of locomotion*, Plenum Press, New York, 1976.

108. Grillner, S., Zangger, P. "On the central generation of locomotion in the low spinal cat." *Experimental Brain Research* 34 (1979), 241-261.
109. Grimes, D.L. *An active multi-mode above knee prosthetic controller*. Ph.D. Th., Massachusetts Institute of Technology, 1979.
110. Grundman, J., Seireg, A. "Computer control of a multitask exoskeleton for paraplegics." *On Theory and Practice of Robots and Manipulators -- Second CISM-IFTOMM Symposium, Warsaw* (1976), 241-248.
111. Gubina, F. *Stability and dynamic control of certain types of biped locomotion*. IV Symp. on External Control of Human Extremities, Dubrov, 1972.
112. Gubina, F., Hemami, H., McGhee, R.B. "On the dynamic stability of biped locomotion." *IEEE t. on Biomedical Engineering BME-21*, 2 (1974), 102-108.
113. Gupta, S. Estimation of lower limb joint forces and moments using on-line measurements and computations. Master Th., Ohio State University, Columbus, Ohio, 1975.
114. Gurfinkel, E.V.. *Physical foundation of the stabilography*. Symposium International de Posturographic Smolenile, 1973.
115. Gurfinkel, V.S., Shik, M.I. The control of posture and locomotion. In *Motor Control*, Gydikou, A.A., Tankou, N.T., Kosarov, D.S., Ed., Plenum, New York, 1973, pp. 217-234.
116. Harris, R.I., Beath, T. "Hypermobility flat-foot with short tendo achillis." *J. Bone and Joint Surg.* 30-a (1948), 116-140.
117. Hartrum, T.C. Biped locomotion models. Tech. Rept. Technical Report 272, The Ohio State University, Columbus, Ohio, 1971.
118. Hartrum, T.C. *Computer implementation of a parametric model for biped locomotion kinematics*. Ph.D. Th., The Ohio State University, Columbus, Ohio, 1973.
119. Hatze, H. "A complete set of control equations for the human musculo-skeletal system." *J. Biomechanics* 10 (1977), 799-805.
120. Havill, J.R., Ratcliff, J.W. A twin-gyro attitude control system for space vehicles. NASA Technical Note TN D-2419, 1964.
121. Heglund, N.C.; Taylor, C.R.; McMahon, T.A. "Scaling stride frequency and gait to animal size: Mice to horses." *Science* 186 (1974), 1112-1113.

122. Hemami, H.. *Pole assignment by mode feedback*. Proc. 9th Annual Allerton Conference on Circuit and System Theory, Evanston, Ill., 1971.
123. Hemami, H., Weimer, F.C., Koozckanani, S.H. "Some aspects of the inverted pendulum problem for modelling of locomotion systems." *IEEE t. on Automatic Control AC-18*, 6 (1973), 658-661.
124. Hemami, H., Weimer, F.C. Further considerations of the inverted pendulum. , Proc. of the Fourth Iranian Conference on Electrical Engineering, Pahlavi University, Shiraz, Iran, 1974, pp. 697-708.
125. Hemami, H.. *Reduced order models for biped locomotion*. Proc. of 7th Pittsburgh Conf. on Modelling and Simulation, Pittsburgh, Pa., 1976.
126. Hemami, H., Camana, P.C. "Nonlinear feedback in simple locomotion systems." *IEEE t. on Automatic Control 21*, 6 (1976).
127. Hemami, H., Cvetkovic, V.S.. *Postural stability of two biped models via Lyapunov second method*. Proc. of 1976 JACC. West Lafayette, Indiana, 1976.
128. Hemami, H., Farnsworth, R.L. "Postural and gait stability of a planar five link biped by simulation." *IEEE t. on Automatic Control AC-22*, 3 (1977), 452-458.
129. Hemami, H., Golliday, C.L., Jr. "The inverted pendulum and biped stability." *Mathematical Biosciences 34* (1977), 95-110.
130. Hemami, H., Jaswa, V.C. "On a three-link model of the dynamics of standing up and sitting down." *IEEE t. Systems, Man, and Cybernetics SMC-8*, 2 (1978), 115-120.
131. Hemami, H., Wall, C., III, Black, F.O. "Single inverted pendulum biped experiments." *J. of Interdisciplinary Modeling and Simulation 2(3)* (1979), 211-227.
132. Hemami, H., Tomovic, R., Ceranowicz, A.Z. "Finite state control of planar bipeds with application to walking and sitting." *J. Bioengineering 2* (1979), 477-494.
133. Hemami, H., Wyman, B.F. "Modeling and control of constrained dynamic systems with application to biped locomotion in the frontal plane." *IEEE t. on Automatic Control AC-24*, 4 (1979), 526-535.
134. Hemami, H., Wyman, B.F. "Indirect control of the forces of constraint in dynamic systems." *Journal of Dynamic Systems, Measurement, and Control 101* (1979), 355-360.
135. Hemami, H. "A feedback on-off model of biped dynamics." *IEEE t. on Systems, Man, and Cybernetics SMC-10*, 7 (1980), 376-383.

136. Hemami, H., Robinson, D.J., Ceranowicz, A.Z. "Stability of planar biped models by simultaneous pole assignment and decoupling." *Int. J. Systems Science* 11, 1 (1980), 65-75.
137. Hemami, H., Robinson, D.J., Ceranowicz, A.Z. "On stability, pole assignment and decoupling of some biped models." *Submitted to IEEE t. on Automatic Control* ().
138. Hemami, H., Weimer, F.C., Robinson, C.S., Stockwell, C.W., Cvetkovic, V.S. "Analysis of some derived models of otoliths and semicircular canals." *1977 JACC* ().
139. Herman, B., Cook, T., Cozzens, B., Freeman, W. Control of postural reaction in man: the initiation of gait. In *Control of Posture and Locomotion*, R.B. Stein, K.G. Pearson, R.S. Smith, J.B. Redford, Eds., Plenum Press, New York, N.Y., 1973, pp. 353-388.
140. Hicks, J.H. The three weight bearing mechanisms of the foot. In *Biomechanical Studies of the Musculo-Skeleton System*, F.G. Evans, C.C. Thomas, Eds., Springfield, Ill., 1961.
141. Higdon, D.T., Cannon R.H., Jr. On the control of unstable multiple-output mechanical systems. Proc. of Winter Annual Meeting, ASME Winter Annual Meeting, 1963.
142. Hildebrand, "Motion of the running cheetah and horse." *J. Mammalogy* 40, 4 (1959), 481-495.
143. Hildebrand, M. "How animals run." *Scientific American* (1960), 148-157.
144. Hildebrand, "Symmetrical gaits of horses." *Science* 150 (1965), 701-708.
145. Hildebrand, M. "Analysis of the symmetrical Gaits of Tetrapods." *Folia Biotheoretica* 4 (1966), 9-22.
146. Hill, J.C. A model of the human postural control system. , 8th IEEE Symp. Adaptive Processes: Decision and Control, 1969.
147. Hirose, S., Umetani, Y.. *The basic motion regulation system for a quadruped walking vehicle*. ASME Conference on Mechanisms, Los Angeles, 1980.
148. Hirose, S.; Umetani, Y. A cartesian coordinates manipulator with articulated structure. Tokyo Inst. of Tech., Japan, .
149. Hirose, S.; Oda, S.; Umetani, Y. An active cord mechanism with oblique swivel joints and its control. Tokyo Inst. of Tech. and Toshiba Elec. Co., Tokyo, Japan, .
150. Hollerbach, J.M. "A recursive formulation of lagrangian manipulator dynamics." *IEEE t. Systems, Man, and Cybernetics* 10 (1980), 730-736.

151. Horn, B.K.P., Raibert, M.H. Configuration space control. MIT Artificial Intelligence Laboratory Memo 458. December, 1977
152. Horn, B.K.P. The fundamental EEL equations, Working Paper 116, MIT, AI, 1975.
153. Howell, R.. *Speed in animals*. Univ. of Chicago Press, Chicago, 1944.
154. Hristic, D., Vukobratovic, M.. *A new approach to the rehabilitation of paraplegic persons* , 1971.
155. Hughes, G.M. "The coordination of insect movements." *J. Exp. Biol.* 29 (1952), 267-285.
156. Jain, A.K. Measurement of gait in children. Tech. Rept. Tech. Note No.1. The Ohio State University, 1972. Communication and Control Systems Lab, Dept. of Electrical Engineering
157. Jain, A.K. A Study of regularly realizable gait matrices. Master Th., The Ohio State University, Columbus, Ohio, .
158. Jaswa, V.C. Dynamic stability and control of a three link model of a human being. Master Th., Ohio State University, Columbus, Ohio. 1975.
159. Jaswa, V.C. *An experimental study of real-time computer control of a hexapod vehicle*. Ph.D. Th., Ohio State University, Columbus, Ohio, 1978.
160. Johnston, R.C., Smidt, G.I.. "Measurement of hip-joint motion during walking." *J. Bone & Joint Surg.* 51-A (1969). 1083-1094.
161. Jones, R.L. "The human foot -- An experimental study of its mechanics and the role of its muscle and ligaments in the support of the arch." *Am. J. Anat.* 68 (1941), 1-39.
162. Jones, F.W.. *Structure and function as seen in the foot, Edition 2*. Bailliere, Tindall and Cox, London, 1949.
163. Jones, G.M. "Observations on the Control of Stepping & Hopping Movements in Man." *J. Physiol* 219 (1971), 709-727.
164. Juricic, D., Vukobratovic, M. "Mathematical modelling of bipedal walking system." *ASME Publication* 72-WA BHF-13 (1972).
165. Kanayama, Yutaka, Iijima, Jun'ichi, Ochiai, Hajime, Watarai, Hiroshi, Ohkaw, Kohichi. A self-contained robot 'Yamabiko'. , 3rd USA-Japan Computer Conference, 1978.
166. Kane, T.R., and Vebison, D.A. "Formulation of equations of motion for complex spacecraft." *J. of Guidance and Control* 3, 2 (1980), 99-112.

167. Kato, I., Matsushita, S., Kato, K. A model of human posture control system. In *Advances in External Control of Human Extremities*, M.M. Gavrilovic, A.B. Wilson Jr., Eds., , Belgrade, 1969, pp. 443-464.
168. Kato, I., Tsuiki, H. The hydraulically powered biped walking machine with a high carrying capacity. In *IV Symp. on External Control of Human Extremities*, , Dubrovnik, Yugoslavia, 1972.
169. Kato, T., Takanishi, A., Jishikawa, H., Kato, I. The realization of the quasi-dynamic walking by the biped walking machine. 4th Symposium on Theory and Practice of Robots and Manipulators, IFTMoM, 1981.
170. Keith, A. "The history of the human foot and its bearing on orthopedic practice." *J. Bone and Joint Surg. II* (1929), 10-32.
171. Kenny, J.D. Investigation for a walking device for high efficiency lunar locomotion. , American Rocket Society Annual Meeting, Philadelphia, Penna., 1965.
172. Kettelkamp, D.B., Johnston, R.C., Smidt, G.L., Chao, E.Y.S., Walker, M. "An electrogoniometric study of knee motion in normal gait." *J. Bone & Joint Surg. 51-A* (1970), 775-790.
173. Khadelwal, B.M., Frank, A.A. On the dynamics of an elastically coupled multi-body biped locomotion model. Proceedings of Joint Automatic Control Conference, Austin, Texas, 1974.
174. Khosravi-Sichani, B. A preliminary study of a two segment artificial foot. Master Th., The Ohio State University, Columbus, Ohio, 1979.
175. Kimura, T; Endo, B. Comparison of force of foot between quadrupedal walking of dog and bipedal walking of man. Dept. of Anthropology, Univ. of Tokyo, .
176. Kinch, E.A.. *Patent No. 1669906. Volume : Vehicle propelling device.* , 1928.
177. Klein, C.A., Briggs, R.I.. "Use of active compliance in the control of legged vehicles." *IEEE t. on Systems, Man, and Cybernetics SMC-10*, 7 (1980), 393-400.
178. Klein, C.A.; Patterson, M.R. Computer coordination of limb motion for a three-legged walking robot. research Unclass /54 28721, Ohio State Univ. EE Dept., NASA, 1980.
179. Klien, Charles. *Limb motion for a 3 legged walking machine.* , 1980.
180. Kljajic, M., Trnkoczy, A. "A study of adaptive control principle orthoses for lower extremities." *IEEE t. On Systems, Mans, and Cybernetics SMC-8*, 4 (1978), 313-321.
181. Koozekanani, S.H., McGhee, R.B. "Occupancy problems with pairwise exclusion constraints -- an aspect of gait enumeration." *Journal of Cybernetics* 2, 4 (1973), 14-26.

182. Koozckanani, S.H., Stockwell, C.W., McGhee, R.B., Firoozmand, F. "On the role of dynamic models in quantitative posturography." *IEEE t. Biomedical Engineering* (1980).
183. Kuce, B. "Movement of two legged system of pendulum type." *Mekhanika Tverdogo Tela* 2 (1975), 58-61. In Russian
184. Kugushev, E.I., Jaroshevskij, V.S.. *Problems of selecting a gait for an integrated locomotion robot*. Institute of Applied Mathematics, USSR Academy of Sciences, Moscow, .
185. Larin, J.B. "Stabilization of biped walking apparatus." *Izv. AN SSSR. Mekhanika Tverdogo Tela* 11, 5 (1976), 4-13.
186. Larin, V.B. "Control of a jumping robot, I. Choice of programmed trajectory." *14, 6* (1979), 27-32.
187. Leimanis, E.. *The general problem of the motion of coupled rigid bodies about a fixed point*. Springer-Verlag, 1965.
188. Liberson, W.T. "Biomechanics of gait: a method of study." *Arch. Phys. Med. Rehabilitation* (1965).
189. Lindholm, L.E., Oberg, K.E.T.. *An optoelectronic instrument for remote on-line movement monitoring*. Chalmers University of Technology Goteborg, Sweden, 1979.
190. Liston, R.A.. *Walking machine*. Annual Meeting of the American Society of Agricultural Engineers, University of Georgia, 1965.
191. Liston, R.A., Mosher, R.S. A versatile walking truck. Proc. Transportation Engineering Conference, ASME, Washington, D.C., 1968.
192. Luh, J.Y.S., Walker, M.W., Paul, R.P. "On-line computational scheme for mechanical manipulators." *Dynamic Systems, Measurement, and Control* 102 (1980), 69-77.
193. Mackerle, J. "Walking riders." *T-68 12* (1968), 776-777.
194. Manter, J. "Dynamics of quadrupedal walking." *J. of Experimental Biology* 15, 4 (1938), 522-539.
195. Marr, D. "A theory of cerebellar cortex." *J. Physiol.* 202 (1969).
196. Matsuoka, K. A model of repetitive hopping movements in man. Proc. of Fifth World Congress on Theory of Machines and Mechanisms, IFIP, 1979.
197. Matsuoka, K. "A mechanical model of repetitive hopping movements." *Biomechanisms* 5 (1980), 251-258. In Japanese

198. Matsuoka, K. "Study on robot legs." *Bulletin of ME Dept. 11* (1976), 65-69. Written in Japanese
199. McGhee, R.B. *Finite state control of quadruped locomotion*. Proc. of the Int. Symp. on External Control of Human Extremities, Dubrovnik, Yugoslavia, 1967.
200. McGhee, R.B. "Finite state control of quadruped locomotion." *Simulation* (1967).
201. McGhee, R.B. "Some finite state aspects of legged locomotion." *Math. Biosciences*. 2 (1968), 67-84.
202. McGhee, R.B., Frank, A.A. "On the stability properties of quadruped creeping gaits." *Math. Biosciences*. 3 (1968), 331-351.
203. McGhee, R.B., Frank, A.A. "Some considerations relating to the design of autopilots for legged vehicles." *J. of Terramechanics* 6, 1 (1969).
204. McGhee, R.B., Kuhner, M.B. On the dynamic stability of legged locomotion systems. *Advances in External Control of Human Extremities*, Belgrade, 1969, pp. 431-442.
205. McGhee, R.B. *A mathematical theory for legged locomotion systems*. Proc. 1970 Midwest Symposium on Circuit Theory, 1970.
206. McGhee, R.B., Jain, A.K. "Some properties of regularly realizable gait matrices." *Mathematical Biosciences* 13, 1/2 (1972), 179-193.
207. McGhee, R.B., Pai, A.L. "An approach to computer control for legged vehicles." *J. Terramechanics* 11 (1972), 9-27.
208. McGhee, R.B., Orin, D.E. *An interactive computer-control system for a quadruped robot*. Proc. Symposium on Theory and Practice of Robots and Manipulators, Udine, Italy, 1973.
209. McGhee, R.B., Sun, S.S. *On the problem of selecting a gait for a legged vehicle*. Proc. of VI IFAC Symposium on Automatic Control in Space, Tsakhkadzor, Armenian SSR, U.S.S.R., 1974.
210. McGhee, R.B., Backett, J.R. "Hexapod." *Interface Age* (1977).
211. McGhee, R.B., Koozkanani, S.H., Weimer, F.C., Rahmani, S. Dynamic modelling of human locomotion. Proceedings of Joint Automatic Control Conference, 1979.
212. McGhee, R.B., Iswandhi, G.I. "Adaptive locomotion of a multilegged robot over rough terrain." *IEEE Transactions on Systems, Man, and Cybernetics SMC-9*, 4 (1979), 176-182.
213. McGhee, R.B. Robot locomotion with active terrain accommodation. Proc. NSF Robotics Research Workshop, Univ. Rhode Island, 1980.

214. McGhee, R.B.; Frank, A.A. "On the stability of quadruped creeping gaits." *Math. Biosciences* 3, 3/4 (1968), 331-351. Amer. Elsevier Pub. Co., Inc.
215. McGhee, R.B.; Waldron, K.J. Design study for an actively terrain-adaptive off-road vehicle. OSU, 1980. DARPA
216. McKenney, J.D. Investigation for a walking device for high efficiency lunar locomotion. Tech. Rept. Paper 2016-61, American Rocket Society Space Flight Report to the Nation, New York, 1961.
217. McMahon, T.A. "Using body size to understand the structural design of animals: quadrupedal locomotion." *Journal of Applied Physiology* 39, 4 (1975), 619-627.
218. McMahon, T.A., Greene, P.R. "Fast running tracks." *Scientific American* 239, 6 (1978), 148-163.
219. McMahon, T.A. "Scaling Physiological Time." *American Mathematical Society* 13 (1980), 131-163.
220. McMahon, T.A. Allometry. In , McGraw-Hill, 1976, pp. 49:57. In 1977 McGraw-Hill Yearbook of Science and Technology
221. McMahon, T.A. "Gravitational scale effects." *The Physiologist* 22, 6 (1979), S-5 & S-6. Harvard Univ., Div. of Applied Sciences
222. McMahon, T.A.; Greene, P.R. "The influence of track compliance on running." *J. Biomechanics* 12 (1979), 893-904. Pergamon Press Ltd. in Great Britain
223. McMahon, T.A. Studies in locomotion and muscle mechanics. Proposal to SDF. Nov, 1982
224. Melvill-Jones, G. and Watt, D.O.D. "Observations on the control of stepping and hopping movements in man." *J. Physiol.* 219 (1971a), 709-727.
225. Melvill-Jones, G. and Watt, D.O.D. "Muscular control of landing from unexpected falls in man." *J. Physiol.* 219 (1971b), 729-737.
226. Mihajlov, D., Chang, C.W., Bekey, G.A., Perry, J. "Computer graphics in the study of normal and pathological human gait." *Medinfo* 77 (1977), 561-564.
227. Miller, D.L., Nelson, R.C., *Biomechanics of sport*. Lea & Febiger, Philadelphia, Pennsylvania, 1973.
228. Milner, M. et al. "Angle diagram in the assessment of locomotor function." *S.A. Medical Journal* 47 (1973), 951-957.
229. Milner, M., Brennan, P.K., Wilberforce, C.B.A. "Stroboscopic polaroid photography in clinical studies of human locomotion." *S.A. Medical Journal* 47 (1973), 948-950.

230. Miura, H., Shimayama, I. "Computer control of an unstable mechanism." *J. Fac. Eng.*, 17 (1980), 12-13. In Japanese
231. Miyazaki, Fumio. "A Control Theoretic Study and Dynamic Linked Locomotion." ??(1980).
232. Mocci,U., Petternella,M., Salinari,S. Experiments with six-legged walking machines with fixed gait. Tech. Rept. Report 2-12, Institute of Automation, University of Rome, 1972.
233. Mochon, S.; McMahon, T.A. "Ballistic Walking: An improved model." *Mathematical Biosciences* 52 (1980), 241-260. Harvard Univ. Div. of Applied Sciences
234. Morrison,R.A. Iron mule train. , Proc. Off-Road Mobility Research Symposium, Washington, D.C., 1968, pp. 381-400.
235. Morrison,J.B. "The mechanics of the knee joint in relation to normal walking." *J. Biomechanics* 3 (1970), 51-61.
236. Morrison,J.B. "The mechanics of muscle function in locomotion." *J. Biomechanics* 3 (1970), 431-461.
237. Morrison, R.A. Iron mule train. , Off-Road Mobility Research Symposium, Washington, 1968, pp. 381-400 and pictures pgs. 8:10, 12, 14. Space Div. Aerojet Gen. Corp., El Monte, CA
238. Morton,D.J.. *The human foot*. Columbia University Press, New York, 1935.
239. Morton,D.J.. *Human Locomotion and Body Form*. , University of Columbia, Baltimore, 1952.
240. Mosher,R.S. Design and fabrication of a full-scale, limited motion pedipulator. General Electric report, 1965.
241. Mosher,R.S. Test and evaluation of a versatile walking truck. , Proc. Off-Road Mobility Research Symposium, Washington, D.C., 1968, pp. 359-379.
242. Murray,M.P., Drought,A.B., Kovry,R.C. "Walking patterns of normal men." *J. Bone & Joint Surg.* 46-A, 2 (1964), 335-360.
243. Murray,M.P. "Gait as a total pattern of movement." *Am. J. Phys. Med.* 46, 1 (1967), 290-333.
244. Murray,M.P., Seirig,A., Scholz,R.C. "Center of gravity, center of pressure and supportive forces during human activities." *J. of Applied Pysiology* 23, 6 (1967), 831-838.
245. Murthy, S.S., Raibert, M.H. 3D Balance in Legged Locomotion: Modeling and Simulation for the One-Legged Case. , ACM Inter-Disciplinary Workshop on Motion: Representation and Perception, 1983.

246. Muybridge, E. *The human figure in motion*. Dover Publications, New York, 1955. First published in 1901, Chapman and Hall, Ltd., London.
247. Muybridge, E. *Animals in motion*. Dover Publications, New York, 1957. First Published in 1899, Chapman and Hall, Ltd., London
248. Napier, J. "The antiquity of human walking." *Scientific American* 216, 4 (1967), 56-66.
249. Narinyani, A.S., Pyatkin, V.P., Kim, P.A., Dementyev, V.N. "Walking robot: a non-deterministic model of control." ( ).
250. Nashner, L.M. "A model describing vestibular detection of body sway motion." *Acta Otolaryng.* 72 (1971), 429-436.
251. Nashner, L.M. Vestibular and reflex control of normal standing. In *Control of Posture and Locomotion*, R.B. Stein, K.G. Pearson, R.S. Smith, J.B. Redford, Eds., Plenum Press, New York, N.Y., 1973, pp. 291-308.
252. Nashner, L.M. "Adapting reflexes controlling the human posture." *Experimental Brain Research* 26 (1976), 59-72.
253. Nashner, L.M. "Fixed patterns of rapid postural responses among leg muscles during stance." *Experimental Brain Research* 30 (1977), 13-24.
254. Nashner, L.M. "Visual contribution to rapid motor responses during postural control." *Brain Research* 150 (1978), 403-407.
255. Nashner, L.M., Woollacott, M., Tuma, G. "Organization of rapid responses to postural and locomotor-like perturbations of standing man." *Experimental Brain Research* 36 (1979), 463-476.
256. Nashner, L.M. "Balance adjustments of humans perturbed while walking." *J. Neurophysiology* 44, 4 (1980), 650-664.
257. Navinyani, A.S., Pytkin, V.P., Kim, P.A. Walking robot: a non-deterministic model of control. , Siberian Brnch, Novosibirs, .
258. Nilson, F.A. *Supporting and Propelling Mechanism for Motor Vehicles*, , 1926.
259. Nilsson, N.J. A mobile automaton: An application of artificial intelligence techniques. , Proc. Int. Jt. Conf. A.I., Washington, DC, 1969, pp. 509-520.
260. Okhotsimskii, D.E., Platonov, A.K., et al. *Control algorithms of legged vehicle capable of mastering obstacles*. Proc. of 5th IFAC Symp. on Automatic Control in Space, Geneva, 1973.

261. Okhotsimskii, D.E., Platonov, A.K.. *Control algorithm of the walker climbing over obstacles*. Proc. 3rd IJCAI, Stanford, California, 1973.
262. Okhotsimskii, D.E., Gurfinkel, V.S., Devyanin, E.A., Platonov, A.K. Integrated walking robot development. Conference on Cybernetic Models of the Human Neuromuscular System, 1977.
263. Orin, D.E. A simulation study of a computer-assisted manual control system for legged vehicles. Master Th., The Ohio State University, Columbus, Ohio, 1972.
264. Orin, D.E. *Interactive control of a six-legged vehicle with optimization of both stability and energy*. Ph.D. Th., The Ohio State University, Columbus, Ohio, 1976.
265. Orin, D.E., McGhee, R.B., Vukobratovic, M. "Kinematic and kinetic analysis of open-chain linkages utilizing Newton-Euler methods." *Mathematical Biosciences* 43 (1979), 107-130.
266. Orin, D.E., Oh, S.Y. "Determination of joint positions from limb segment constraints in robotic systems." *Proc of Fifth World Congress on Theory of Machines and Mechanisms* (1979), 860-863.
267. Orin, D.E. "A three degree-of-freedom leg for a hexapod locomotion vehicle." (1980).
268. Orin, D.E. "CARM: General-purpose subroutine package for robot linkage systems simulation." (1980).
269. Orin, D.E. Supervisory control of a multilegged robot. Tech. Rept. Tech Note #23, EE, Ohio State Univ., 1981.
270. Orin, D.E. Three-axis joystick control of a hexapod vehicle over constant-slope terrain. Tech. Rept. Tech Note #23, EE, Ohio State Univ., 1981.
271. Pai, A.L. *Stability and control of legged locomotion systems*. Ph.D. Th., The Ohio State University, Columbus, Ohio, 1971.
272. Pearson, K. "The control of walking." *Scientific American* (1976), 72-86.
273. Pedley, T.J.. *Scale effects in animal locomotion*. Academic Press, London, 1977.
274. Pedotti, A. "A study of motor coordination and neuromuscular activities in human locomotion." *Biological Cybernetics* 26 (1977), 53-62.
275. Pedotti, A., et.al. "Optimization of muscle-force sequencing in human locomotion." *Math. Bioscience* 28 (1978), 57-76.

276. Perry, J. Foot floor contact guide. Rancho Los Amigos Hospital Kinesiology Service.
277. Petternella, M., Salinari, S. Six legged walking vehicles. Tech. Rept. Report No.74-31, University of Rome, 1974. Istituto di Automatica, Rome Italy
278. Plagenhoef, S.. *Patterns of Human Locomotion: A Cinematographic Analysis*. Prentice Hall, Englewood Cliffs, New Jersey, 1971.
279. Proffitt, D.R.; Cutting, J.E.; Stier, D.M. "Perception of wheel-generated motions." *J. of Exp. Psychol. - Human Perception and Performance* 5, 2 (1979), 289-302.
280. Pugh, L.G.C.E. "The influence of wind resistance in running and walking and the mechanical efficiency of work against horizontal or vertical forces." *J. Physiology* 213 (1971), 255-276.
281. Raibert, M.H. "Analytical equations vs. table look-up for manipulation: A unifying concept." *Proc. IEEE Conf. on Decision and Control* (1977), 576-579.
282. Raibert, M.H. "A model for sensorimotor control and learning." *Biological Cybernetics* 29 (1978), 29-36.
283. Raibert, M.H., Horn, B.K.P. "Manipulator control using the configuration space method." *The Industrial Robot* 5, 2 (1978), 69-73.
284. Raibert, M.H., Brown, H.B., Jr., Chepponis, M., Hastings, E., Shreve, S.T., Wimberly, F.C. Dynamically Stable Legged Locomotion. Tech. Rept. CMU-RI-81-9, Robotics Institute, Carnegie-Mellon University, 1981.
285. Raibert, M.H. Dynamic stability and resonance in a one legged hopping machine. Conference on Theory and Practice of Robots and Anthropomorphic Systems, IFTMoM, 1981.
286. Raibert, M.H. "Hopping in legged systems -- Modelling and simulation for the 2D one-legged case." *IEEE Tran. Systems, Man, and Cybernetics*, Submitted (1982).
287. Raibert, M.H., Brown, H.B., Jr. "Experiments in balance with a 2D one-legged hopping machine." *ASME J. Dynamic Systems, Measurement, and Control*, Submitted (1982).
288. Raibert, M.H., Wimberly, F.C. "A new tabular method for robot dynamics with focus on legged locomotion." *In preparation* (1982).
289. Raibert, M.H., Brown, H.B., Jr., Chepponis, M., Hastings, E., Murthy, S.S., Wimberly, F.C. Dynamically Stable Legged Locomotion -- 1982 Annual Report. Tech. Rept. CMU-RI-82, Robotics Institute, Carnegie-Mellon University, 1982.

290. Raibert, M.H., Sutherland, I.E. "Machines That Walk." *Scientific American* 248, 1 (1983), 44-53.
291. Ralston, H.J. "Energy-speed relation and optimal speed during level walking." *Int. Z. Angew. Physical Einsch. Arbeits Physiol. Bd. 17* (1958), 277-283.
292. Ralston, H.J. Energetics of human walking. In *In Neural Control of Locomotion*, R.N. Herman, S. Grillner, P.S. Stein, D.G. Stuart, Eds., Plenum Press, New York, 1975, pp. 77-98.
293. Roberts, W.M., Levine, W.S., Zajac, F.E., III. "Propelling a torque controlled baton to a maximum height." *IEEE t. Automatic Control AC-24*, 5 (1979), 779-782.
294. Robinson, D.J., Stockwell, C.W., Koozekanani, S.. *A method for evaluation of vestibular postural control in humans*, Boston, Mass., 1976. 29th ACEM:B
295. Rugg, L.A.. *Mechanical horse*, 1893.
296. Saltzman, E. "Levels of sensorimotor representation." *J. Mathematical Psychology* 20, 2 (1979).
297. Saund, E. "The physics of one-legged mobile robots - Part I - A general discussion." *Robotics Age* (1982), 38-45.
298. Saund, E. "The physics of one-legged mobile robots - Part II - The mathematical description." *Robotics Age* (1982), 35-37, 53.
299. Saunders, J.B., Imma, V.T., Eberhart, H.D. "The major determinants in normal and pathological gait." *The Journal of Bone & Joint Surg. 35-A*, 3 (1953), 543-558.
300. Schneider, A. Yu., Gurfinkel, E.V., Kanaev, E.M., Ostapchuk, V.G. A system for controlling the extremities of an artificial walking apparatus. In Russian Report No.5, Physio-Technical Institute, 1974. General and Molecular Physics Series, Moscow, USSR
301. Schwartz, R.P., Heath, A.L., Morgan, D.W., Towns, R.C. "A quantitative analysis of recorded variables in the walking patterns of normal adults." *J. Bone & Joint Surg. 46-A* (1964), 324-334.
302. Seifert, H.S. "The lunar pogo stick." *J. Spacecraft and Rockets* 4, 7 (1967).
303. Seifert, H.S. Small scale lunar surface personnel transporter employing the hopping mode. Tech. Rept. Report No.397, Stanford University Dept. Aeronautics and Astronautics, 1968, 1970.
304. Seireg, A., Arvikar, R.J. "A mathematical model for the evaluation of forces in lower extremities of the musculo-skeletal system." *J. of Biomechanics* 6 (1973), 313-326.

305. Severin, F.V., Orlovskii, G.N., Shik, M.L. "Work of the muscle receptors during controlled locomotion." *Biophysics* 12, 3 (1967), 575-586.
306. Shigley, R. Mechanics of walking vehicles. Tech. Rept. Report No. 7, OTAC, Detroit, Michigan, 1957. Land Locomotion Laboratory
307. Shik, M.L., Orlovskii, G.N. Coordination of the limbs during running of the dog. Institute of Biological Physics, 1965. Academy of Sciences, Moscow, U.S.S.R.
308. Shik, M.L., Orlovsky, G.N., Severin, F.V. "Locomotion of the mesencephalic cat elicited by stimulation of the pyramids." *Biofizika* 13 (1968), 127-135.
309. Silver, W.M. On the equivalence of Lagrangian and Newton-Euler dynamics for manipulators. .
310. Simons, J., Van Brussel, H., De Schutter, J., Verhaert, J. "A self-learning automaton with variable resolution for high precision assembly by industrial robots." *IEEE t. Automatic Control* AC-27, 5 (1982), 1109-1112.
311. Sindall, J.N. "The wave mode of walking locomotion." *Journal of Terramechanics* 1, 4 (1964), 54-73.
312. Smoliar, Stephen W.. *A lexical analysis of labanotation*. University of Pittsburgh Tech. Report. July 1978.
313. Snell, E.. *Reciprocating Load Carrier*. , 1947.
314. Speckert, Glen. "A computerized look at cat locomotion or one way to scan a cat." , A.I. Memo 374 (1976).
315. Steindler, A.. *Mechanics of normal and pathological locomotion*. Charles C. Thomas, Springfield, IL, 1935.
316. Stepaneko, Y. Dynamics of complex mechanisms. Mathematical Institute, . Belgrade
317. Stewart, G. W.. *Introduction to Matrix Computations*. Academic Press, New York, 1973.
318. Stuart, D.G., Withey, T.P., Wetzel, M.C., Goslow, G.E., Jr. Time constraints for inter-limb coordination in the cat during unrestrained locomotion. In control of posture and locomotion, New York, 1973, pp. 537-560.
319. Sun, S.S. *A theoretical study of gaits for legged locomotion systems*. Ph.D. Th., , 1974.
320. Sutherland, I.E.. *A Walking Robot*. The Marcian Chronicles, Inc., Pittsburgh, 1982.
321. Taylor, C.R.; Rowntree, V.J. "Running on two or four legs: Which consumes more energy?" *Science* 179 (1973), 179 and 187.

322. Taylor, C.R.; Shkolnik, A.; Dmpel, R.; Baharav, D.; Borut, A. "Running in cheetahs, gazelles, and goats: energy cost and limb configuration." *Amer. J. of Physiology* 227, 4 (1974), 848-850. Harvard Univ., Tel-Aviv Univ., Hebrew Univ.
323. Taylor, C.R.; Heglund N.C.; McMahon, T.A.; Looney, T.R. "Energetic cost of generating muscular force during running." *J.Exp.Biol.* 36 (1980), 9-18. Printed in Great Britain
324. Tomovic,R. "On the synthesis of self-moving automata." *Automation and Remote Control* 26 (19-5).
325. Tomovic,R. "A general theoretical model of creeping displacement." *Cybernetics IV* (1961), 98-107. English translation
326. Tomovic,R., Karplus,W.R.. *Land locomotion -- simulation and control.* , Opatija, Yugoslavia, 1961. Proc. Third International Analogue Computation Meeting
327. Tomovic,R., McGhee,R.B. "A finite state approach to the synthesis of bioengineering control systems." *IEEE t. on Human Factors in Electronics* 7, 2 (1966), 65-69.
328. Tomovic,R., Bellman. "Systems approach to muscle control." *Math. Biosci.* 8 (1970).
329. Trnkoczy,A., Bajd,T., Malezic,M. "A dynamic model of the ankle joint under functional electrical stimulation in free movement and isometric conditions." *J. of Biomechanics* 9 (1976), 509-519.
330. Urschei,W.E.. *Walking Tractor.* , 1949.
331. Vukobratovic,M., Frank,A.A. Legged locomotion studies. In *Advances in External Control of Human Extremities*, M.M. Gavrilovic, A.B. Wilson Jr., Belgrade, Eds., , 1969. pp. 407-430.
332. Vukobratovic,M., Juricic',D. "Contribution to the synthesis of biped gait." *IEEE t. on Biomedical Engineering BME-16* (1969).
333. Vukobratovic,M., Frank,A.A., Juricic',D. "On the stability of biped locomotion." *IEEE t on Biomedical Engineering BME-17* (1970).
334. Vukobratovic,M., Juricic',D., Frank,A.A. "On the control and stability of one class of biped locomotion systems." *t. ASME Journal of Basic Engineering* (1970), 328-332.
335. Vukobratovic,M. "Contributions to the study of anthropomorphic systems." *Kibernetika* 2 (1972).
336. Vukobratovic,M., Ciric,V., Hristic,D., Stepanenko,J. Contribution to the study of anthropomorphic robots. , Paper 18.1, Proc. IFAC V World Congress, Paris, 1972.

337. Vukobratovic, M., Stepaneko, Y. "On the stability of anthropomorphic systems." *Mathematical Biosciences* 14 (1972), 1-38.
338. Vukobratovic, M., Stepaneko, Y. "Mathematical models of general anthropomorphic systems." *Mathematical Biosciences* 17 (1973), 191-242.
339. Vukobratovic, M. Dynamics and control of anthropomorphic active mechanisms. First Symposium on Theory and Practice of Robots and Manipulator Systems, IFTMoM, Udine, Italy, 1973, pp. 313-332.
340. Vukobratovic, M., et al. "Development of active exoskeletons." *Medical and Biological Engineering* (1973).
341. Vukobratovic, M., Hristic, D., Stojiljkovic, Z. "Development of active anthropomorphic exoskeletons." *Medical and Biological Engineering* (1974), 66-80.
342. Vukobratovic, M., Okhotsimiskii, D.E. "Control of legged locomotion robots." *Proc. International Federation of Automatic Control Planary Session* (1975).
343. Vukobratovic, M.. *Legged locomotion robots and anthropomorphic systems*. Research monograph, Institute Mihailo Pupin, Belgrade, Yugoslavia, 1975.
344. Vukobratovic, M. Legged locomotion robots: mathematical models, control algorithms and realizations. , 1975. Unpublished report
345. Vukobratovic, M., Hristic, D., Stekic', D., Gluhajic', N. "New method of artificial motion synthesis and application to locomotion robots and manipulators." ( ).
346. Walker, M.W., Orin, D.E. "Efficient Dynamic Computer Simulation of Robotic Mechanisms." *ASME J. Dynamic Systems, Measurement, and Control* 104, 3 (1982), 205-211.
347. Wetzel, M.C., Atwater, A.E., Stuart, D.G. Movements of the hindlimb during locomotion of the cat. In *Neural control of locomotion*, R.N. Herman, S. Grillner, P.S. Stein, D.G. Stuart, Eds., Plenum Press, New York, 1975.
348. Wetzel, M.C., Stuart, D.G. "Ensemble characteristics of cat locomotion and its neural control." *Progress in Neurobiology* 7 (1976), 1-98.
349. Whitney, W.M. Human vs autonomous control of planetary roving vehicles. , IEEF Symp. on Sys., Man and Cybernetics, Dallas, 1974, pp. 1-4.
350. Williams, M., Lissner, H.R.. *Biomechanics of human motion*. W.B. Saunders Company, Philadelphia, 1962.

351. Wilson, D.M. "Insect walking." *Annual Review of Entomology* 11 (1966), 103-121.
352. Wilson, D.M. "Stepping patterns in tarantula spiders." *J. Exp. Biol.* 47 (1967), 133-151.
353. Winter, D.A., Greenlaw, R.K., Hobson, D.A. "Television-computer analysis of kinematics of human gait." *Computer and Biomedical Research* 5 (1972).
354. Winter, D.A., Robertson, D.G.E. "Joint torque and energy patterns in normal gait." *Biological Cybernetics* 29 (1978).
355. Wirta, R.W., Herman, R.. *Some observations of relations among gait variables.* , 1975. Krusen Center for Research and Engineering Temple University, Moss Rehabilitation Hospital, Philadelphia
356. Witt, D.C. A feasibility study on automatically-controlled powered lower-limb prosthesis. University of Oxford, . Department of Engineering Science Report
357. Wittenburg, J.. *Dynamics of systems of rigid bodies.* B. G. Teubner, 1977.
358. Yang, P. *A study of electronically controlled orthotic knee joint systems.* Ph.D. Th., The Ohio State University, Columbus, Ohio, 1976.
359. Zheng, Y. *The study of a nine link biped model with two feet.* Ph.D. Th., OSU, 1980. Report #TH-80-HH-058